Thermal conditions and kinematics associated with final emplacement of the Lyngen Nappe

—

Erik Klaebo

Master thesis in GEO-3900
Spring 2017

Abstract

The tectonic boundary of between the Lyngen magmatic complex and the underlaying Nordmannvik have been examined for kinematic indicators. This boundary is characterised by an amphibole facies garnet-mica-kyanite gneiss overlain by a greenschist facies amphibolite/meta-gabbro succession separated by heavily foliated and lineated garnet-mica schist, phyllites and quartzites. Two main populations of lineation were identified: A West verging and a NW verging. Field observations and thin section analyses indicate an overall top to the WNW sense of shear. Not all kinematic indicators show emplacement in this direction; a cluster of indicators located in a synform NE of Nordkjosbotn showed a consistently top to the SE sense of shear. Top to the WNW kinematic indicators were also found on the East side of Storfjorden, 8 km to the east of the Lyngen nappe/Nordmannvik boundary. The emplacement is interpreted to have happened in greenschist facies conditions based on the presence of chlorite in schist and phyllites. Quartz CPO indicate that the temperatures were high enough that rhomb and prism a-slip was dominant with grain boundary migration as the dominant recrystallization mechanism. A top WNW sense of shear indicate that the Lyngen nappe could have been displaced due to extensional collapse or possibly extrusion wedging.

Contents

Introduction

Aim

The aim of this thesis is to characterize the kinematics and metamorphic conditions of the Lyngen nappe during its final emplacement. This is done by studying the boundary between the Lyngen nappe and the underlying Nordmannvik nappe running from Lyngseidet to Nordkjosbotn in the east Lyngen Alps, Troms for kinematic indicators and minerals that characterise metamorphic facies.

Study area

FIGURE 1: STUDY AREA IS CONTAINED WITHIN STIPPLED LINE AND STRETCHES 45 KM FROM NORDKJOSBOTN TO LYNGSEIDET.

Study area is located North of Norway, in Troms a two hours' drive from the regional capital of Tromsø. The Lyngen Alps are known for their easily accessible glaciers and spectacular alpine peaks, featuring skiers and hikers all year long. Nordkjosbotn bounds the area in the South and Lyngseidet in the North with the fylkesvei 868 serving as the logistical connection between them. This road follows along the Lyngen/Nordmannvik tectonic boundary and serves as a natural starting point when examining it. Going up into the mountain are several sheep trails and hiking paths, making surveying the boundary rather convenient.

The area is dominated by a gently west tilting plain that is either by sea level or a few hundred meters up after a steep slope in the South. Steep alpine mountains are cut into by rounded valleys that might feature a glacier at the end. From these rivers flow, creating waterfalls and stepped river beds as they prefer to traverse down the east slopes of the mountain. These rivers might follow the rock beds, sometimes creating angular almost 90 degrees bends as they break through one unit, leaving behind barren riverbeds that form natural paths through the terrain. Pine trees grow in distinct belts in the lowermost valleys in a fauna otherwise dominated by birch. Giving way to moss and marches higher up followed by a belt of grass below bare peaks.

Regional geology

The Caledonides
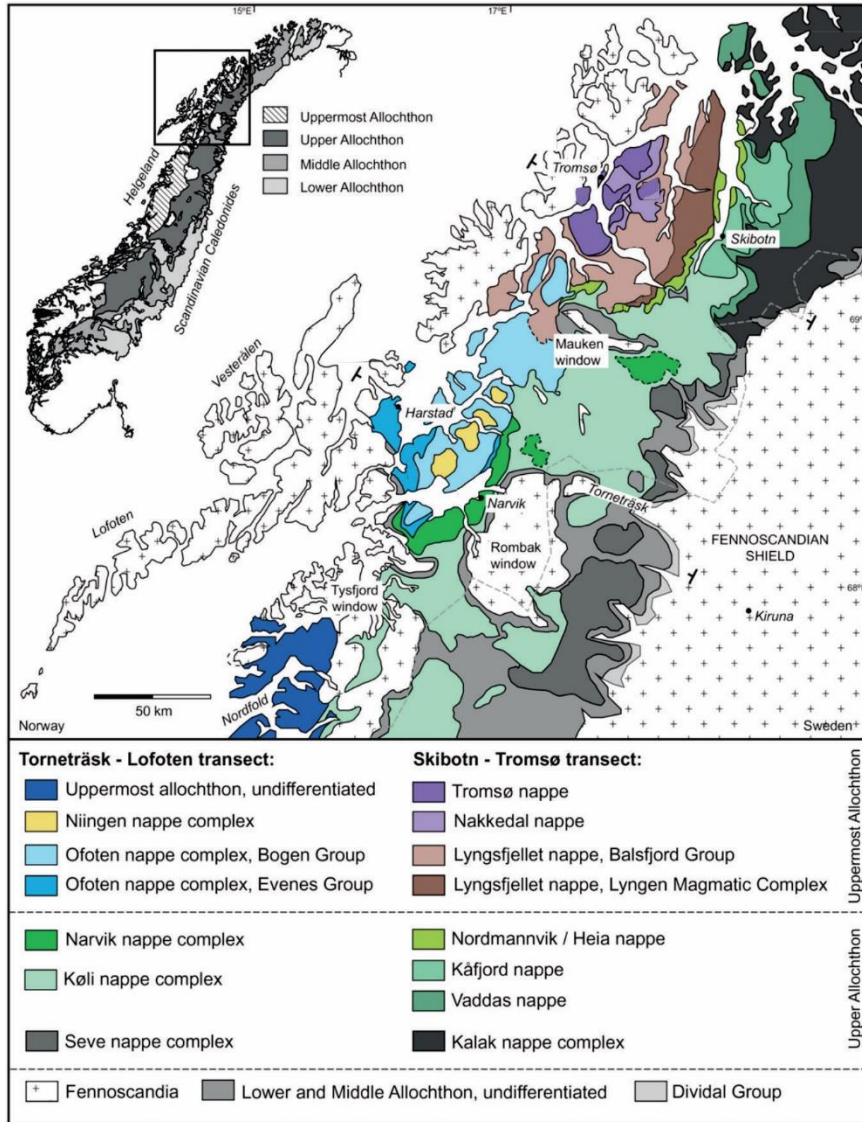
FIGURE 2: THE SCANDINAVIAN CALEDONIDES. FIGURE MODIFIED FROM (AUGLAND, ANDRESEN, GASSER, & STELTENPOHL, 2014A)

The Caledonide orogen of Scandinavia comprises a tectonostratigraphy of thin extensive nappes that were emplaced ESE on to the Baltic craton (Ramsay, Sturt, Zwaan, & Roberts, 1985). These nappes are traditionally separated into the lower, middle, upper and uppermost allochton based on affinity to Baltica (D. D. G. G. Roberts, 1985). The lower allochton is derived from Baltica, the middle from Baltica margin, the upper allochton represent Iaepetus and the uppermost is derived from the Laurentian margin (D. Roberts, Nordgulen, & Melezhik, 2007; Stephens, 1985). Alternatively the Caledonides can be divided into non genetic sections; North, Central and South, based on distinct tectonic differences

along strike of the orogen to encompass for complex palaeographical relationships(F. Corfu, Andersen, & Gasser, 2014).

The Scandinavian Caledonides extends for about 1500 km from Stavanger in the South to the Barents Sea in the North. The basement consists of Archaean to Neoproterozoic rocks of the Fennoscandian shield with the oldest rocks situated in the North of the orogen. Uncomformably overlaying the basement is a thin autochthonous sedimentary cover of Neoproterozoic to Palaeozoic age. Overlaying these rocks are allochtonous tectonic units of both metaigneous and metasedimentary rocks bounded by major thrusts, extensional faults and strike-slip faults. To the west and north the orogen is covered by younger Palaeozoic to Cenozoic sedimentary rocks(F. Corfu et al., 2014).
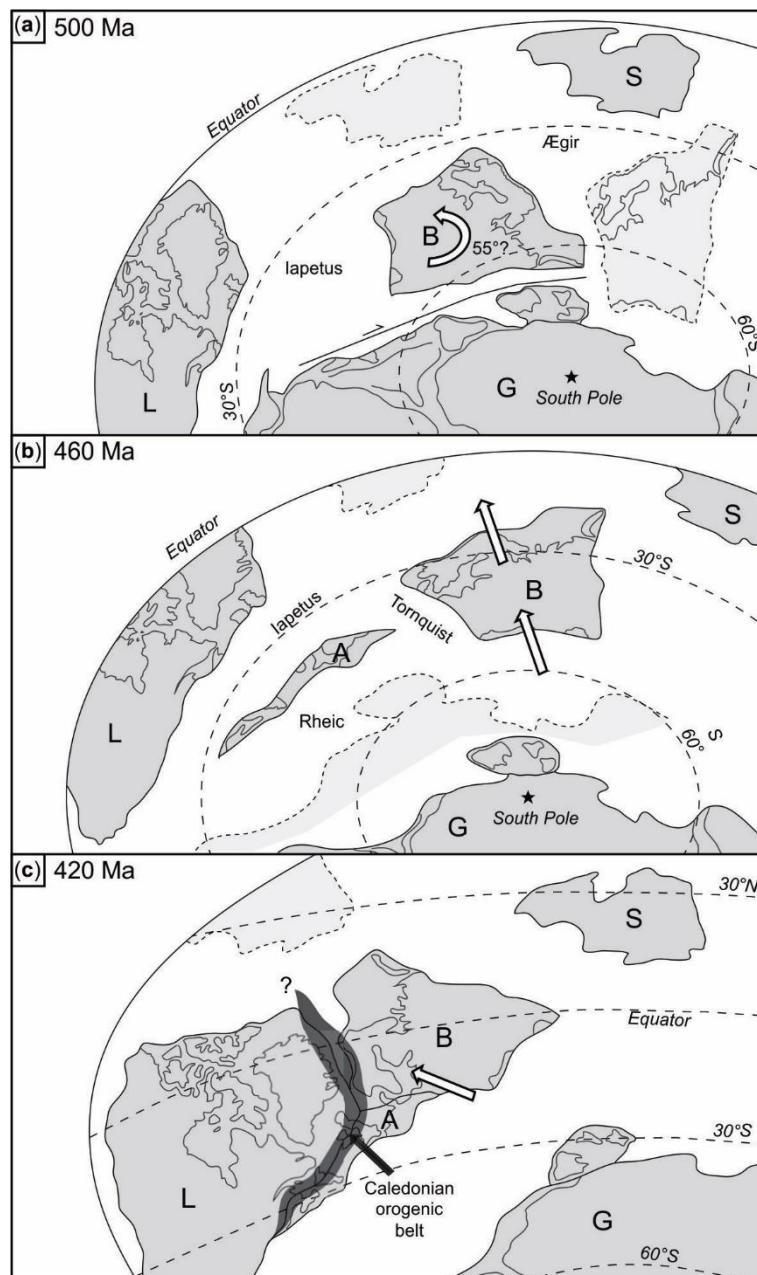
FIGURE 3: OVERVIEW OF POSSIBLE PALAEOGRAPHIC POSITIONS OF THE PALEOZOIC CONTINENTS IN THE TIMESPAN LEADING UP TO THE SCANDIAN EVENT. L – LAURENTIA, B – BALTICA, A – AVALONIA, S – SIBERA, G - GONDWANA. FIGURE COPIED FROM (F. CORFU ET AL., 2014). A) BALTICA ROTATES ANTICLOCKWISE TO

4

The formation of the Caledonian orogeny happened over a time interval of 200 Ma from the Cambrian into the Devonian and relates to the tectonic events associated with the development and closure of the part of Iaepetus ocean situated between Baltica and Laurentia. This closure involved several phases of arc-arc, arc-continent and continent-continent collisions; sometimes synchronous, sometimes diachronous. The arc-arc and arc-continent collisions were involved in the earlier phases while the later phases involved continent-continent collisions (McKerrow, Mac Niocaill, & Dewey, 2000).

In the Late Cambrian (513-490 Ma) the margins of virtually all cratons underwent the onset of orogenesis or initiation of subduction, including Baltica and Laurentia. This might have been due to a global-scale plate reorganization due to the terminal suturing between East and West Gondwana resulting in compensatory changes elsewhere in the global plate circuit to maintain a zero sum for all plate motion. (Boger & Miller, 2004; van Staal & Hatcher, 2010) The subduction initiation in the Iaeptus happened along the passive margins of Baltica and Laurentia, even though passive margins in themselves are deemed unsuitable for the initiation of subduction due to being characterized by old, strong oceanic lithosphere(Cloetingh, Wortel, & Vlaar, 1982).

Around 480 Ma the Iaeptus ocean reached its widest point and consequent closure started with steady narrowing through the Ordovician. Baltica rotated counterclockwise from facing Siberia to facing Laurentia and moved northward approaching close enough to Laurentia to share similar fauna. Avalonia rifted off Gondwana and the Tornquist Ocean between Avalonia and Baltica started narrowing with subduction under Avalonia until Baltica and Avalonia merged in the Ordovician-Silurian boundary time. By around 425 Ma the Iaeptus ocean between Laurentia and Baltica closed resulting in the Scandian orogeny and formation of Laurussia (Torsvik et al., 1996). The Baltoscandian margin was partially subducted beneath Laurentia in the mid-late Silurian and was followed by rapid exhumation of the highly-metamorphosed hinterland in the early Devonian. Late Scandian collapse of the orogen occurred on major extensional detachments into the late Devonian.(Gee, Fossen, Henriksen, & Higgins, 2008)

The formation of the Scandinavian Caledonides is divided into four to five major phases chronically listed as: Finnmarkian, Trondheim, Taconian, Scandian and Solundian(D. Roberts, 2003). The Finnmarkian phase has come under criticism and the term is recommended to be dropped as Pb-U dating shows that the Kalak Nappe Complex has undergone tectonic events atypical for the autochronous Baltic margin. Indicating that it is an exotic terrane in respect to Baltica that has been translated and accreted on to Baltica during the Scandian collisional phase.(F. Corfu, Roberts, R. J., Torsvik, T. H., Ashwal,L. D. & Ramsay, D. M., 2007; C. L. Kirkland, Daly, & Whitehouse, 2008)

Trondheim event

The event, affecting mostly central Norway, marks a principal phase of deformation and metamorphism that includes ophiolite obduction and bueschist metamorphic parageneses.(D. Roberts, 2003) Some of the supra-subduction ophiolites have been dated to have U-Pb zircon ages in the rage 493-482 Ma(Dunning, 1987) while the obduction events age range from Mid Ordovician to Llandovery, Silurian (Eide & Lardeaux, 2002). The origin of

the ophiolites are uncertain as it yields both Baltoscandian geochemical signatures(Andersson, 1985) while showing dominance of Laurentian fauna (T. Grenne, Ihlen, & Vokes, 1999; Tor Grenne & Roberts, 1998). One scenario is that an arc or a microcontinent existed in the late Cambrian between Baltica and Siberia with ongoing intra-ocenaic subduction. Baltica starts rotating counterclockwise in early Ordovician and move towards Laurentia in the middle Ordovician, sweeping through series of arc-subduction and back-arc rift associated settings, obducting ophiolites and causing blueschist metamorphism, before docking with Laurentia in late Silurian(Eide & Lardeaux, 2002).

Taconian event

The event is characterized by mid to late Ordovician metamorphism and likely ophiolite obduction with west-directed thrusting that occurred along the Laurentian margin.(D. Roberts, 2003; Yoshinobu et al., 2002) The evidence for this episode is largely confined to the uppermost allochthon in the Central and South section of the Scandinavian Caledonides. Shelf and adjacent slope/rise successions and magmatic arc complexes are considered to have been incorporated into the Taconian accretionary wedge on the margin of Laurentia due to oceanward subduction. These successions were then deposited on top of Baltica during the Scandian Laurentia-Baltica collision.(D. Roberts, 2003) An upper constraint on the event in the upper Central part of the Scandinavian Caledonides is provided by faunas of Ordovician-Early Silurian age in a basin that accumulated material partly from the deformed and inverted Lyngen ophiolite (Bjørlykke & Olaussen, 1981).

Scandian event

The orogenesis is generally seen as a product of oblique collision between Baltica and Laurentia in Late Silurian to Early Devonian with the margin of Baltica subducted below Laurentia. It is the principal tectonometamorphic event resulting in the characteristic Caledonide allochton distribution in Norway and Sweden. The timing of the Scandian event varies transversely and laterally due to the obliquity of the collision and the presence of arcs and microcontinental blocks. (D. Roberts, 2003) Subduction to maximum depths of ca 125 km occurred at maximum age of 407 Ma with rapid rates of initial exhumation that flattened out into late Devonian(Terry, Robinson, Hamilton, & Jercinovic, 2000). Overall the Scandian tectonometamorphism was a short event of perhaps less than 10 Ma involving all principle allochthones including those influenced by the Taconian and Trondheim events. With the uppermost allochthon shown to be detached Laurentia-derived Taconian outliers transposed onto Baltica(D. Roberts, 2003).

Extensional phase

A period of extensional collapse followed the Scandian phase partially due to gravitational collapse resulting in Devonian sedimentary basins. The deformation varied in intensity across the orogen, both vertically and W-E. A change of tectonic transport also resulted from the extension characterised by a top-west directed sense of shear. The extension did not affect the Fennoscandian basement in the eastern part of the Caledonides, but is prevalent in the west as basement windows with top-to-the-west shear zones. In the west of Norway initial extensional deformation commenced at greenschist-facies conditions and became increasingly more brittle and localized as the nappes were exhumed in the Late Silurian to Middle Devonian.(Andersen, 1998) While the extension was unidirectional in Western

Norway, occurring under greenschist facies conditions, there is evidence of bidirectional orogen parallel transport happening in medium-grade conditions in Central Norway. This resulted in uplift of the high-grade central Norway basement by tectonic denudation and a less pronounced metamorphic break between the upper and lower plates. Connecting these two regimes in the Devonian was the Møre-Trøndelag fault complex with steep subvertical transfer faults(Braathen et al., 2000). North Norway lacks Devonian sedimentary basins and the most Northern Devonian extensional detachment is thought to be the Eidsfjord detachment at Lofoten. This detachment has a low-angle and hinterland dipping geometry with top to the west kinematics, similar to detachments in West Norway(Mark G Steltenpohl et al., 2011). While the late orogenic extension structures in West Norway show progressive development of decreasing pressure and temperature, the Ofoten detachment zone in North Norway indicate a steady level at the mid-crustal level throughout the late-extensional event. This might be explained by a difference in position between the two regions with regards to distance to the syn-orogenic thrust front and to different amount of extension. West Norway being further from the syn orogenic thrust front experiencing more uplift due to isostatic rebound than Ofoten which is closer to the thrust front (Rykkelid & Andresen, 1994). Protracted cooling history of the region preclude significant extensional unroofing during the Devonian period and indicate that post-orogenic extensional collapse was a less important factor in the North of the Caledonides compared to the more Southerly segments.(Northrup, 1997)

Troms Caledonides

The Troms area is situated on the border between the Northern and Central segment of the Scandinavian Caledonides and comprises of an Archaean to Palaeoproterozic basement overlain by an extensive autochthonous to paraautochthonous Neoproterozoic to Palaeozoic sedimentary cover, overlain by Mesoproterozoic meta-sedimentary and igneous rocks of the Kalak nappe complex, overlain by Palaezoic rocks with mainly oceanic affinities topped by nappe stack of Precambrian continental crust.(F. Corfu et al., 2014)

Fennoscandian shield

The NE domain of the Fennoscandian shield consists of a granite-gneiss association with greenstone, paragneiss and granulitic complexes of Archaen age whose formation can be understood in terms of collisions of lithospheric plates. Its architecture is attributed to accretionary-collisional processes with several phases of accretions and at least one collisional event.(Slabunov et al., 2006)

Dividal Group

Overlaying the Fennoscandian shield is a sequence of autochronous Neoproterozoic to Cambrian meta-sedimentary deposits collectively known as the Dividal group. The group crops out as a narrow belt of shelfal and platform sediments along and structurally below the Caledonian thrust front. Dated zircons indicate a Timanian source area from the NE margin of Baltica and indicate that the Dividal group represents a Late Neoproterozoic to Early Cambrian foreland basin setting(Andresen, Agyei-Dwarko, Kristoffersen, & Hanken, 2014) alternatively the group represent the thermally controlled subsidence of a passive margin(Kumpulainen & Nystuen, 1985).

Kalak nappe complex

The complex is a composite stack of more than 10 thrust sheets with variable tetonometamorphic histories that dominate most of the northern segment of the Caledonides. The nappes are dominated by clastic sedimentary rocks with lesser amounts of para- and orthogneisses and minor limestones. (Gayer, Humphreys, Binns, & Chapman, 1985) Zircon dating indicate that meta sedimentary sequence consists of at least three different successions; the Sværholt succession deposited at 1030-980 Ma, the Sørøy succession deposited 910-840 Ma and the Åfjord pelites and Falknes limestones deposited at 760-710 Ma. (Christopher L Kirkland, Stephen Daly, & Whitehouse, 2007; T. Slagstad et al., 2006) Both the Sværholt and the Sørøy succession is intruded by mafic to felsic intrusions, but the timing is different, with the oldest intrusions occurring in the Sværholt succession. (C. L. Kirkland, Daly, Eide, & Whitehouse, 2006) Seiland igneous province intrudes into the Sørøy succession, distinguished from the earlier mentioned and older intrusions by zircon dating.(R. J. Roberts, Corfu, Torsvik, Ashwal, & Ramsay, 2006) Both successions are intruded by 440-420 Ma pegmatites and granitic veinlets formed by metamorphism associated with the juxtaposition of the Kalak Nappe Complex on top of Baltica Several episodes of pre Scandian deformation episodes have affected the Kalak Nappe Complex in the early Proterozoic, affecting specific nappes in separate events.(Fernando Corfu, Gerber, Andersen, Torsvik, & Ashwal, 2011)

Reisa/Skibotn nappe complex

The complex consists from bottom to the top of the Vaddas, Kåfjord and Nordmannvik nappe and is tectonically equivalent to the Narvik Nappe complex further South.(Andresen & Steltenpohl, 1994) The vaddas nappe constitute a relatively undisturbed right way up stratigraphic and magmatic succession with a twofold depositional history. A continental succession deposited in shallow-water separated by a non-tectonic hiatus with an overlaying transgressive Late Ordivician-Silurian formation. Metamorphic grade varies from upper greenschist to lower amphibolite. (Lindahl, Stevens, & Zwaan, 2005)
The Kåfjord nappe is composed of metapsammite, marble, garnet-mica schists in the basal section with the upper section composed of mylonitic gneisses with locally boudinaged amphibolite layers. Metamorphic grade is typically middle amphibolite.(Dallmeyer & Andresen, 1992) A blastomylonitic high-strain zone marks the boundary between Kåfjord and the overlaying Nordmannvik nappe.
The Nordmannvik nappe is dominated by migmatized garnet mica schist and gneisses that includes lenses of amphibolite, calc-silicates and marbles with a few bodies of diorite/ gabbro occurring locally. (Augland, Andresen, Gasser, & Steltenpohl, 2014b) It contrasts with all structurally underlaying tectonic units because of its record of a polyphase metamorphic evolutions and its high metamorphic grade. (Dallmeyer & Andresen, 1992) Geothermobarometric studies on relict equilibrium mineral assemblages from the porphyroclasts show that upper amphibolite- to granulite facies conditions with P-T estimates of 9,2 plus/minus 1,0 kBar and temperatures up to 715 plus minus 30 degrees were reached.(S. Elvevold, 1988)

Lyngsfjell Nappe Complex

A greenschist-grade shear zone marks the transition from the Nordmannvik nappe to the overlaying Lyngsfjell Nappe Complex. The Lyngsfjell Nappe Complex consists of the Lyngen Magmatic Complex and the unconformably overlaying Barlsfjord group. The Lyngen Magmatic Complex comprises the Lyngen Gabbro, the Aksla Volcanics and the Kjosen

Greenshists.(A. J. S. Kvassnes, A. H. Strand, H. Moen-Eikeland, & R. B. Pedersen, 2004)
The Kjosen Greenschists defines the easternmost part of the Lyngen Magmatic Complex and comprises pillow lavas, volcaniclastics and undifferentiated greenschists of MORB to island-arc theoleiite. The Aksla volcanics are mainly deformed greenschist facies pillow-lavas, hyaloclastite breccias and dikes MORB to IAT.(Furnes & Pedersen, 1995)

The Lyngen gabbro is wedge shaped(Chroston, 1972) with maximum thickness in the west and has been subdivided into a Western and Eastern suite. Large shear zones separate the Western and Eastern suite, named Rypdalen Shear zone. (D. Slagstad, 1995) Based on magmatic proximity between the western and eastern suite and the non-tectonic transition between the two it is thought that the Lyngen Gabbro represents the lower crustal section of an incipent arc or outer-arc of an Ordivician (469 Ma) oceanic supra-subduction zone(A. Kvassnes, A. Strand, H. Moen-Eikeland, & R. Pedersen, 2004; Oliver & Krogh, 1995) This ophiolite fragment is suggested to have been dismembered during the Scandian event and placed on top of the Reisa Nappe complex possibly by out of sequence thrusting and duplication involving late activation of the basement (Anderson, Barker, Bennett, & Dallmeyer, 1992)

The Balsfjord group is separated by the underlaying Lyngen gabbro by an unconformity that is thought to be late Ordovician based on the oldest fossils recovered. The group consists of Silurian dolomites, calcareous schists and schists with a progression from carbonate rich sediments at the base to sequences dominated by psammite-schist in the top. (Bjørlykke & Olaussen, 1981)

Nakkedal nappe complex

The Nappedal nappe complex consists of high grade quartzfeldspathic paragneiss and amphibolitic magmatic rocks and the mafic Skattøra Migmatite Complex with the contact between the paragneiss and the skattøra migmatite complex being gradational and crosscut by anorthosite dykes. Dating of the anorthostic dykes in the Skattøra migmatite complex yields an age of 456 Ma while the origin of the dykes is suggested to be due to water rich fluids escaping from a subduction zone invaded the crust of an active continental margin. The original tectonic setting of this unit is considered to correspond to that of a rifted margin based on the sedimentary rock association and the inferred alkaline composition of gabbroic protoliths in the Skattøra Migmatite Complex(Selbekk, Skjerlie, & Pedersen, 2000). Finally the boundary zone between the Skattøra Migmatite Complex and the overlaying eclogite facies Tromsø Nappe is characterized by mylonites without anorthositic dykes.(Andresen, Fareth, Bergh, Kristensen, & Krogh, 1985)

Tromsø nappe

The Tromsø nappe is comprised of pelitic to semi-pelitic schists, marbles, calc-silicate rocks, metabasites, quartzo-feldspathic gneisses, retrograded eclogites and ultramafic bodies. U-Pb dating of zircons present in the felsic gneiss yields an age of 493 Ma for the formation of the protolith and suggest a rifted margin to be the original tectonic setting. Pressure and temperature calculations on some of these eclogites indicate subduction-related prograde UHP metamorphism to pressures exceeding 3 GPa at temperatures up to 735 degrees Celsius occurring at 452 Ma. It is suggested that the Tromsø nappe was put on top of the underlying Skattøra Migmatic Complex during the exhumation from 80 km depth following the subduction related event. The Scandian event juxtaposed both the Tromsø nappe and Nakkedal nappe complex on top of the Balsfjord group of the Lyngen Nappe Complex, possibly by underthrusting along a deep crustal shear zone causing a inversed metamorphic

gradient in the balsfjord group. This metamorphic event reached pressures of 1,0 - 1,0 GPa and temperatures of 665 degrees Celsius and is dated by Ar-Ar of Muscovite to be 432 Ma. (F. Corfu, Ravna, & Kullerud, 2003; Krogh, Andresen, Bryhni, Broks, & Kristensen, 1990; Selbekk et al., 2000)

Previous work in the area

(Andresen & Bergh, 1985) describe the equivalent units further west around Balsfjord, noting the jump from lower amphibolite facies in Dyrøy and Senja Nappes (Skibotn/Reisa nappe complex) to upper greenschist facies in the Lyngen magmatic complex.

(Synnøve Elvevold, 1987) determined the metamorphic peaks in the Heia and Vaddas nappes to be granulite and lower amphibolite facies respectively and determined that the Heia napped went through several metamorphic events.

(Oliver & Krogh, 1995) maps one section of the study area with emphasis on the Kjosen area, dating zircons from metatonalites and dated the minimum age of the Kjosen unit to be 469 Ma.

(A. J. S. Kvassnes et al., 2004) describes the gabbro units in the area and concludes them to be the lower crustal section of an incipient arc.

(Hibelot, 2013) worked north of the study area investigating the relationship between metamorphism and deformation in the Nordmannvik nappe concluding that the nappe should be placed in the middle allochton as the protolith are sediments from the outermost Baltica margin.

Methods

Fieldwork was done to obtain samples and make a map of the field area. Most emphasis was put on the Southern and northern section of the study area due to logistical reasons. Thin sections were then made based on potential for sense of shear, presence of clear lineation and in the case of quartz; grain size. These thin sections were then analysed and described with emphasis on potential sense of shear indicators. A petrological microscope was utilized as well as two electron microscopes with differing caps on Voltage. The scanning electron microscopes produced backscatter images showing the contrast between heavy and light elements; thus minerals, as well as using energy-dispersive X-ray spectroscopy to detect the presence of single elements. The quartz thin sections were analysed with focus on dynamic recrystallization mechanisms. A few of them were then selected to undergo electron backscatter diffraction analysis based (EBSD) on location and the presence of domains of orientated quartz grain. This data was then used to make pole figures of the quartz preferred orientation as well as grain maps using (Heilbronner, 2000) Lazy Grain boundary method using Fiji Image J. This grain map was then used to describe grain sizes and fabric using Kaleidagraph and Word Excel to systemize the data and a program named Stripstar to represent the grain sizes in three dimensions. (Philpotts & Ague, 2009) was used for petrological interpretations, (Cees W. Passchier, Trouw, & SpringerLink, 2005) for sense of shear indicators and (Heilbronner & Barrett, 2014) for grain maps and statistical plots.

Sense of shear indicators in a mylonitic shear zone

Mylonites are characterised by small grain size and regular planar foliation and straight lineation. Porphyroclasts may be present; remnants of resistant larger grains than the matrix. These might feature distinct tails that form a sigma or delta clast (Figure 4b) depending on mantle thickness and rotation of the porphyroclast. These tails can indicate the sense of shear, with the flat portions indicating flow direction. Mineral fish (Figure 4 c) are elongate lozenge or lens shaped and lack evidence of rotation. Mica often form these shapes, though other minerals can as well if it has a poor bonding with the matrix.
Shear bands are manifested as small angle shear zones transecting mica preferred orientation (Figure 4 c and d). There are two types: C-type and C'-type which relates to whether the shear planes are parallel or at an angle to the dominant foliation. C'-types have shear band cleavage oblique to the shear zone boundaries with angles varying from 15 to 35 degree. They develop mainly in strongly foliated mylonites and characteristically fails to continue into less foliated layers. Usually only one set of C'-type fabrics are developed, but a second less developed fabric might occur orthogonally to the main set. A younger set can also overprint an older set with a gentler inclination. C-type shear bands have shear planes parallel to the shear zone boundary are more continuous than C'-type fabric. C-type form in weakly foliated mylonites with a small percentage of mica being most common in medium grade shear zones and deformed granites.
Minerals can exhibit a lattice preferred orientation (Figure 4 f and j) develop a monoclinic oblique fabric with respect to the foliation. Equant minerals also develop a monoclinic symmetry of lattice preferred orientation with axes oriented asymmetrically to foliation(Cees W. Passchier et al., 2005).
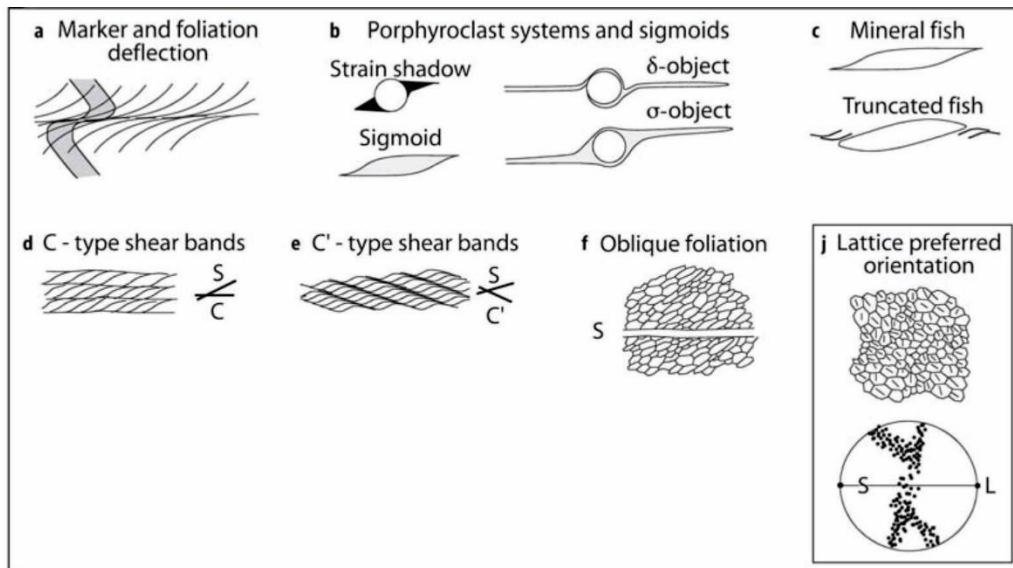
FIGURE 4: STRUCTURES USED AS SENSE OF SHEAR INDICATORS IN THIN SECTIONS THAT ARE COMMON IN A MYLONITIC ZONE, ALL DEXTRAL IN THIS CASE. FIGURE MODIFIED FROM (CEES W. PASSCHIER ET AL., 2005) A) DEFLECTION OF MARKER BANDS INDICATING SENSE OF SHEAR. B) SIGMA CLASTS FEATURING STRAIN SHADOWS. C) PORPHYROCLAST WITH MANTLE FORMING A DELTA- AND A SIGMA CLAST. C) ELONGATED LOZENGE SHAPED MINERAL FISH. D) CONTINUOUS C TYPE SHEAR BANDS. E) C'-TYPE SHEAR BANDS WITH SHEAR PLANES AT AN ANGLE TO FOLIATION. F) OBLIQUE ORIENTATION OF ELONGATED MINERALS. J) LATTICE PREFERRED ORIENTATION OF MINERALS.

Quartz lattice preferred orientation

Non-coaxial progressive deformation is not symmetrical and favours deformation along one a-axis resulting in one maxima more developed than the others. This leads to a monoclinic symmetry with the c-axis being tilted with the sense of shear, normal to the favoured a-axis, but at an angle less than 90 degrees to the external reference line. Initially this results in a double a-axis maximum being replaced by a single a-axis maximum (Figure 5) due to basal, rhomb and prism slip. The dominant slip system is determined by temperature, lower temperatures favouring basal a-slip and higher temperatures favouring prism a-slip and until slip happens along the c-axis.

The practical consequence is that the girdle moves away from the stereo net periphery depending on dominant slip mechanism and ends up with a monoclinic symmetry relative to an external line of reference. Strain and dynamic recrystallization can affect this pattern by removing grains that are oriented unfavourable. (Cees W. Passschier et al., 2005)
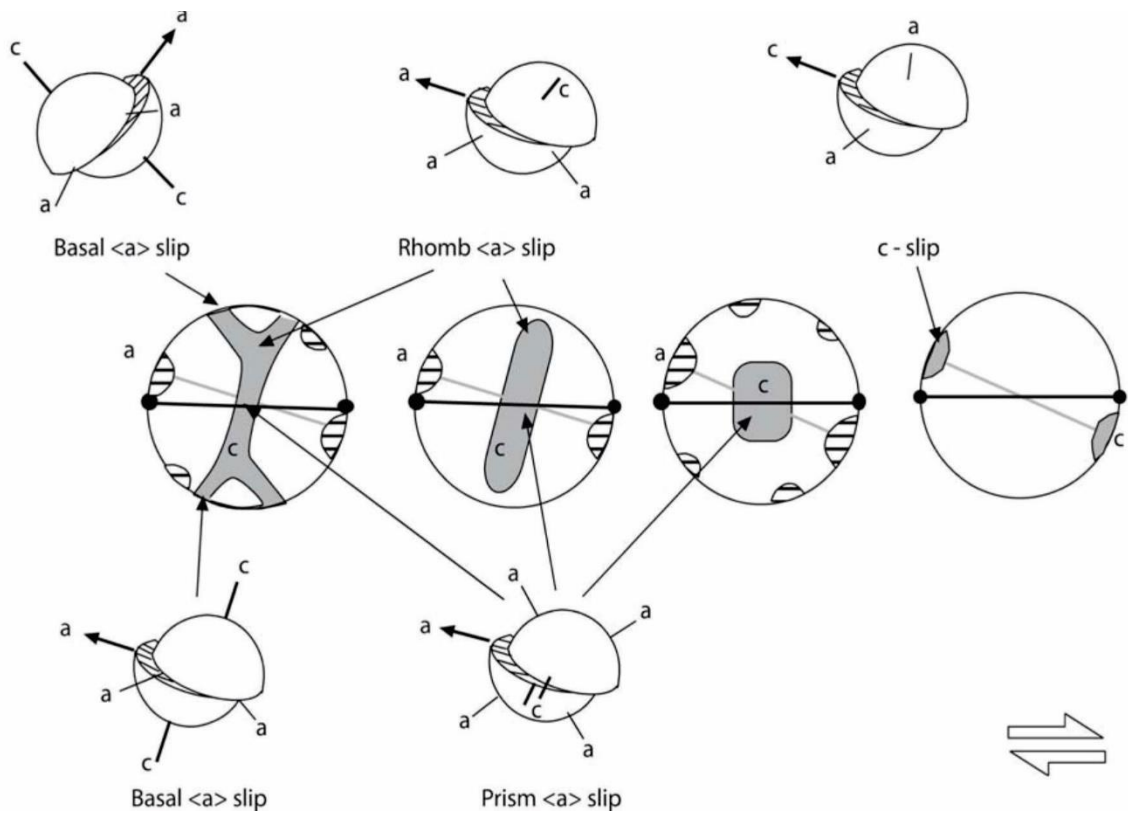
FIGURE 5: STEREOPLOTS OF C-AXIS AND A-AXIS ORIENTATION DURING NON-COAXIAL SLIP. A-AXES MARKED WITH STIPLED AREAS, C-AXES WITH DARK GREY. BLACK LINE IS EXTERNAL SYMMETRY SUCH AS LINEATION, WHILE GREY LINE IS INTERNAL SYMMETRY. MODIFED FROM (CEES W. PASSCHIER ET AL., 2005). FROM LEFT TO RIGHT, GRIDLE SHAPE REFLECTING THE DOMINANT SLIP MECHANISM. LEFT GIRDLE SHOQ A COMBINATION OF BASAL, RHOM AND PRISM SLIP. PROGRESSIVE DEFROMATION CAHNGES DOMINANT SLIP MECHANISM FROM BASAL TO RHOMB, FROM RHOMB TO PRISM AND FINALLY TO C-SLIP.

Results

Overview

Study area was characterised by six principal units. Nordmannvik gneiss and schist, Koppangen/Kjosen phyllites, chlorite schist, amphibolite and gabbro. The gneiss tended to form steep outcrops and gently westerly dipping plateaus with sparse vegetation. Where units of marble were present pine trees would be more common. Otherwise there tended to be marshes and birch in the lower-laying areas. Rivers would be diverted along strike following erosion-resistant layers before breaking through creating step relict river beds. The gently west dipping foliation with easily erodible schist and phyllites caused rivers and lakes to form along the transition between gneiss and phyllites. Phyllites would form steep slopes covered with grass and subsequently sheep trails as these would tend to favor this pasture over the lower laying grasses growing in the soil generated by the gneiss. As the phyllites had a quartzite rich cap they could also form low hills and plateaus. Overlaying the phyllites, the greenschist would form peaks and plateaus relative to the phyllites, but would be eroded by glaciers and form slopes when overlain by gabbro. The gabbros formed peaks generally everywhere with glaciers situated at the gabbro-amphibolite/chlorite schist boundary making smooth channels in the more easily eroded greenschist.

Units would vary N-S along the strike of Lyngen, undulating and varying in thickness, overall dipping gently to the North. Nordmannvik would almost disappear below sea level north and south of Furuflaten(Figure 7 a and b), barely sticking out of the water. Thus, it would make its characteristic west dipping plateau at sea level at Furuflaten, but make the same plateau 500 meters higher up further into Storfjorden.

The phyllites seemed to taper out southward, losing thickness and the hard quartzite cap that allowed it to make out a plateau north of Lyngseidet, disappearing SW of Storvatnet. The greenschist also varied in thickness, being prominent at Furuflaten and further north when Nordmannvik is almost at sea level. Further South it tapers out, not necessarily correlated to the phyllites as the variation in thickness seems more abrupt, thickening again South of nordkjosbotn where the unit lays directly on top of the Nordmannvik gneiss along a steep N-S oriented fault.

Foliation would generally dip west, usually with a 20-degree dip for the gneiss and phyllites and around 40 degrees for the chlorite schist and gabbro (Figure 6). Locally the dip would vary, probably due to large scale folding. East of Storvatnet a km wide asymmetric synform folded the foliation. This synform dipped North and had a near vertical fold limb in the east and more gently dipping fold limb in the west. Smaller possibly parasitic folds could be observed along the west limb.
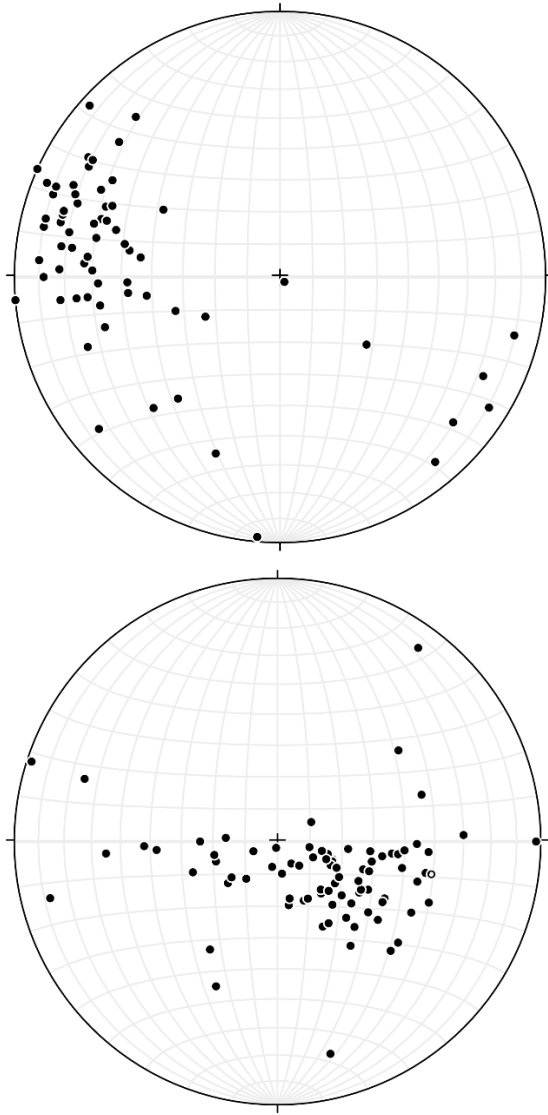
Figure 6: Equal hemisphere pole plots of area stretching lineation to the left and pole plots of the study area foliation to the right. **L**ineation is generally oriented **W-NW** and is dipping **20-30** degrees. **F**oliation is generally striking **S-SW** with right hand rule.
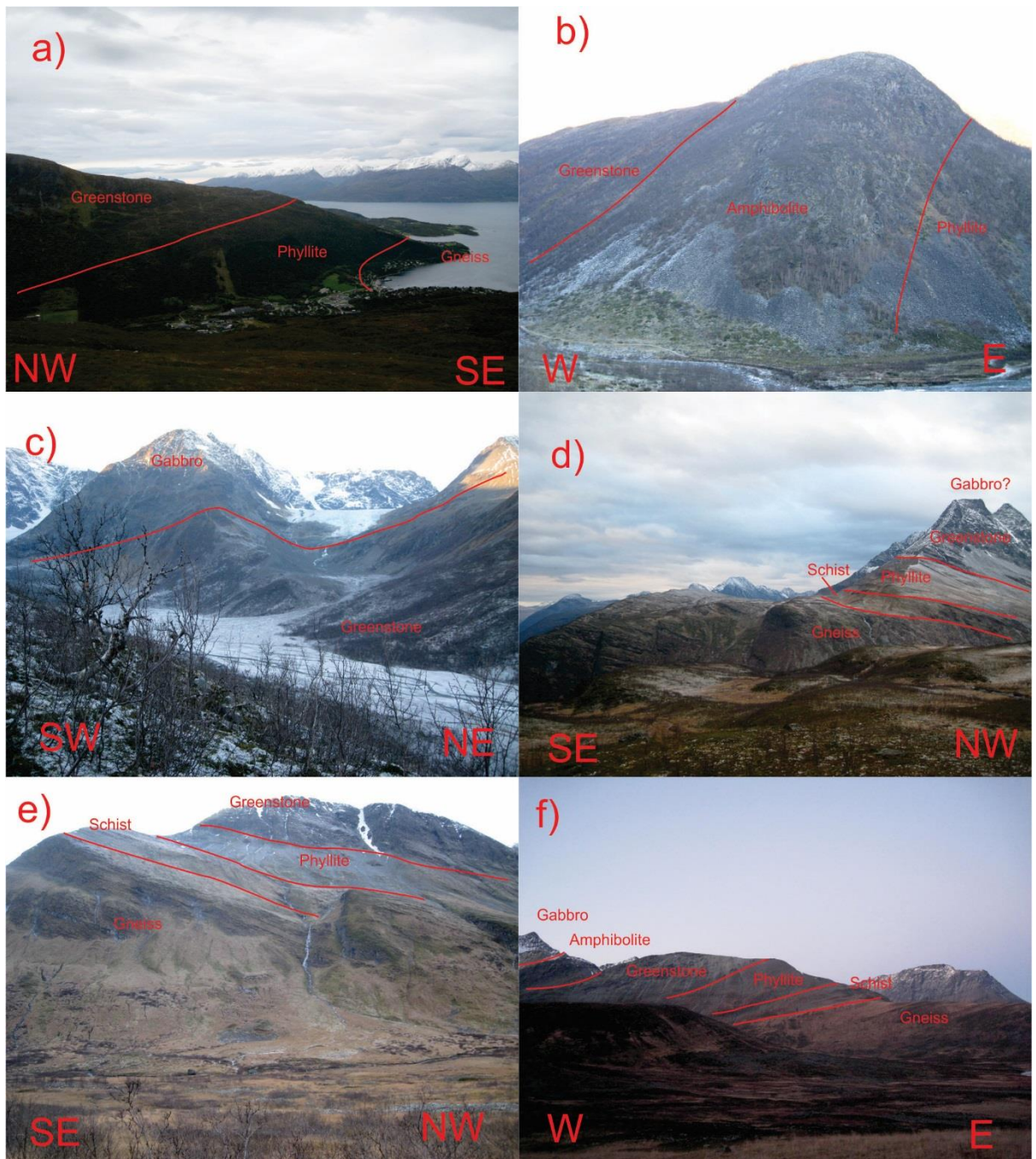
FIGURE 7: N-S OVERVIEW OF THE MAPPED AREA. A) VIEW OF LYNGSEIDET LOOKING NE FROM KAVRINGTINDEN, THE NORDMANNVIK UNIT OF GARNET MICA GNEISS IS BARELY VISIBLE ABOVE THE WATER LINE, RISING UP FURTHER NORTH AND SOUTH AS IT UNDULATES ALONG STRIKE OF THE SHORELINE. KOPPANGEN IS THE PHYLLITES BECOMING MORE QUARTZITIC HIGHER UP IN THE SUCCESSION CREATING LOCAL PEAKS IN THE TERRAIN. B) VIEW OF POLLFJELLET LOOKING NORTH FROM LYNGSDALEN, ANOTHER LOCATION WHERE THE NORDMANNVIK UNIT UNDULATES ALMOST BELOW SEA LEVEL. SHOWING A STEEP BOUNDARY BETWEEN THE KOPPANGEN PHYLLITES AND KJOSEN AMPHIBOLITES AND GREENSTONE. UNUSUAL HERE BEING META GABBRO LOWER IN THE SUCCESSION THAN METAVOLCANICS DIRECTLY ON TOP OF KOPPANGEN PHYLLITES. C) VIEW OF GASKAJIEHKICOHKKA FROM DALTINDEN LOOKING NW. BOUNDARY BETWEEN LYNGEN GABBRO AND UNDERLAYING GREENSTONE WITH GLACIERS SITUATED ON THE BOUNDARY. D) VIEW OF STEINDALSTINDEN LOOKING SW FROM RASTEBYFJELLET, THE HARD NORDMANNVK UNIT WITH SPARSE VEGETATION MAKING A GENTLY WEST DIPPING PLATFORM BEFORE TURNING INTO WEAKER SCHIST AND PHYLLITES MAKING STEEP SLOPES COVERED WITH GRASS CULMINATING IN GABBRO AND GREENSTONE

FORMING SNOW COVERED PEAKS. E) VIEW OF STALLOBORRI LOOKING SW FROM RIIDAVARRI, NORDMANNVIK GNEISS FORMING SPARSE MARSH TERRAIN WITH POOR DRAINAGE TURNING INTO GRASS COVERED SCHIST, TURNING INTO STEEP SLOPES OF PHYLLITE WITH GREENSTONE/AMPHIBOLITE FORMING THE PEAK. F) VIEW OF STALLOBORRI LOOKING NORTH FROM GIEVDNEVAHCAHCA, NORDMANNVIK GNEISS FORMING MARSH AND WEST DIPPING PLATEAU, OVERLAIN BY SCHIST AND PHYLLITES MAKING STEEP SLOPES, OVERLAIN BY GREENSTONE, AMPHIBOLITE AND GABBRO.
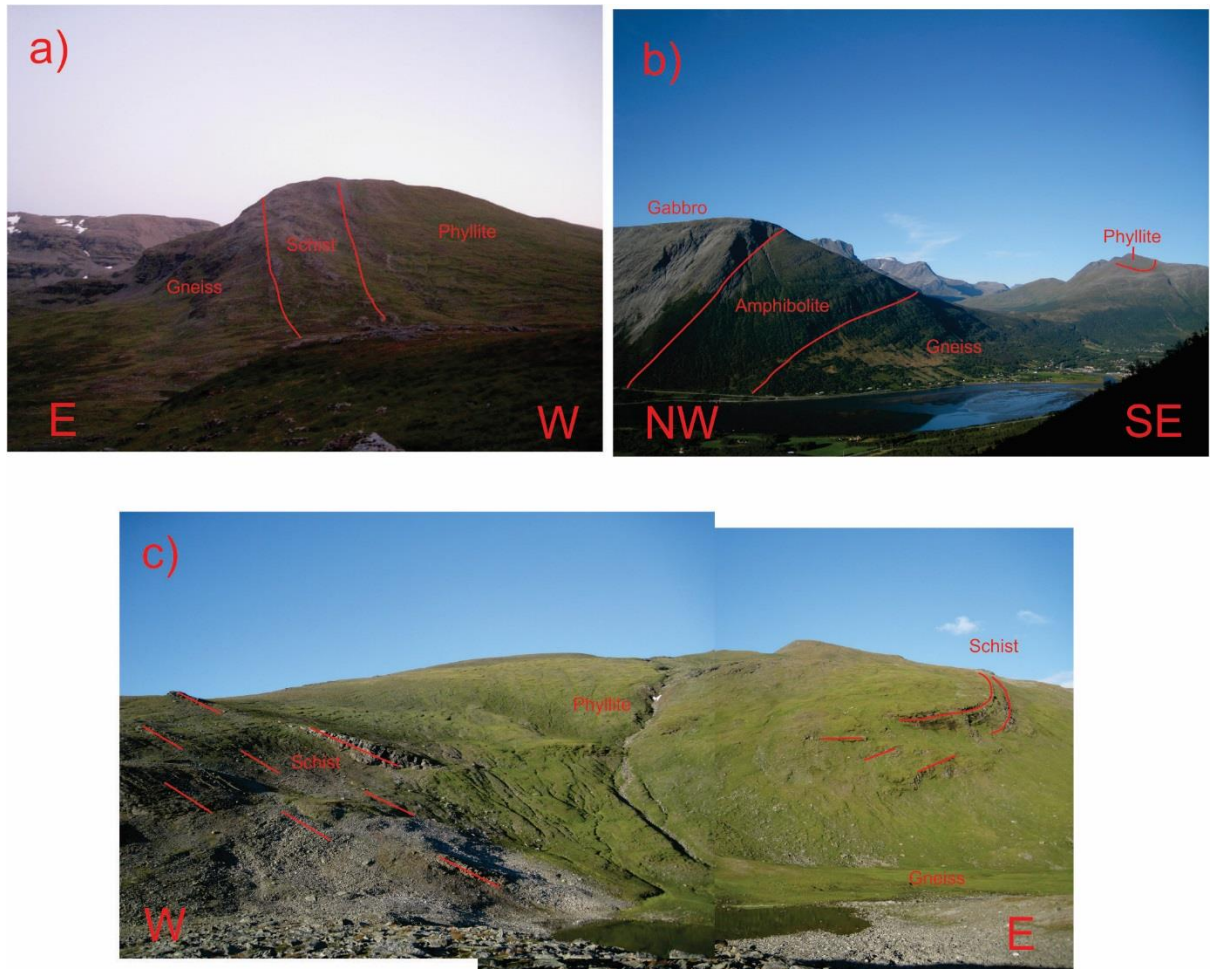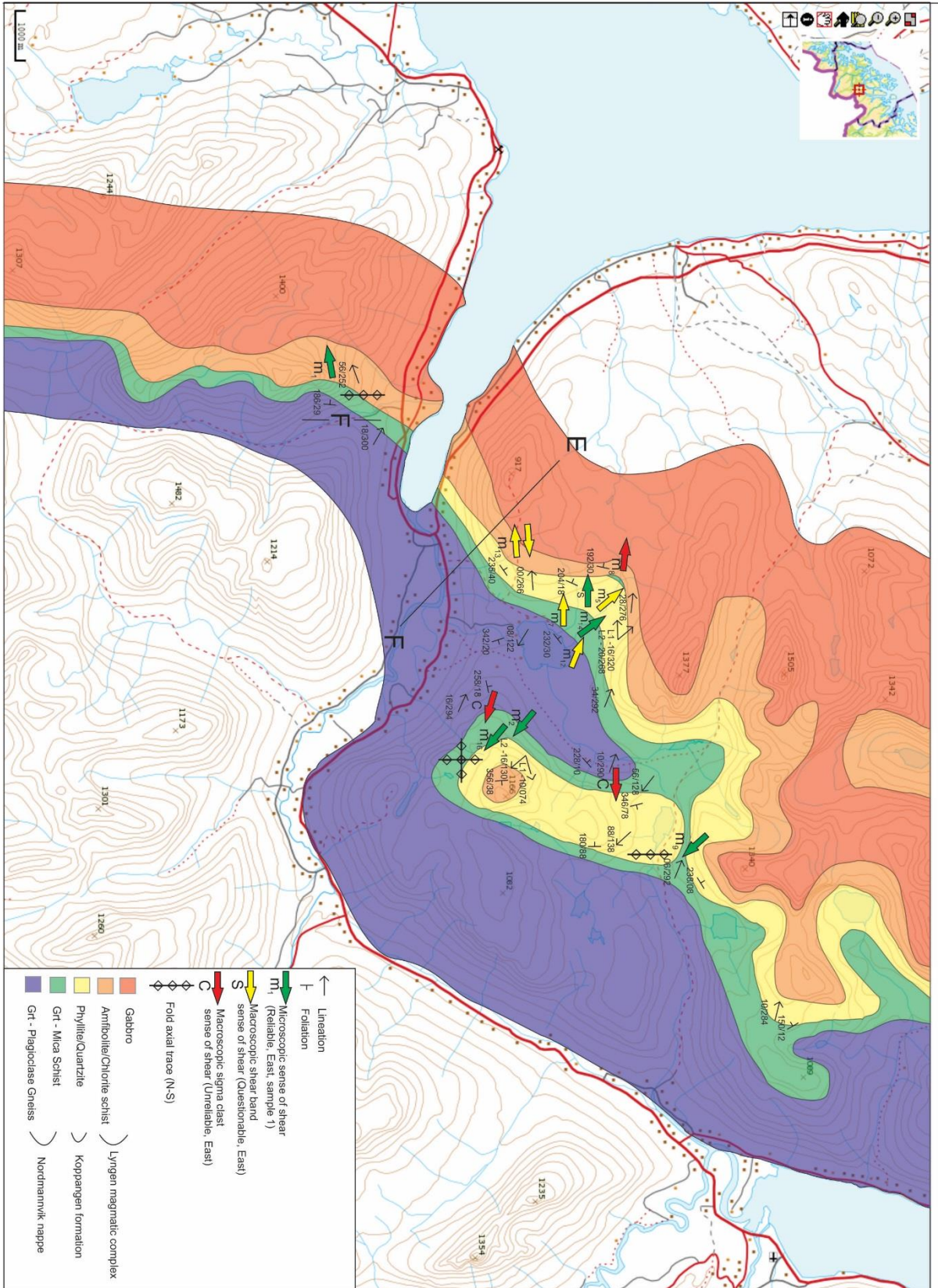

FIGURE 8: CONTINUATION OF FIGURE 1. A) VIEW OF RASSEVARRI LOOKING SOUTH FROM THE SLOPE OF RIEPPETINDEN, SCHIST WITH VERTICAL FOLIATION SEPARATING GNEISS AND PHYLLITES WITH FOLIATION FORMING A SYNFORM. B) VIEW OF PERSTINDEN LOOKING NE FROM NORTH SLOPE OF STORE RUSSETINDEN, GNEISS OVERLAIN BY MOSTLY AMPHIBOLITE, WITH THIN UNITS OF PHYLLITE AND GREENSTONE OVERLAIN BY GABBRO FORMING THE PEAK. C) VIEW OF RASSEVARRI LOOKING NORTH FROM BRENNMOTINDEN, RED STIPPLED LINES MARKING FOLIATION, PHYLLITES FORMING A SYNFORM WITH SCHIST UNDERLAIN BY GNEISS.
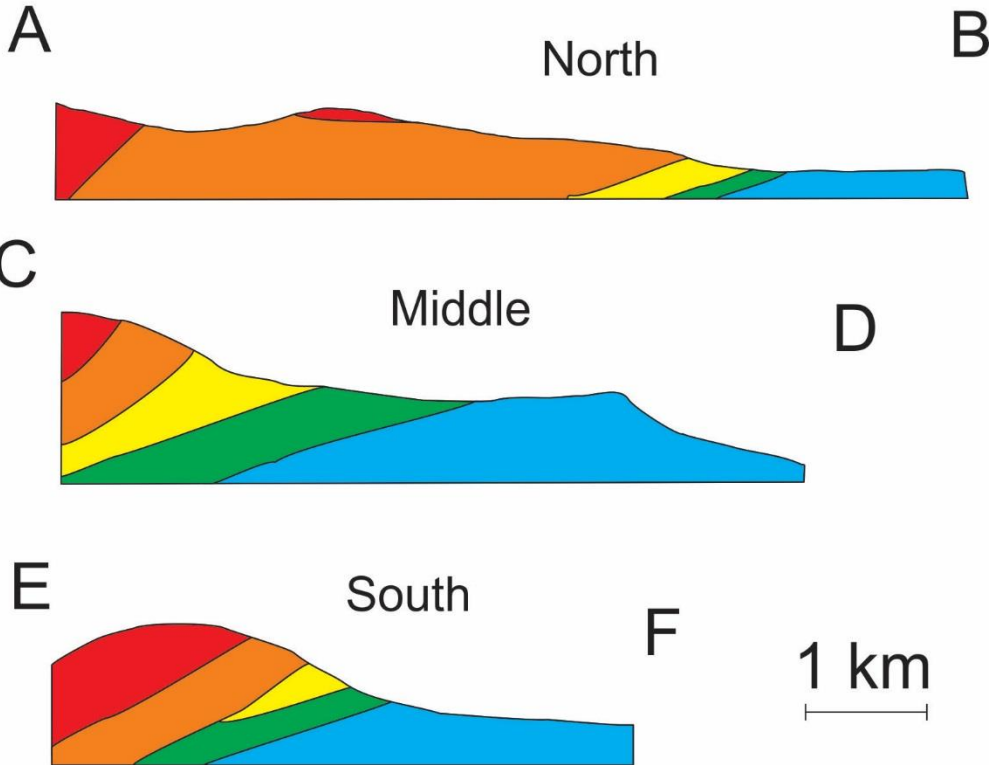
Legend:

↑ Lineation
⊥ Foliation

m$_1$ Microscopic sense of shear (Reliable, East, sample 1)

S Macroscopic shear band sense of shear (Questionable, East)

C Macroscopic sigma clast sense of shear (Unreliable, East)

◇◇◇ C Fold axial trace (N-S)

Gabbro
Amfibolite/Chlorite schist
Phyllite/Quartzite
Grt - Mica Schist
Grt - Plagioclase Gneiss

Lyngen magmatic complex
Koppangen formation
Nordmannvik nappe

1000 m

Profiles

FIGURE 9: PROFILES FROM CROSS SECTIONS MARKED ON THE MAP: RED IS GABBRO, ORANGE IS
GREENSCHIST/AMPHIBOLTE, YELLOW IS PHYLLITE, GREEN IS SCHIST AND BLUE IS NORDMANNVIK. THE UNITS
OF GABBRO AND GREENSCHIST/AMPHIBOLITE ARE STEEPER THAN THE UNDERLAYING PHYLLITE, SCHIST AND
GNEISS MAKING THE PHYLLITE SEEMINGLY TAPER OUT. THE GREENSTONE/AMPHIBOLITE APPEAR THICKER IN
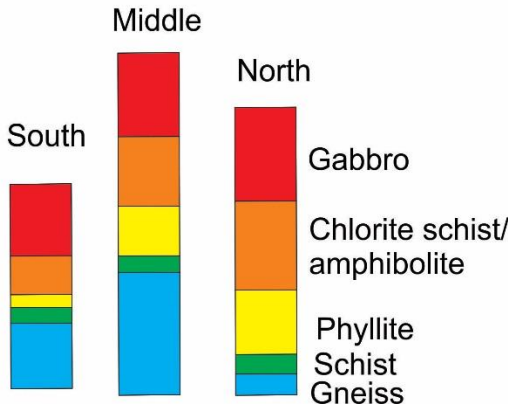THE NORTH THAN THE SOUTH.

Stratigraphic coloumns

FIGURE 10: STRATIGRAPHIC COLUMNS OF THE UNITS ALONG THE EAST LYNGEN ALPS, THE BASE IS SEA LEVEL
AND THE TOP ROUGHLY MARKS THE HEIGHT OF THE PEAKS. THEY INDICATE THAT THE NORDMANNVIK
GNEISS UNIT VARIES ALONG STRIKE OF THE LYNGEN PENINSULA WHILE THE PHYLLITES SEEMS TO TAPER OUT
SOUTHWARD.

Nordmannvik gneiss

Field description
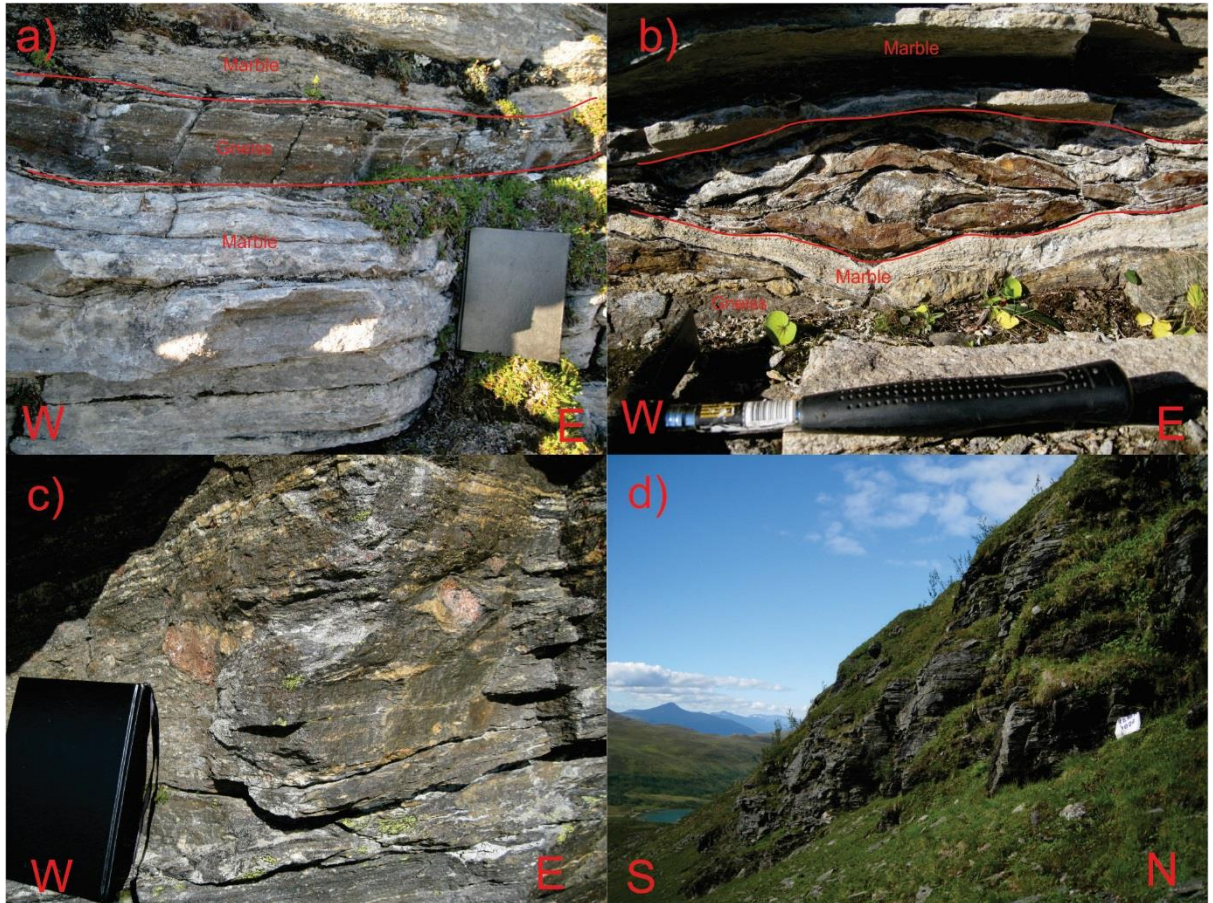
FIGURE 11: NORDMANNVIK GNEISS WITH UNITS OF MARBLE. A) INTERFINGERING LAYERS OF MARBLE AND GNEISS, BOOK FOR SCALE. B) LENS OF UNKNOWN ROCK WITH WHAT APPEAR TO BE A REACTION RING IN MARBLE, HAMMER FOR SCALE. C) GARNET – PLAGIOCLASE GNEISS WITH GARNET SIGMA CLASTS AND A MYLONITIC FOLIATION. BOOK FOR SCALED) OUTCROP OF GARNET-PLAGIOCLASE GNEISS MAKING STEEP OUTCROPS IN THE TERRAIN. WHITE PLASTIC BAG FOR SCALE.

Petrology

The unit is a garnet-mica-plagioclase gneiss of grey to black colour sometimes featuring mm to several cm sized granoblasts of garnets that make a augen texture, sometimes with a rim of plagioclase. It also featured mm sized white trains or layers of plagioclase interpreted to be leucosomes. Mineral content seemed to vary and the gneiss had a distinct alternating layering of garnet and plagioclase rich sections. Some units appeared more weathered than others with a black weathering that suggest carbonates. The garnets appeared vitreous red-purple and could vary a lot in size from a few mm to a diameter at some locations. Inclusions were common and seemed to be of the same material as that of the matrix; mica and plagioclase. Foliation would be folded around the granoblastic garnets and some had tails of mica and/or plagioclase forming sigma clasts. Plagioclase occurred in thin coherent to decoherent layers parallel to foliation that appeared drawn out and sheared folding around

garnets. Black biotite up to a cm in size would make out the foliation, bending around clasts of garnet and plagioclase. When cut open the rock would have a virous sheen. The unit would usually form steep slopes as it appears resistant to erosion, leading rivers along strike. It would have varying weathering of grey, yellow and purple. It would occasionally be very weakly magnetic. A few layers of uniform marble with very coarse grains as well as lenses of amphibolite were observed in the gneiss, these would often form overhangs with the gneiss forming the roof. Toward the contact the gneiss gradually turns into a schist, with the gneiss occurring as lenses before ceasing altogether. Garnet grain size would generally decrease down to a few mm or less. Larger grains seemed to have been fragmented. Layers of plagioclase ceased to be and instead there would be trains of subhedral to euhedral grains a few cm or less in size. In general the rock would look more dull and grey, seemingly losing some of the black biotite. Units of gneiss did occur higher up into the succession, but it is not clear whether it got there as erratics left by glaciers or due to thrusting/folding.

Structures

The gneiss had a distinct mylonitic foliation that became more prominent and closer spaced as you moved up in the succession. It also featured a NW/W lineation (Figure 12b). Several populations of sigma clasts of amphibole and garnet was observed and tended to indicate a SE top sense of shear.
Slickensides (Figure 12a) was observed along a riverbed cutting into the gneiss/greenschist contact where gneiss would be on the east side of the river and greenstone on the west. East of Storvatnet distinct outcrops of gneiss would make meter sized drumlin shaped hill with a West-East orientation.
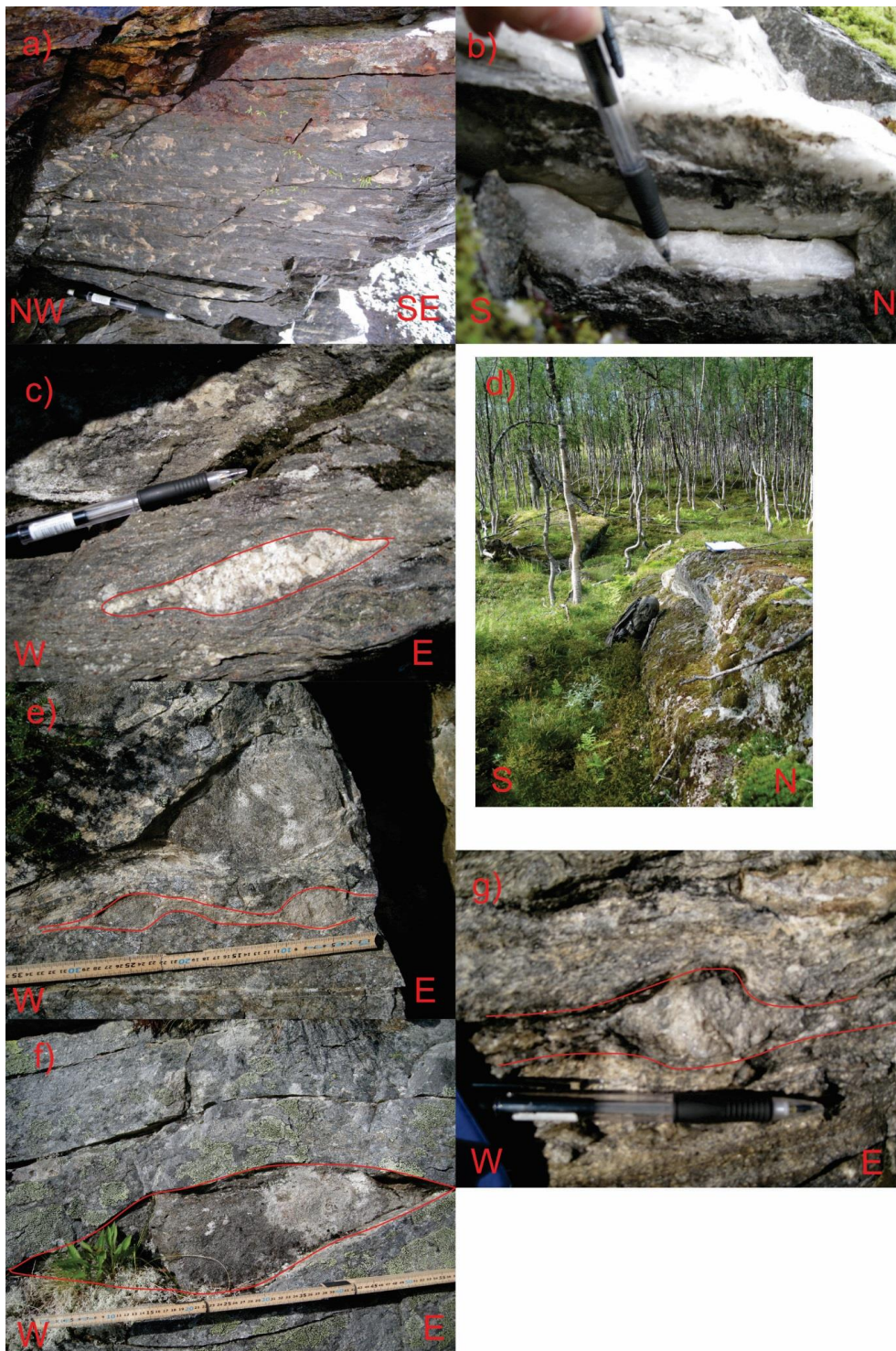
Figure 12: Structures observed in the Nordmannvik unit. a) Slick and slides of possibly epidote on planar surfaces of garnet plagioclase gneiss right by gneiss/greenstone boundary west of Nordkjosbotn. Pen for scale b) Westerly lineation on a lens of quartz, pen for scale. c) sheared lens of plagioclase possibly a sinistral top west sense of shear, pen for scale. d) one of series of west-east elongated outcrop of garnet – plagioclase gneiss, mega lineation? White bag for scale. e) Sigma clasts of amphibolite in mylonitic gneiss interpreted to be dextral roughly top east sense of shear indicators. ruler for scale f) sigma clast of amphibole in mylonitic gneiss interpreted to be roughly top east sense of shear indicator. g) Sigma clast of quartz(/plagioclase in mylonitic gneiss indicated to be rough west sense of shear indicator, pen for scale.

Thin section description

Two thin section were made from this unit. Sample 9 was gathered from a black-white outcrop of garnet-plag-biotite gneiss South of Rieppetinden in the synform. The outcrop lacked the distinct blue-grey colour that the Nordmannvik gneiss tends to exhibit.

Sample 11 was gathered at the East side of Storfjorden, the idea being to gather from an outcrop far from the boundary between Nordmannvik and the Lyngen magmatic complex. The outcrop was a mylonitic gneiss with almost horizontal foliation interspaced with schist by a roadside.

Thin section 9 – Nordmannvik Garnet plagioclase gneiss
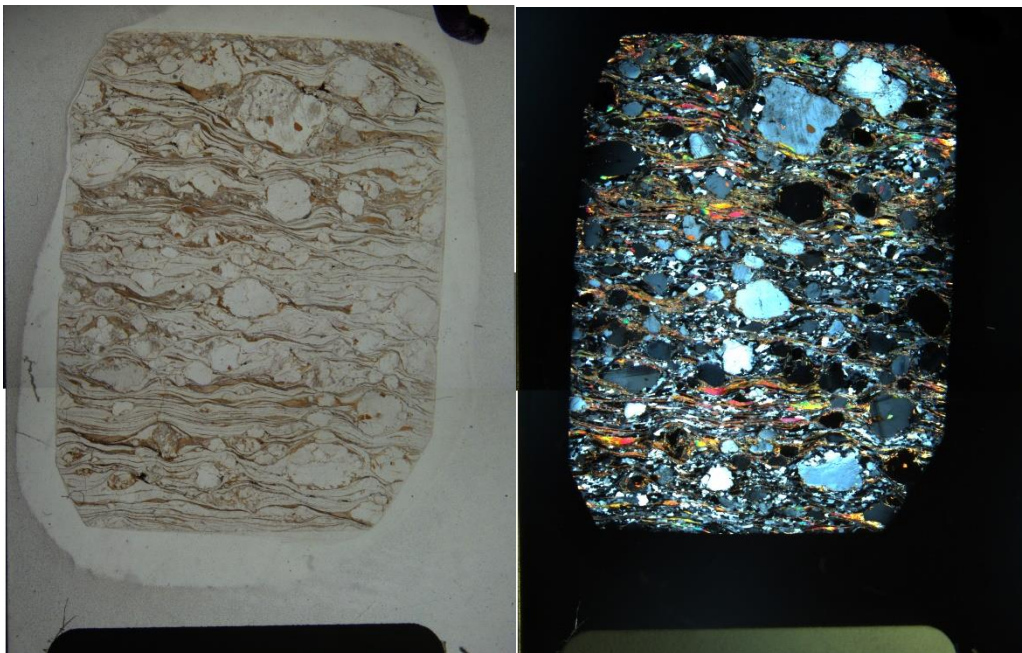
FIGURE 13: THIN SECTION OF SAMPLE 9, PLAGIOCLASE GNEISS FROM SOUTH FLANK OF RIEPPETINDEN. LEFT SIDE IN THIN SECTION IN PLANE POLAR LIGHT, RIGHT IS WITH CROSSED POLARS. VIEW IS ABOUT 5 BY 3 CM. PORPHYROCLASTS OF PLAGIOCLASE IN A FINER GROUNDMASS OF QUARTZ AND BIOTITE.

Minerals: Plagioclase (65 %), quartz (20 %), biotite (15 %), garnet (1 %)

Accessories: Ilmenite, apatite, zircon

Occurence: Quartz appear as small grained matrix with biotite. Plagioclase occurs as porphyroclasts of andesine composition. A bit plagioclase in the matrix, but not much. Garnet is present as a cluster of porphyroclasts.

Description:
Phenocrysts of plagioclase with mostly abrupt extinction, curved grain boundaries, polysynthetic and simple twins, deformation twins and inclusions of biotite occur in a matrix of biotite and quartz. The grains are from 0,4 mm to 2 mm in size and appear rounded with tails of coarse to silt sized grains of muscovite. Ribbons of quartz 25 to 400 micron thick

alternates with ribbons of biotite 10 to 200 microns thick forming a spaced disjunctive foliation. The foliation spacing varies laterally, usually increasing to fold around plagioclase porphyroclasts. Widened biotite ribbons occurs at systemic intervals and in the tails of porphyroclasts forming mica fish. The cleavage domains appear smooth with discrete transitions that are and mostly parallel only joining when encountering porphyroclasts. A few fine to coarse sized garnets occur as aggregate porphyroclasts with plagioclase. These appear with biotite filled cracks and curved grain boundaries. Ilmenite occur as opaques, while zircon appear with halos in the ribbons of biotite.
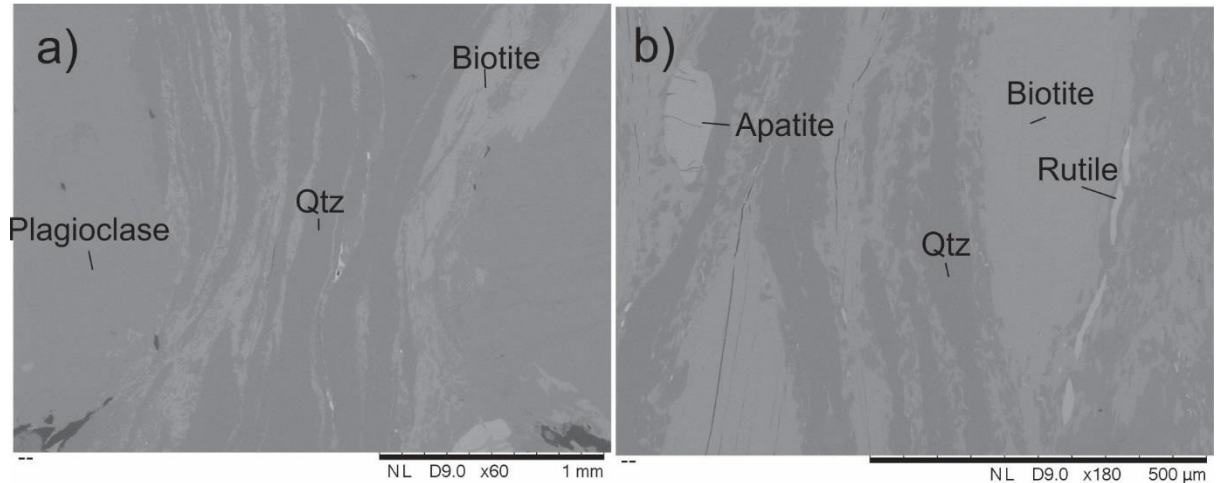
FIGURE 14: BACKSCATTER IMAGES FROM SAMPLE 9 SHOWING BANDS OF MOSTLY DARK QUARTZ (SEEN FROM THE PRESENCE OF MOSTLY SILICON IN EDS) AND LIGHTER BIOTITE FLOWING AROUND PHENOCRYSTS OF PLAGIOCLASE. A SINGLE GRAIN OF APATITE IS VISIBLE AS WELL AS SOME ELONGATED GRAINS OF RUTILE.

EDS data from some of the plagioclase porphyroclasts indicate an andesine composition, while garnets consists of high levels of iron, and some magnesium and calsium suggesting a mixture of Pyrope, Almandine and grossular.

| Plag comp	Na atom C %	Ca atom C %	Al atom C %	Si atom C %		Anorthite %	
1	4,45	2,5	11,4	20,49		35,97122302	Andesine
2	4,47	2,65	11,26	20,87		37,21910112	Andesine
3	4,63	3,38	11,34	20,26		42,19725343	Andesine

FIGURE 15: DATA FROM EDS OF SOME OF THE PLAGIOCLASE GRAINS IN SAMPLE 9. THE NUMBERS INDICATE MOLE PERCENTAGE OF PRESENT ELEMENTS IN ANALYSED AREA. THE RATIO BETWEEN SODIUM AND CALCIUM DETERMINE THE MEMBER OF PLAGIOCLASE WHICH MIGHT BE ANDESINE IN THIS CASE.

| garn comp	Na atom C %	Ca atom C %	Al atom C %	Si atom C %	Fe atom C %	Mg atom C %
1	0	2,59	8,61	14,64	9,44	3,51
2	0	2,06	7,7	14,09	10,52	2,19

FIGURE 16: EDS DATA FROM SOME OF THE GARNETS IN SAMPLE 9. ELEVATED CONTENT OF IRON, SLIGHTLY LOW CONTENT OF ALUMINIUM AND NO MANGANESE COMPARED TO GARNETS FROM OTHER SAMPLES.

Structures:
Dextral lenticular shaped mica fish with recrystallized rims was observed in the optical microscope along with S-C' fabric outlined by the mica foliation and the porphyroclasts of plagioclase. These shear bands had was at 20-30 degree angle to lineation and was consistently dextral.
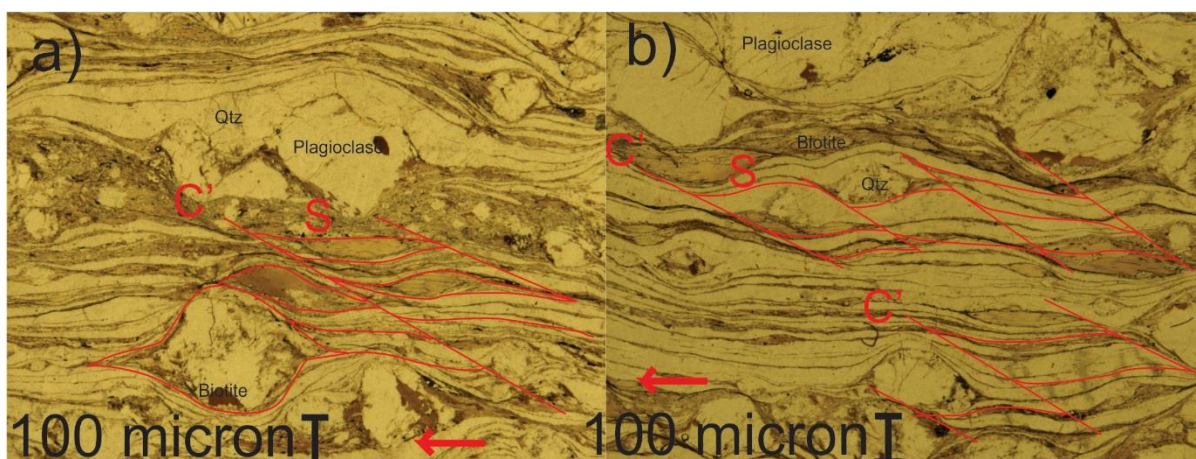
FIGURE 17: SENSE OF SHEAR INDICATOR IN SAMPLE 9. RED MARKINGS INDICATE S-PLANES AND C' PLANES. A) LENTICULAR GRAINS OF MICA INDICATING THE PRESENCE OF SHEAR BANDS AND A S-C' FABRICS. SHEAR PLANES SEEM TO FOLLOW EDGE OF PLAGIOCLASE PHENOCRYSTS. INTERPRETED TO INDICATE A DEXTRAL SENSE OF SHEAR. B) SIMILAR TO A) AT ANOTHER LOCATION. HERE SMALL LENSES OF QUARTZ ALSO OUTLINE THE S-C' FABRIC, ALSO DEXTRAL SENSE OF SHEAR.
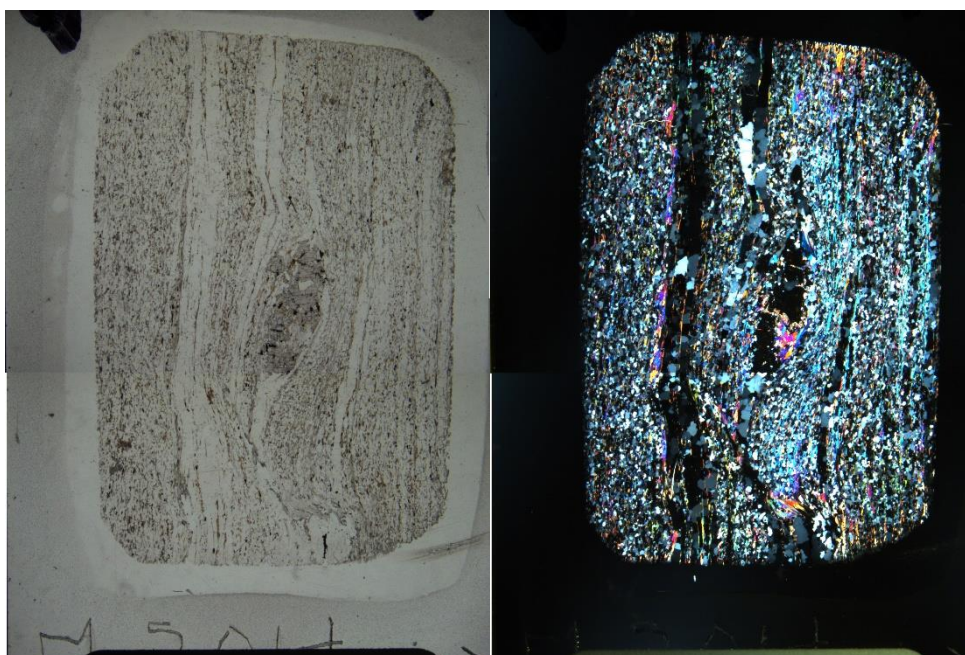
FIGURE 18: OVERVIEW OF THIN SECTION SAMPLE 11, LEFT IN PLANE POLAR LIGHT, RIGHT WITH CROSSED POLARS. BANDS OF QUARTZ SHOW UNIFORM EXTINCTION AND OUTLINES AN ALMOST SHEAR-BAND LOOKING FABRIC. PORPHYROCLAST OF GARNET IN CENTRE INTERPRETED TO INDICATE A SINISTRAL SENSE OF SHEAR FORMING A SIGMA/DELTA CLAST. FIELD OF VIEW ABOUT 5 BY 3 CM.

Minerals: Quartz (60 %), muscovite (10 %), biotite (10 %), chlorite (5 %), garnet (5 %), ilmenite (3 %), pyrite (3 %), calcite (2 %), titanite (1 %), plagioclase (1 %)

Accessories: rutile, zircon, apatite, tourmaline

Occurrence: Matrix of mostly quartz, muscovite and biotite with lesser amounts of chlorite. Bands of quartz run parallel to lineation. A few grains of Ca-Na plagioclase are observed in the matrix. Large titanite crystals occur in the garnet.

Description:
 A single porphyroclast of a 2mm in diameter wide garnet occur in a matrix of quartz, mica and chlorite. The garnet is elongated obliquely to foliation and feature inclusion of coarse anhedral titanite, euhedral rutile, zircon and anhedral quartz. Grains of opaque sulphides grow around the garnet edge and cracks are filled with fine muscovite, chlorite and quartz. Muscovite, biotite and chlorite form a spaced foliation, separated by 0,6 mm thick ribbons of quartz. Overall the mica, chlorite foliation make up about 80 % of the area with the quartz ribbons being mainly grouped into discrete parallel bands running from one edge of the thin section to the other. Quartz ribbons also make up the tails of the garnet porphyroclast. Muscovite grain size varies, with alternate larger and smaller grain sizes when traversing perpendicular to foliation (0,1 to 1 mm long respectively with only slight variation in thickness). A third grouping of muscovite grain sizes can be observed in the garnets shadow zone, here the muscovite is oriented at an angle to the foliation and tend to be of a lower aspect ratio than the muscovite in the surrounding matrix. There is also a fine-grained matte of muscovite running around one of the garnet fragments and seemingly nowhere else. Biotite is found intermingled with the muscovite, but tend to be of smaller size and stubbier.

Less biotite is also to be found around the garnet. Biotite also alternates in grain size when traversing perpendicular to lineation, but not necessarily in synchronization with the muscovite.

Chlorite is situated in the garnet cracks, but is most commononly associated with the large bands of muscovite. They tend to form mica fish shaped aggregates of up to 0,2 mm wide elongated parallel to foliation when in the muscovite bands. When found in the matrix they have a more columnar habit and can contain zircon visible by pleochroic halos. Some crystals can be seen to grow across the foliation.

The distribution of ilmenite is not clear, but they tend to be elongated along lineation, cluster around the edge of the garnet and in bands parallel to foliation. They do occur less in the quartz ribbons.

Calcite occur in the mica-chlorite foliation as small fine euhedral grains and in the garnet pressure shadow. There is a local concentration located by what appear to be a small microscopic fold with fold axis perpendicular to lineation.

A few grains of albite have been observed in the SEM, but seems to be missing otherwise.

Structures:

Overall the garnet and fabric of the thin section suggests a sinistral macro size shear band. The single garnet can be interpreted to be a sinistral delta clast. Shear bands were observed, both dextral and sinistral. The sinistral S-C' fabric had C-planes 20-25 degrees to lineation while the dextral S-C' fabric measured around 30 degrees. Only sinistral S-C fabric was observed, thus the overall conclusion of a sinistral sense of shear.
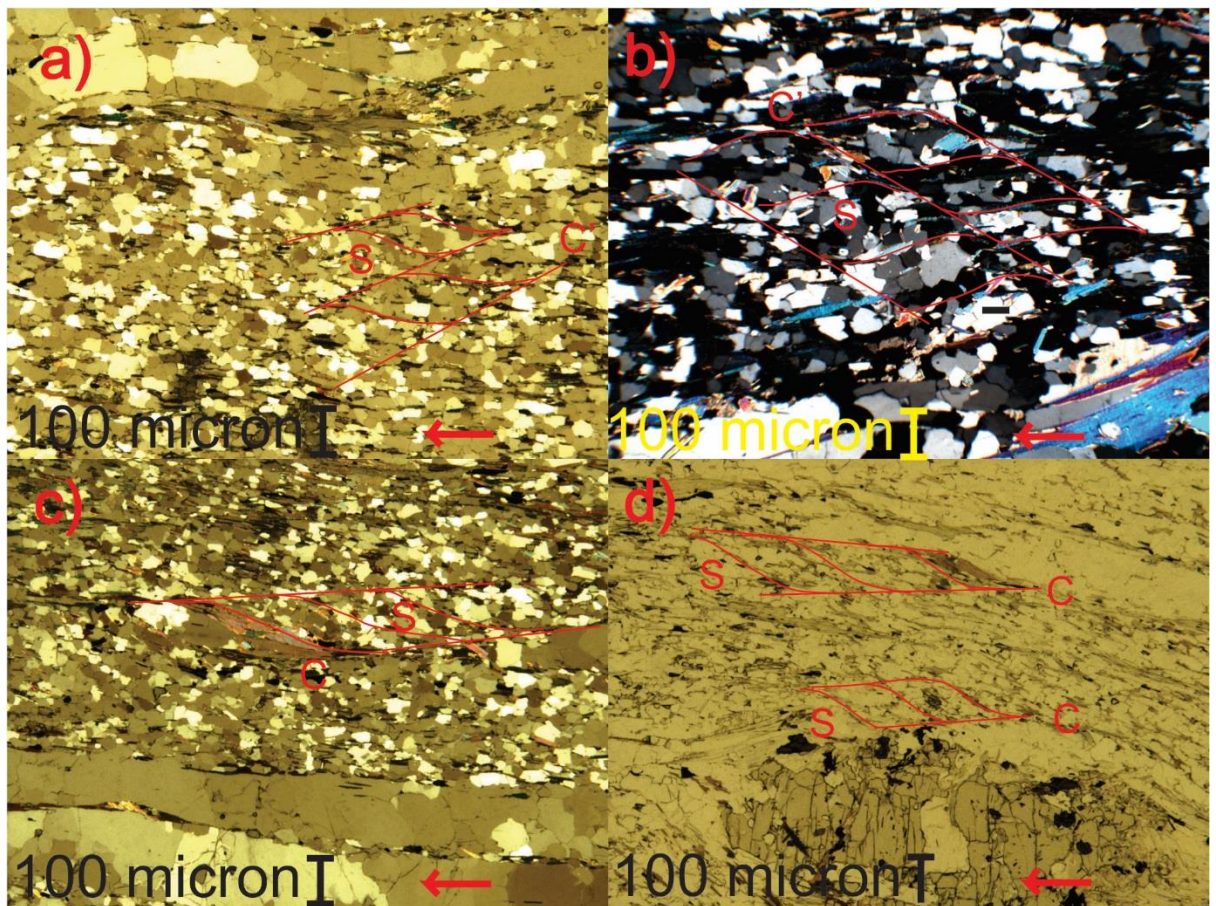
FIGURE 19: OVERVIEW OF SENSE OF SHEAR STRUCTURES IN SAMPLE 11. D) IS PPL WHILE THE OTHER THREE IMAGES ARE XPL. A) SHOW SINISTRAL S-C' FABRIC. B) SHOW DEXTRAL S-C' FABRIC. C) AND D) SHOW SINISTRAL S-C FABRIC.

Quartz sample description

Sample 11 was gathered from a quartz lens at a marble quarry South of Furuflaten just before the Nordmannvik unit dipped below sea level. The outcrop featured two lineations and was white-black in colour due to biotite, again lacking the grey-blue colour normal to Nordmannvik gneiss.

Thin section 3 – Nordmannvik, Quartz sample from a garnet biotite gneiss
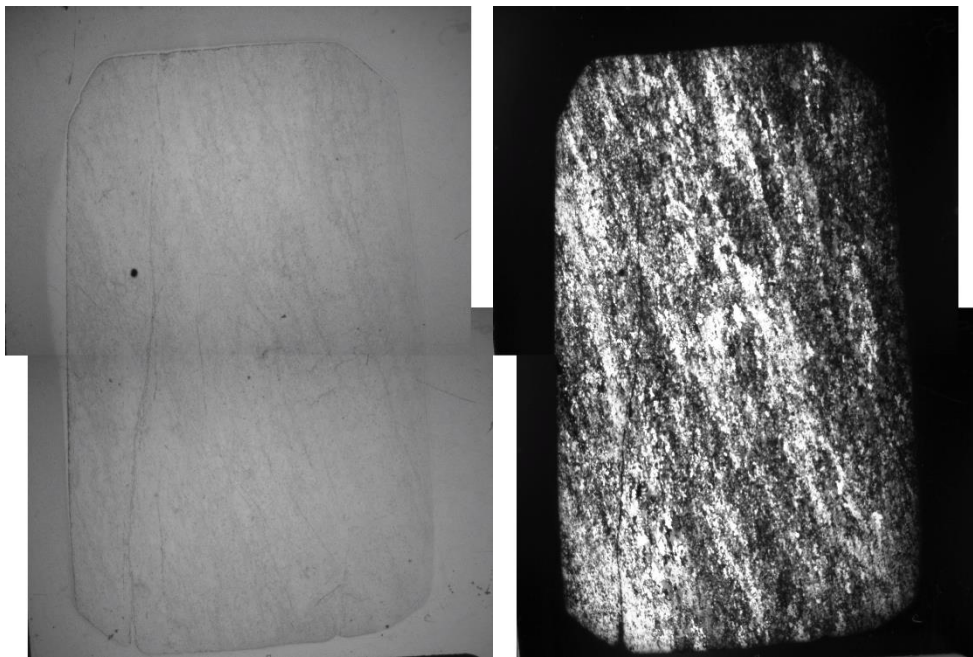
FIGURE 20: SAMPLE 3 IN PPL TO THE LEFT, XPL TO THE RIGHT. FIELD OF VIEW IS ABOUT 3 BY 5 CM. PPL SHOW THE PRESENCE OF TINY CRACKS CRISS-CROSSING THE SAMPLE. RIGHT SHOW DOMAINS OF EXTINCT QUARTZ RUNNING DIAGONALLY ALONG THE THIN SECTION.

Description:

Anhedral mostly equigranular grains of quartz with round to straight grain boundaries form grains of 25-50 microns in size. They exhibit slight elongation at an angle to lineation and a wave like extinction running across the thin section as can be seen in Figure 20. Some larger relict grains are present. Deformation mechanism is interpreted to be mainly by sub grain rotation due to small grain size, varying extinction and rounded grain boundaries. Most of the grains exhibit max birefringence, perhaps suggesting that the sample might have been cut normal to actual lineation.
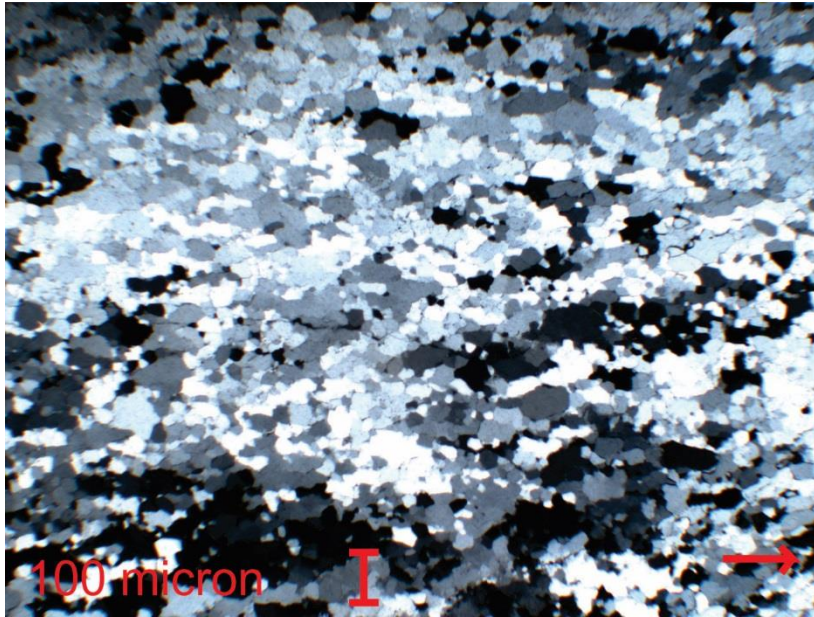
FIGURE 21: AREA OF SAMPLE 3 UNDER XPL. ROUNDED GRAINS AND A WIDE VARIETY OF EXTINCTIONS WITH DIAMETERS OF AROUND 25-50 MICRON INDICATE SUB-GRAIN ROTATION AS DOMINANT RECRYSTALLIZATION MECHANISM.

Nordmannvik Schist

Field description

FIGURE 22: GARNET MICA SCHIST. A) WEST PLUNGING ASYMMETRICAL FOLDED MICA SCHIST, LOOKING NORTH ALONG HINGE. BAG FOR SCALE. B) CLOSE-UP OF MICA GARNET SCHIST AT A FOLD LIMB. C) FOLDED MICA SCHIST, LOOKING WEST ALONG SOUTH DIPPING FOLD HINGE.

Petrology

The garnet-plagioclase mica schist had a grey sheening colour and rounded garnets that would fold the foliation. It would be easily weathered and form depressions between the harder underlying gneiss and the overlaying phyllites marked by small North-South running lakes and streams. Mineralogically it could be similar to the gneiss with porphyroclasts of garnet with mica forming the foliation. Garnets could however be black, more spars and more rounded and be a few mm or less in diameter. There could also be mm sized grains of amphibole elongated parallel to lineation and lenses of quartz. Foliation would be of varying proportions between fine to coarse biotite and sericite. It would at places be interfingering with phyllites making it hard to distinguish between the two units. South of Nordkjosbotn it would appear as lenses above the chlorite schist. Here it would feature very coarse amphibole grains elongated parallel to lineation. Plagioclase would form mm wide bands

folding around medium to very coarse garnets. Marble occurred as thin layers of coarse to granular grains interlayered with quartzite.

Structures

The unit was easily eroded and thus featured few outcrops. It did however feature some sigma clasts and a few folds. The most prominent being the folds shown in Figure 22. At this location (Brennmotinden) there was a set of perpendicular folds. One set features a N-S axial trace while the second set featured a W-E axial trace. The N-S axial trace dipped gently north, was asymmetrical with steep east limb dipping 40-70 degrees and a gentle west limb dipping 20-30 degrees. The single fold with a W-E axial trace plunged 10 degrees to the west and was roughly symmetrical with limbs dipping 20-30 degrees.
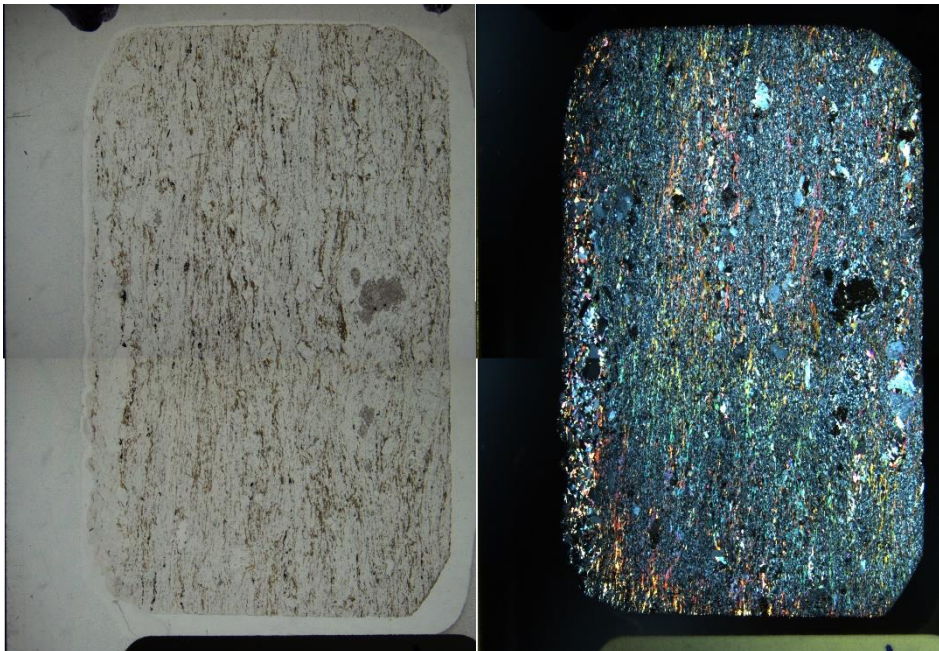
Thin section description

Three thin sections were taken from this unit.

Sample 7 and 12 was gathered along a river that fed Storvatnet from the west.

Sample 16 was gathered from a garnet-plagioclase mylonite, being the host rock of sample 2.

### Thin section 7 – Nordmannvik Biotite Garnet Schist

FIGURE 23: OVERVIEW OF SAMPLE 7, PPL TO THE LEFT, XPL TO THE RIGHT. PORPHYROCLASTS OF PLAGIOCLASE IN A WAVY GROUNDMASS OF BIOTITE, PLAGIOCLASE AND SOME QUARTZ.

Minerals: Plagioclase (60 %), biotite (15 %), quartz (10 %), calcite (5 %), garnet (5 %), ilmenite (4 %), muscovite (1 %)

Accessories: Rutile, apatite, zircon, tourmaline

Occurrence: Porphyroclasts of plagioclase and garnet with tails of calcite and biotite occur in a matrix of albite, biotite, quartz, calcite and a few grains of muscovite.
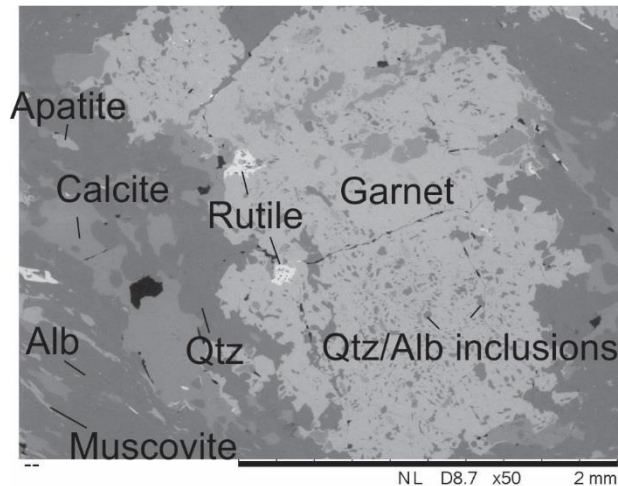
FIGURE 24: BACKSCATTER PICTURE OF GARNET GRAIN SEEN TO THE RIGHT IN FIGURE 17 AS BLACK EXTINCT GRAIN UNDER XPL. FRACTURED POIKILOBLAST OF GARNET WITH INCLUSIONS OF QUARTZ, ALBITE AND SOME GRAINS OF RUTILE. GROUNDMASS OF MOSTLY ALBITE AND MUSCOVITE WITH SOME QUARTZ.

Description:
 The sample has a continuous foliation of small grains of biotite (ranging from less than 2 microns up to 200 microns in length). A coarser grained microlithon of plagioclase, quartz and calcite is visible at the left edge of thin section.

Mylonitic section: Porphyroclasts of plagioclase with a diameter of around 600 microns and less occur with varying aspect ratios depending on orientation to foliation, with the largest aspect ratios occurring when clasts are oriented parallel to foliation length-wise. Most porphyroclasts of plagioclase are oriented with the diagonal at 45 degrees to foliation. The plagioclase porphyroclasts feature polysynthetic twins, simple twins, undulatory extinction and tapering deformation lamellae. Some of the plagioclase porphyroclasts feature inclusions of biotite and muscovite, sometimes arranged as straight lines of disconnected inclusions. A line of plagioclase porphyroclasts appear to have been broken up from on single grain in a brittle way, being separated by cement of calcite. Most of the plagioclase porphyroclasts show serrated grain boundaries with subgrains similar in size to the grains in the matrix. Garnet appear as porphyroclasts with inclusions of calcite, quartz and ilmenite. They appear in a line parallel to foliation with one big garnet followed by several small. Quartz and albite occur in the matrix in unknown proportion with grain sizes of around 2 microns. The proportion between albite/quartz and biotite varies in the matrix; with some areas having a higher biotite proportion while other have a higher quartz/albite proportion. High biotite proportion areas can occur as tails of porphyroclasts or as distinct bands crossing diagonally across foliation. Some of the biotite grains in these bands show undulatory extinction and they are slightly bent.

Microlithon: In the microlithon the plagioclase grain population is larger; up to 800 microns in diameter, featuring simple twins, some undulatory extinction, deformation lamellae and inclusions of muscovite. The plagioclase occurs in a matrix of albite and quartz with a grain size of around 50 microns. There is some biotite, but overall less than in the mylonitic part of the thin section.

A single garnet was analysed with EDS showing presence of manganese, iron and calcite.

gar comp	Na atom C %	Ca atom C %	Al atom C %	Si atom C %	Fe atom C %	Mg atom C %	Mn atom C %
	0	5,19	7,84	14,49	7,77	0	2,21

FIGURE 25: EDS DATA FROM A SINGLE GARNET IN SAMPLE 7.

Structures: Dextral sigma- and delta-clasts of feldspar and garnet. Weak dextral S-C' fabric outlined by mica as shown in Figure 26a as well as sinistral S-C' fabric was observed. Sinistral S-C' fabric tends to have a C-plane aligned 20 degrees to horizontal while the dextral C-planes vary from 30 to 40 degrees. Overall the sense of shear is determined to be dextral due to most shear bands being dextral as depicted in Figure 27.
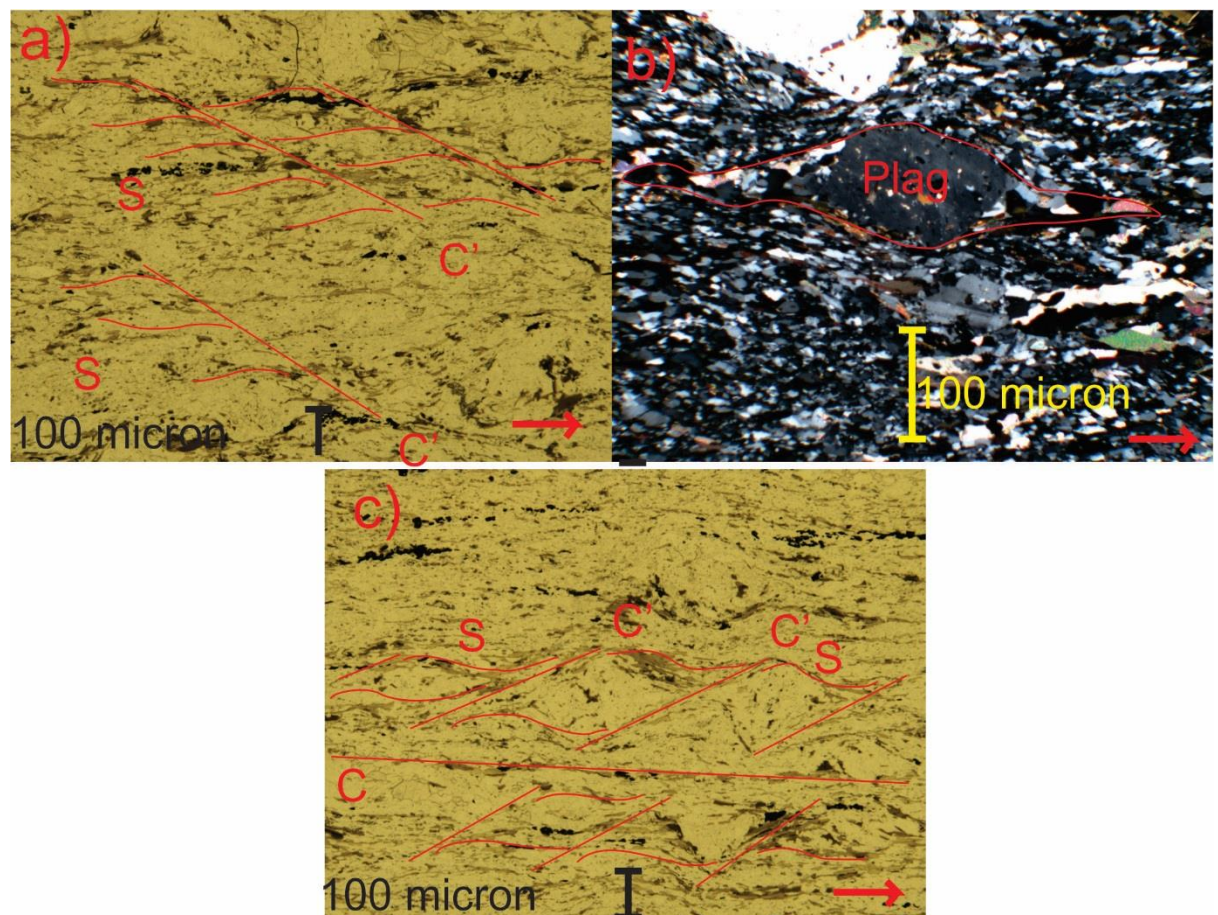
FIGURE 26: OVERVIEW OF SENSE OF SHEAR INDICATORS IN SAMPLE 7. RED MARKINGS INDICATE C/C'-PLANES AND S-PLANES. A) PPL, WEAK DEXTRAL S-C' FABRIC INDICATED BY LENTICULAR SHAPED MICA AND WAVY DOMAINS IN FOLIATION. B) XPL, PORPHYROCLAST OF PLAGIOCLASE FORMING A DEXTRAL DELTA CLAST WITH TAILS MARKING THE PRESENCE OF SHEAR BANDS. C) AND D) PPL, TWO POSSIBLE INTERPRETATIONS OF SHEAR BANDS ALONG THE EDGES OF A SHEARED PORPHYROCLAST OF PLAGIOCLASE. C) INDICATE A SINISTRAL S-C' FABRIC WHILE D) INDICATE A DEXTRAL S-C FABRIC.
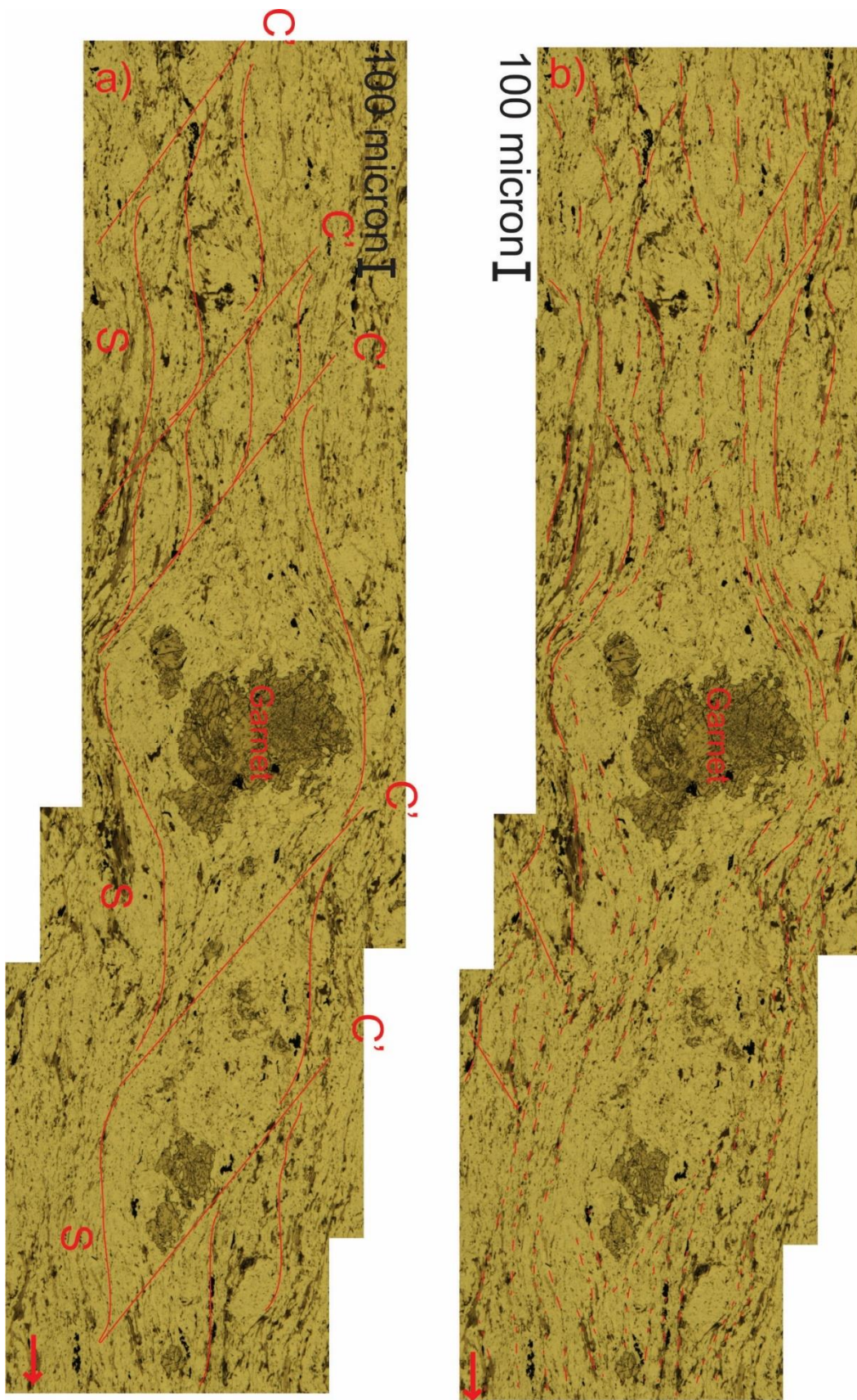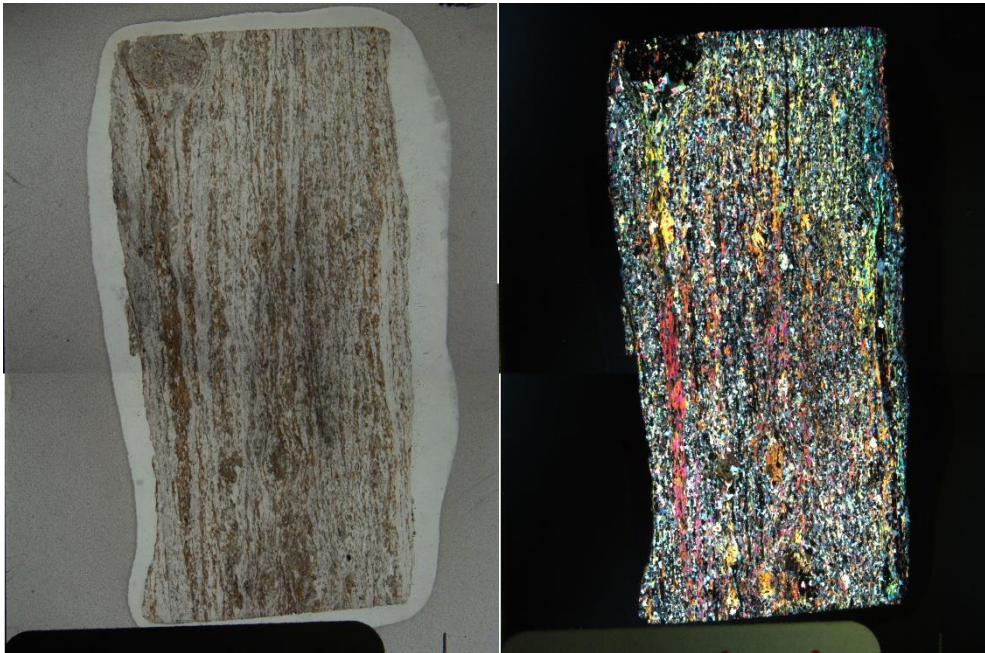
FIGURE 27: SAMPLE 7 COMPOSITE PPL PICTURES. LINEATION MARKED BY RED ARROW. RIGHT PICTURE SHOW MARKED FOLIATION AS IT FOLDS AROUND PORPHYROCLASTS OF GARNET. LEFT IMAGE SHOW

## Thin section 12 – Nordmannvik Garnet mica schist

FIGURE 28: OVERVIEW OF SAMPLE 12, PPL TO THE LEFT, XPL TO THE RIGHT. FIELD OF VIEW ABOUT 5 BY 3 CM. DOMAINS OF BIOTITE AND QUARTZ VISIBLE RUNNING PARALLEL TO LINEATION CURVING AROUND GRAINS OF AMPHIBOLE.

Minerals: Quartz (30 %), biotite 25 %), Hornblende (20 %, distinguished by actinolite by aluminium content), plagioclase (10 %), calcite (10 %), garnet (5 %)

Accessories: Apatite, rutile, titanite, zircon, tourmaline

Occurrence: Some segregation into bands of biotite, plagioclase, quartz and calcite. Porphyroclasts of garnet and grains of amphibole with tails of biotite and calcite. Biotite sub parallel with foliation.
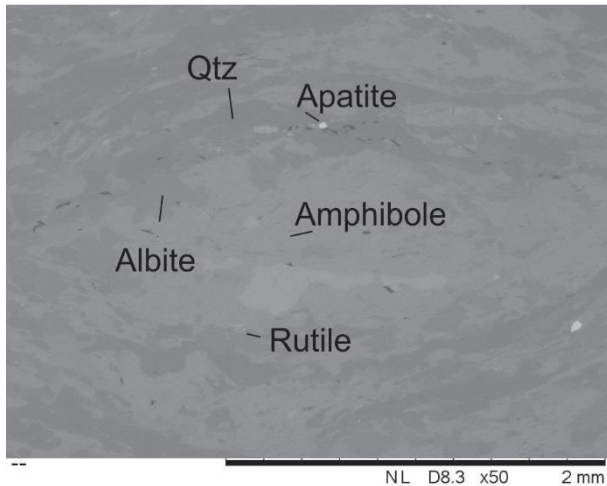
FIGURE 29: BACKSCATTER PICTURE OF SAMPLE 12. A GRAIN OF AMPHIBOLE SURROUNDED BY ALBITE AND QUARTZ. THE AMPHIBOLE MIGHT SHOW SOME ZONING INDICATED BY THE LIGHTER SIGMA SHAPED AREA SURROUNDED BY DARKER AMPHIBOLE.

Description:

Biotite and grains of amphibole form a spaced cleavage with domains characterized by the biotite to quartz and calcite ratio. The transition between the domains are gradual and the domains are anastomosing and vary laterally relative to lineation. There is always a few grains of quartz or biotite in the alternating domains, but calcite disappear in the most quartz and biotite rich domains. The thickest most biotite rich domain, with almost only biotite, is connected to the tail of a garnet porphyroclast.

Biotite occur oriented sub parallel to lineation, locally folding and bending around grains of hornblende. Size vary according to domain; from tens of microns to a few mm, with the larger grain sizes occurring in the biotite rich domains. Inclusions of zircon is common.

Hornblende appears as clasts up to 1 mm in diameter and as smaller fine fragments in the matrix. The clasts are anhedral, sometimes forming aggregates with elongated grains of garnet. They are ubiquitously cracked with mortar of biotite and plagioclase. The clasts are either tilted with the diagonal running parallel to lineation or elongated parallel to lineation. They tend to have tails of calcite and biotite, with calcite tapering out forming a pressure shadow. Some grains are observed to grow across foliation without bending it. Grains of titanite can be observed along the edges of some of the hornblende porphyroclasts.

Plagioclase occur with polysynthetic and simple twins, not clear if they are deformation twins. They occur as rounded subhedral grains up to 0,5 mm in diameter, some with undulatory extinction. Plagioclase also appear as a constituent in hornblende-plagioclase porphyroclast aggregates and as inclusions in garnet and hornblende.

Quartz occur in the matrix as very fine anhedral grains with curved grain boundaries showing no undulatory extinction. A few bands of quartz occur with grains of about 0,2 mm wide elongated parallel to lineation and with boundaries pinned by biotite.

calcite occur as anhedral grains varying in size from ten of microns to hundreds. Grain size is largest when situated in a pressure shadow of garnet or hornblende. In the matrix calcite forms gradual alternating bands with biotite.

Garnet occur as a single 3 mm in diameter porphyroclast and as smaller elongated aggregates with hornblende. The single porphyroclast is ubiquitously cracked with Inclusions of amphibole, biotite, calcite, plagioclase, titanite and tourmaline. It has a strain shadow of mainly calcite and some garnet fragments.

Structures:

Dextral and sinistral sigma clasts of plagioclase and hornblende was observed along with dextral S-C' fabric (Figure 30) that formed C-planes 30 degrees to lineation indicating an overall dextral sense of shear.
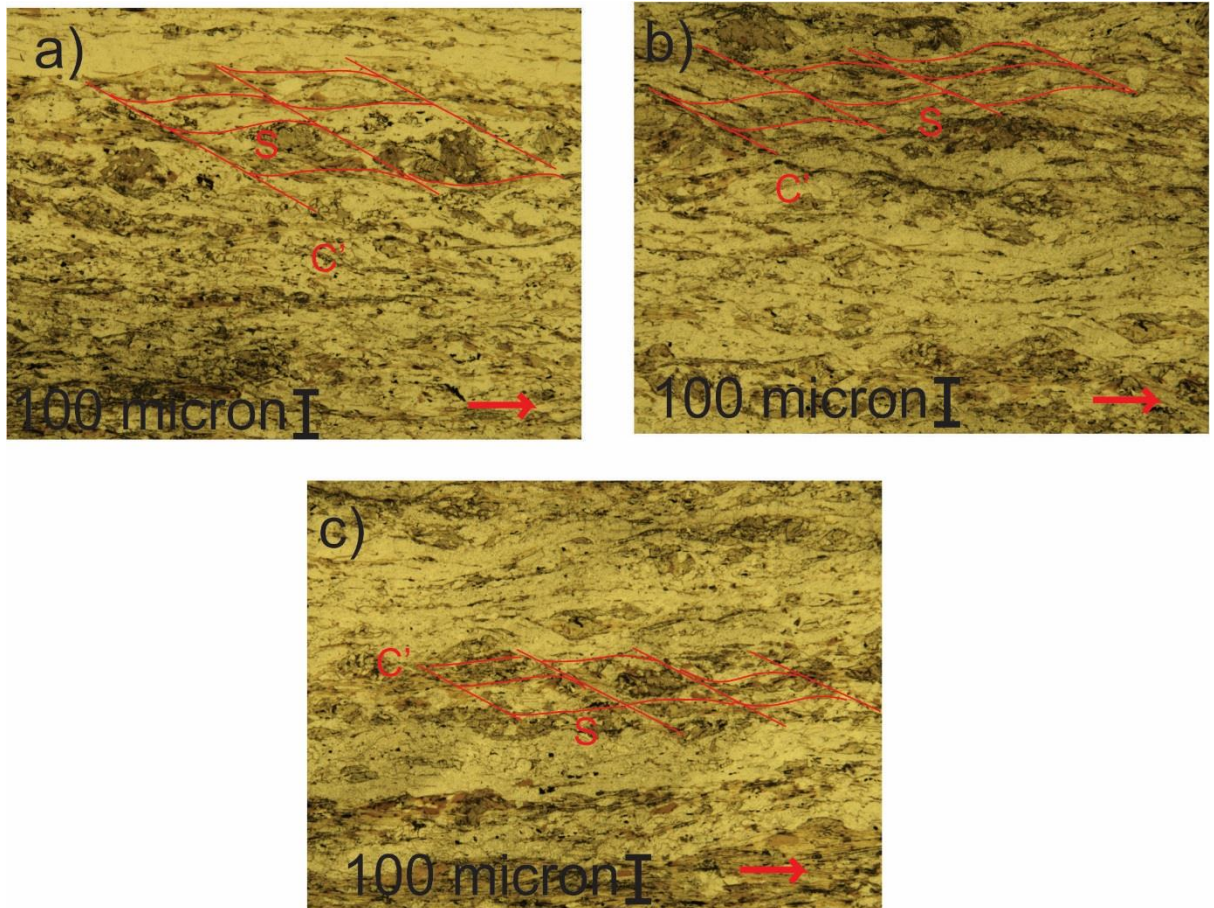
FIGURE 30: SENSE OF SHEAR STRUCTURES IN SAMPLE 12, ALL IN PPL. A)DEXTRAL S-C' FABRIC MARKED BY EDGES OF SHEARED AMPHIBOLE GRAINS. B) DEXTRAL S-C' FABRIC INDICATED BY ALIGNED BIOTITE GRAINS. C) AND D) TWO POSSIBLE INTERPRETATIONS OF SAME STRUCTURE. C) DEXTRAL S-C' FABRIC INDICATED BY THE WAVY FABRIC, FOLDED BIOTITE FOLIATION AND EDGES OF AMPHIBOLE GRAINS. D) SINISTRAL S-C FABRIC INDICATED BY THE PARALLEL TO FOLIATION SHEAR BANDS AND SHEARED AMPHIBOLE GRAINS INDICATING THE S-PLANE.

Thin section 16 – Koppangen phyllite

FIGURE 31: OVERVIEW OF SAMPLE 16 THIN SECTION. LEFT IS PPL, RIGHT IS XPL, FIELD OF VIEW IS 3 BY 5 CM. LINEATION IS VERTICAL. FOLIATION IS VISIBLE AS VERTICAL DOMAINS OF QUARTZ OR DARKER MINERALS. XPL SHOW PATTERNED EXTINCTION.

Minerals: Quartz (60 %), muscovite (20 %), opaques (10 %), biotite (5 %), chlorite (5 %)

Accessories: Rutile, titanite

Occurrence: Layers of differing mineral content. A few quartz-only layers alternating with sections with quartz and mostly muscovite and some layers with mostly muscovite. Chlorite appear with muscovite while single grains of biotite occur throughout.
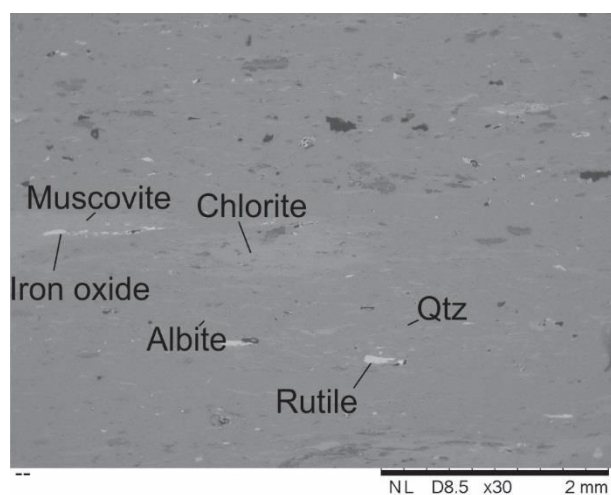
FIGURE 32: BSE IMAGE OF SAMPLE 16. LINEATION IS HORIZONTAL. MOSTLY QUARTZ VISIBLE WITH SOME CHLORITE AND MUSCOVITE.

Description:

Muscovite forms a spaced foliation with biotite and chlorite. The cleavage domains occupy about 90 % of the area, alternating sharply with 0,2 mm thick bands of quartz. In these, muscovite occur as 50 micron or less tabular shaped grains spread out evenly in the matrix. Some variation in concentration occur evident by thin ribbons of higher muscovite proportions than the rest of the matrix.

Biotite occur through the thin section as single tabular to stubby grains 50 to 200 microns wide floating in the matrix usually elongated parallel to lineation. The smallest grain sizes tend to be concentrated along the edges of the quartz ribbons.

Chlorite occurs as 0,3 mm thick aggregates of fibrous grains regularly distributed through the thin section. It tends to form disconnected layers parallel to lineation and tend to be associated with muscovite. It has a yellow discolouring and is associated with rutile and titanite at some locations, but this might be coincidental.

Opaque minerals occur serially from 50 to 300 microns wide anhedral to subhedral tabular shaped grains distributed through the thin section, but also appear enriched in a few discreet bands.

Quartz occurs serially from 20 to 100 microns wide anhedral grains when in the mica rich domains. Grains in ribbons tend to range between 100 and 500 microns in size. Boundaries tend to be slightly elongated parallel to lineation and be straight to curved and frequently be pinned by mica. A few of the larger grains show undulatory extinction.

Structures:

The thin section featured S-C' fabric that was consistently dextral with C-planes around 20 degrees to lineation. This fabric would not be found in mica free areas with larger quartz grains as seen in Figure 33.
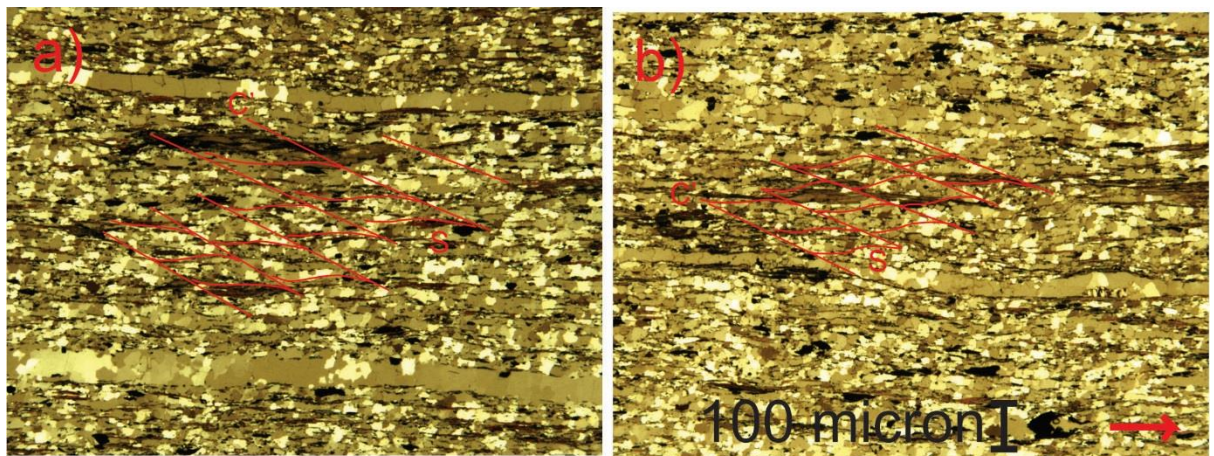

FIGURE 33: OVERVIEW OF STRUCTURES OBSERVED IN SAMPLE 16. RED ARROW MARKS LINEATION. A) AND B) SHOW WEAK DEXTRAL S-C' FABRIC OUTLINED BY WAVY MICA THAT DOES NOT GO INTO THE QUARTZ ONLY DOMAINS.

Quartz sample description

Sample 2 was gathered north of Brennmotinden from a quartz lens in a garnet-plagioclase mylonite just below the phyllite unit.

Sample 5 was gathered at the same location as sample 16, occurring as a lens of quartz in a outcrop of mylonitic garnet plagioclase schist.

Thin section 2 – Nordmannvik, Quartz sample from a garnet biotite gneiss
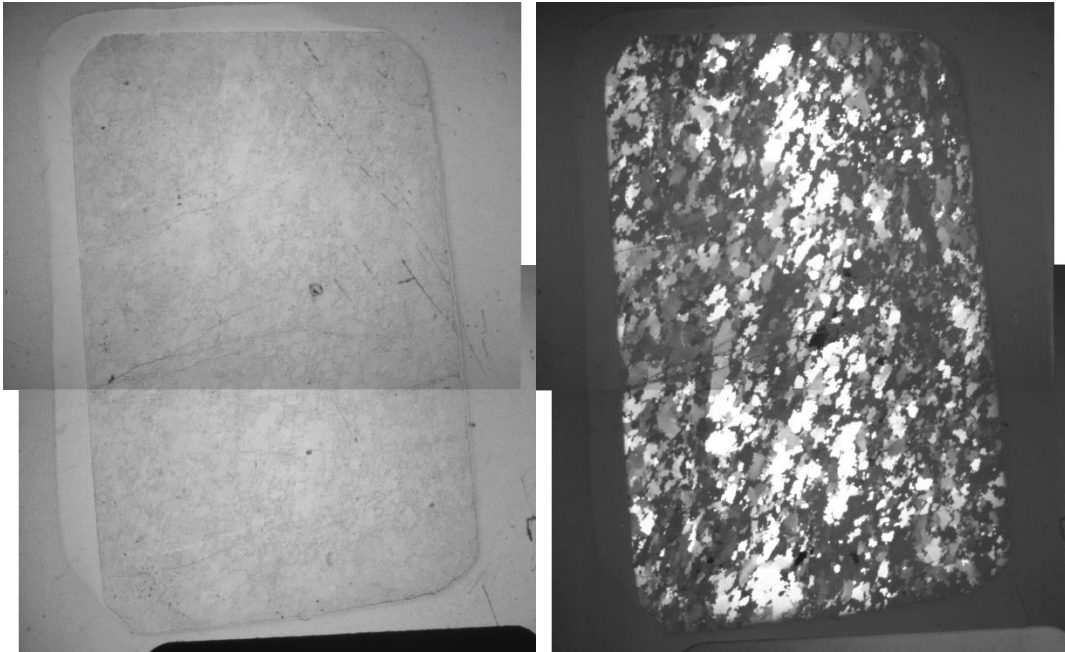
FIGURE 34: OVERVIEW OF SAMPLE 2, PPL TO THE LEFT, XPL TO THE RIGHT. CRACKS VISIBLE IN THE PPL THIN SECTION. RIGHT XPL SHOW DIAGONALLY ELONGATED GRAINS.

Description:

Anhedral grains of quartz show undulatory extinction. Grain boundaries are interlobate and polygonal and the grain distribution is serial. There are indications of both grain boundary migration and sub grain rotation. The interlobating boundaries indicating GBR while SGR is indicated by smaller grains with different orientation than the assumed parent grains.
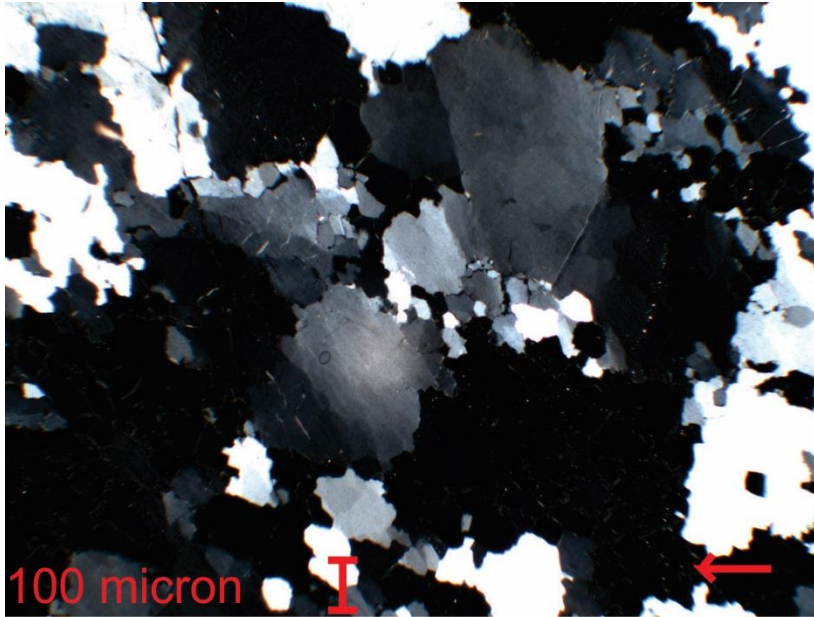
FIGURE 35: CLOSE UP OF AN AREA OF SAMPLE 2, RED ARROW INDICATE LINEATION. LOBATE GRAIN BOUNDARIES INDICATE GRAIN BOUNDARY MIGRATION WHILE SMALL ROUNDED GRAINS WITH DIFFERENT DEGREE OF EXTINCTION COMPARED TO PARENT GRAIN INDICATING SUB GRAIN ROTATION.

## Sample 2 grain size and fabric analysis

The grain map shows that grains tend to be 60 to 100 microns in grain size with a tail of larger grains up to 0,8 mm (Figure 36a). Projecting the grains into equivalent spheres suggests that half of the grains are around 50 microns (Figure 36b) even though 85 % of the volume is occupied by grains larger than that (Figure 36). Comparing the perimeter of the grains with the perimeter of an equivalent circle made of the same area indicate that the grains are lobate or elliptical shaped with a weighted factor of 1,33 (Figure 37a). Grains tend to have a lower axial ratio depending on size, that is larger grains tend to be more elongated compared to smaller grains (Figure 37b). Plots also indicate a preferred orientation of long axes of 60 degrees relative a reference point which is 90 degrees to lineation (Figure 37c). This preferred elongation can be seen in XPL in Figure 34 and translates to 30 degrees clockwise to lineation. Overall the grains show a weighted aspect ratio of 0,519 indicating that long axis tends to be twice as long as short axis (Figure 37d).
SURFOR and PARFOR (Figure 38) also suggests a general preferred orientation of 30 degrees clockwise to lineation with a bulk fabric aspect ratio of 0,808 to 0,816. The larger bulk aspect ratio compared to the weighted aspect ratio suggests that many of the grains have a differing elongated long axis orientation compared to the overall bulk orientation. The figure also indicates a sinistral sense of shear and a monoclinic fabric shape.
CPO analysis of the sample show that basal slip axes are oriented in a hexagonal pattern forming a plane perpendicular to foliation (Figure 7) with the C-axes making an elongated maximum tilted clockwise indicating a dextral sense of shear.
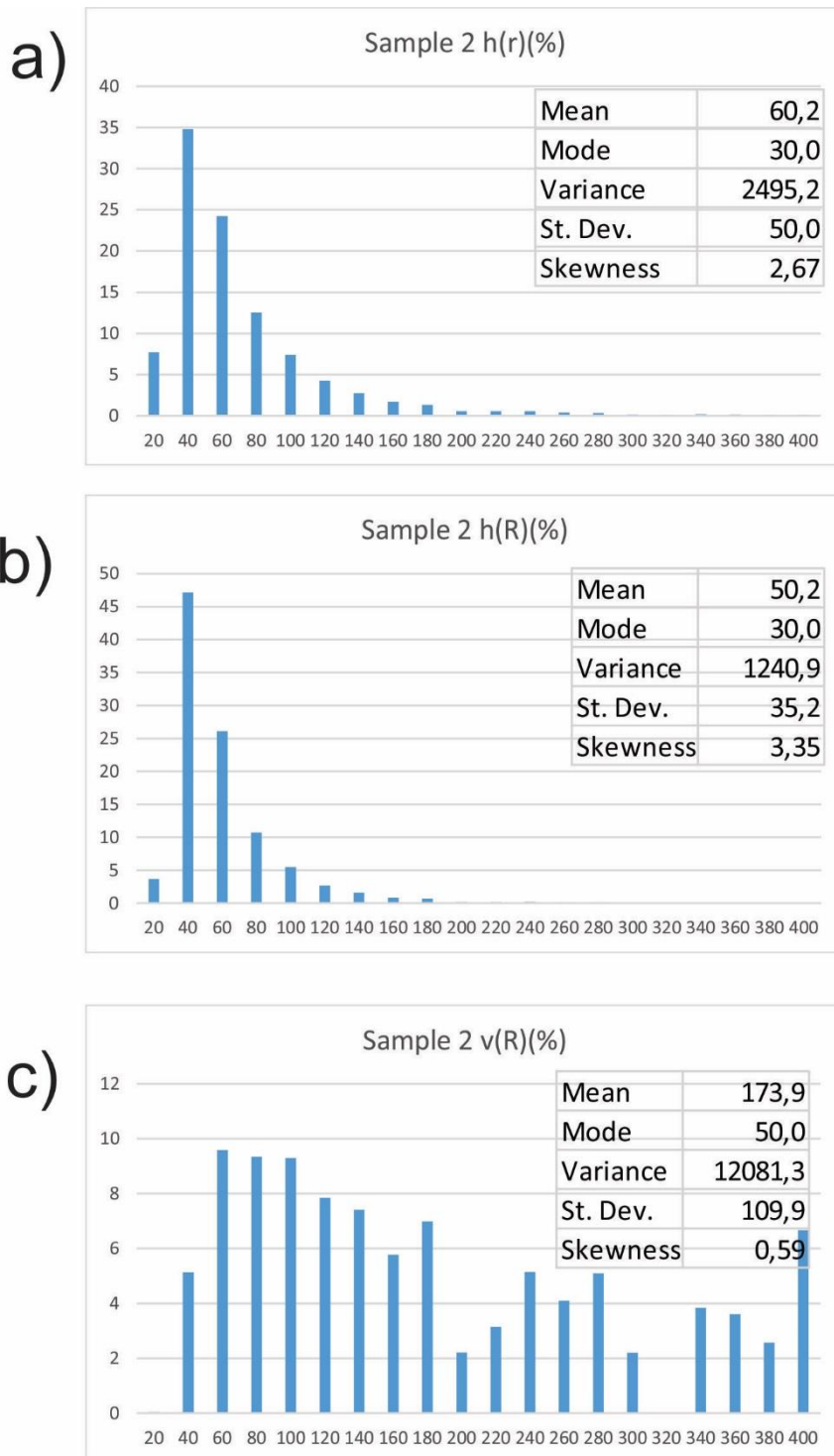
FIGURE 36: GRAIN SIZE DISTRIBUTION OF SAMPLE 2. Y-AXIS IS PERCENTAGE, X-AXIS IS GRAIN RADIUS WITH BIN SIZE OF 20 MICRON. A) HISTOGRAM OF EQUIVALENT GRAIN SIZE RADIUS BASED OF AREA OF GRAINS. MOST COMMON GRAIN SIZE IS AROUND 30 MICRON, WHILE THE MEAN IS 60 MICRON. B) EQUIVALENT GRAIN RADIUS BASED ON PROJECTED VOLUME OF GRAINS. MODE IS STILL AROUND 30 MICRON WHILE THE MEAN HAVE DECREASED TO 50 MICRON. C) VOLUME DISTRIBUTION OF PROJECTED EQUIVALENT GRAINS SHOWING THAT A LARGE FRACTION OF THE SPACE IS OCCUPIED BY A SMALL NUMBER OF LARGE GRAINS.
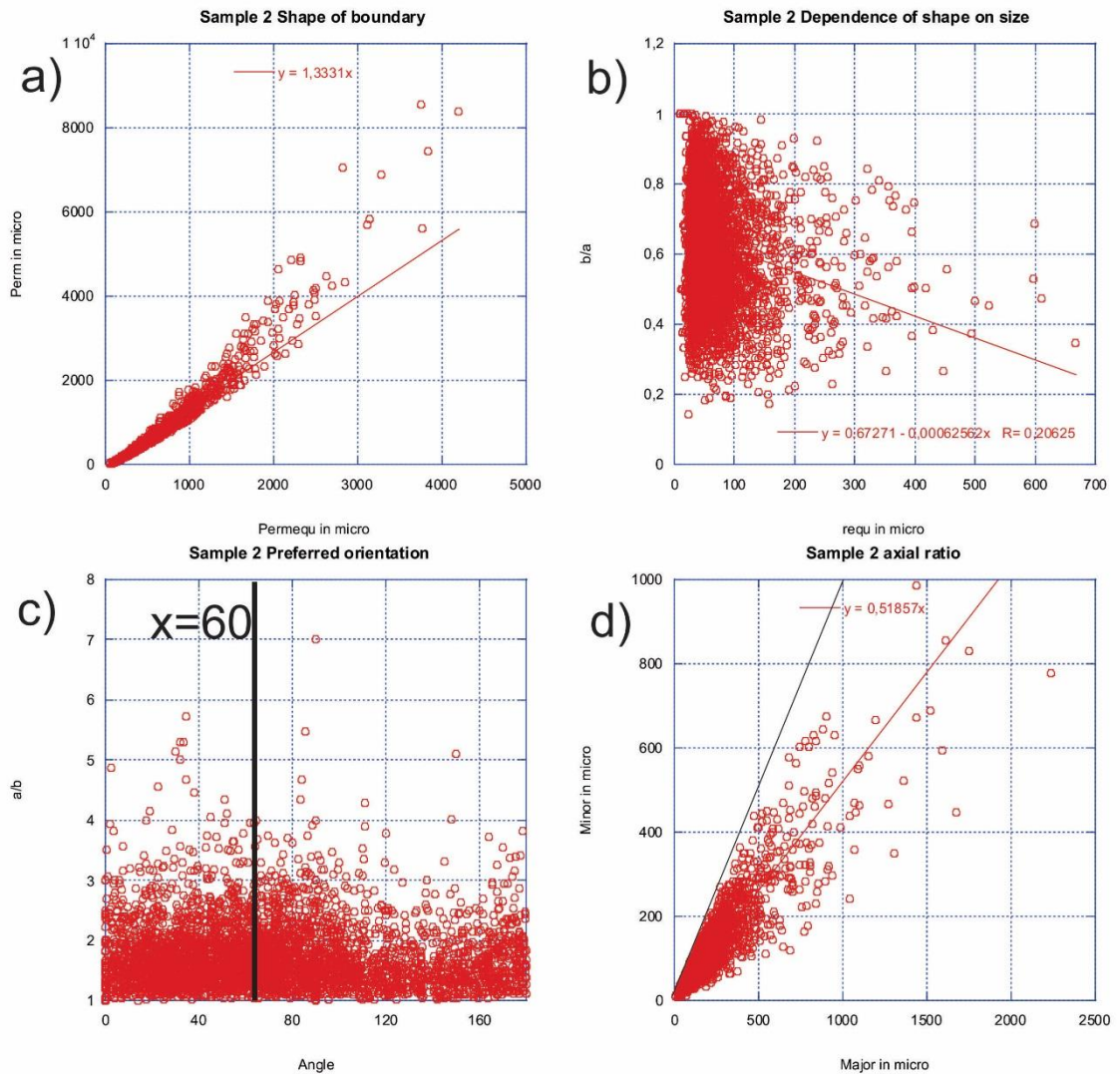
FIGURE 37: SAMPLE 2 CORRELATION PLOTS OF GRAIN ATTRIBUTES. A) Y-AXIS IS PERIMETER OF GRAINS, X-AXIS IS PERIMETER OF EQUIVALENT GRAINS. F(X) IS A LINEAR FIT INDICATING THAT THE GRAIN BOUNDARIES ARE GENERALLY NON-ROUNDED, THAT IS LOBATE. IT ALSO INDICATE THAT THE SMALLER GRAINS ARE MORE ROUNDED THAN THE LARGER GRAINS AS THEY GENERALLY PLOT WITH A HIGHER Y/X RATIO, SUGGESTING TWO POPULATIONS. B) Y-AXIS IS AXIAL RATIO, X-AXIS IS EQUIVALENT RADIUS. F(X) INDICATE THAT LARGER GRAINS GENERALLY TEND TO BE MORE ELONGATED THAN SMALLER GRAINS. C) Y-AXIS IS ASPECT RATIO, X-AXIS IS ANGLE OF LONG AXIS. THE PLOT INDICATE THAT THE LONG AXIS OF MOST OF THE GRAINS TEND TO BE ORIENTATED 60 DEGREES ANTICLOCKWISE TO AN ARBITRARY POINT. IN THIS CASE TRANSLATING TO 30 DEGREES CLOCKWISE TO LINEATION. D) Y-AXIS IS MINOR AXIS OF GRAIN (B), X-AXIS IS LONG AXIS OF GRAIN (A). BLACK LINE IS 1/1 RATIO. F(X) INDICATE THAT THE GRAINS IN GENERAL ARE ELONGATED WITH A MEAN AXIAL RATIO OF 0,51.
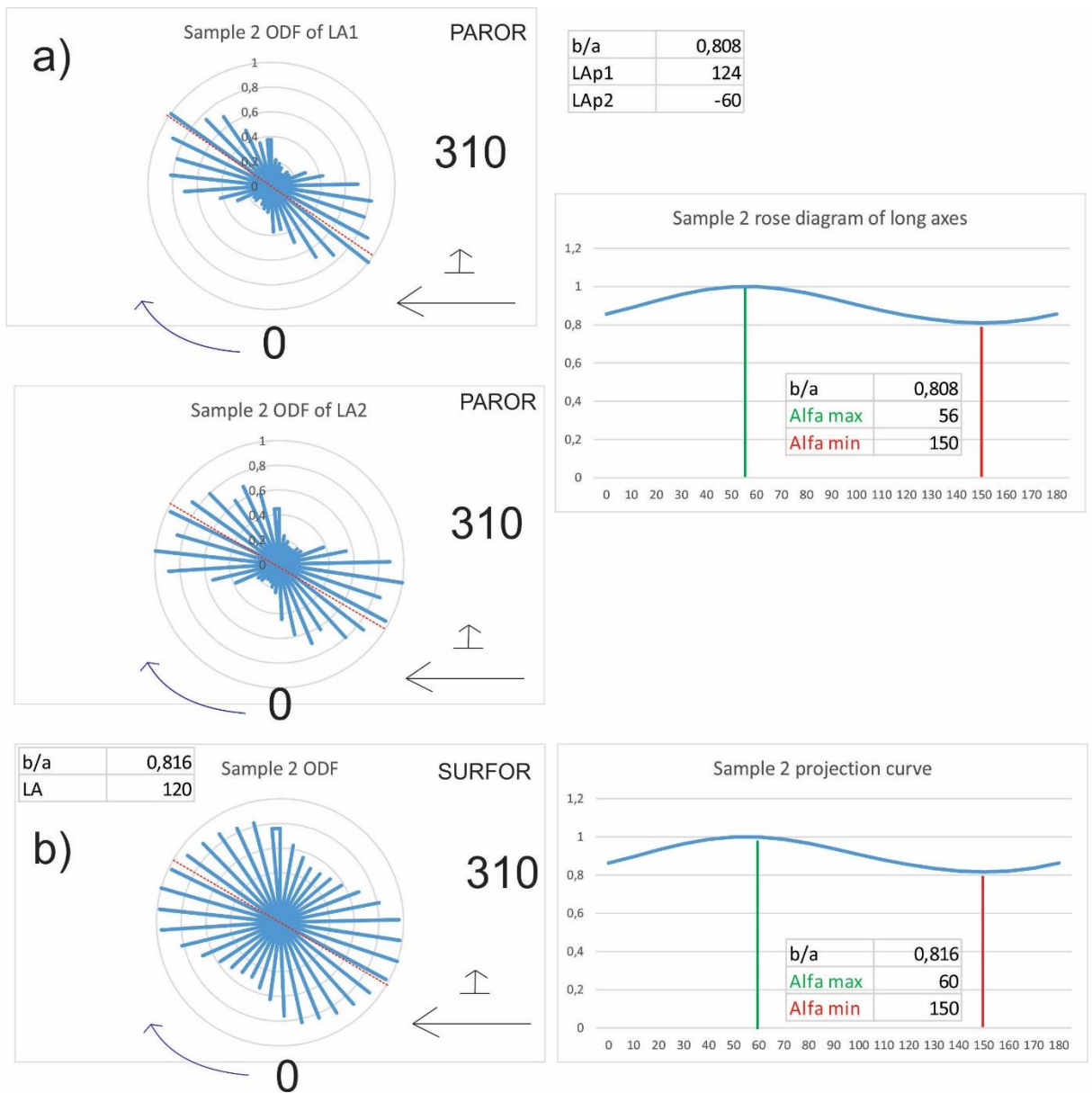
FIGURE 38: SAMPLE 2 PARTICLE AND SHAPE FABRIC. LINEATION IS HORIZONTAL; MARKED BY ARROW, UP IS MARKED BY SMALL ARROW, PERPENDICULAR TO FOLIATION. 0 WITH AN ARROW MARK THE ROSE DIAGRAM POSITIVE AXIS DIRECTION. 310 MARKS ORIENTATION OF RIGHT END OF LINEATION WITH THE LEFT SIDE BEING (310-180) 130 DEGREES. 10 DEGREES RESOLUTION ROSE DIAGRAMS SHOWING LENGTH WEIGHTED ORIENTATION DISTRIBUTIONS (ODF)TO THE LEFT AND ACCOMPANYING PROJECTION CURVES ON THE RIGHT. RED LINE ON ROSE DIAGRAMS MARKS THE BULK PREFERRED ORIENTATION. A) ROSE DIAGRAMS OF LONG AXIS DEFINED BY LONGEST PROJECTIONS SHOWING BULK PREFERRED ORIENTATION TO BE 34 DEGREES TO LINEATION WITH AN AXIAL RATIO OF 0,808. THE SECOND ROSE DIAGRAM SHOWS LONG AXIS DEFINED BY PROJECTIONS NORMAL TO THE SHORTEST SHOWING A SLIGHTLY SMALLER ANGLE BETWEEN THE BULK PREFERRED ORIENTATION OF 30 DEGREES AND LINEATION. A ANGULAR DIFFERENCE OF 56 − (-30) = 84 DEGREES INDICATE A SLIGHTLY MONOCLINIC AND SINISTRAL SHAPE WITH LINEATION AS REFERENCE LINE. B) 10 DEGREE ROSE DIAGRAM OF SURFACE ODF SHOWING A PREFERRED BULK ORIENTATION OF 30 DEGREES TO LINEATION AND AN ASPECT RATIO OF 0,816 ILLUSTRATED BY THE AXIAL RATIO OF THE SURFOR ROSE DIAGRAM. PROJECTION CURVE INDICATE AN ORTHOGONAL SHAPE IN THIS CASE.

49
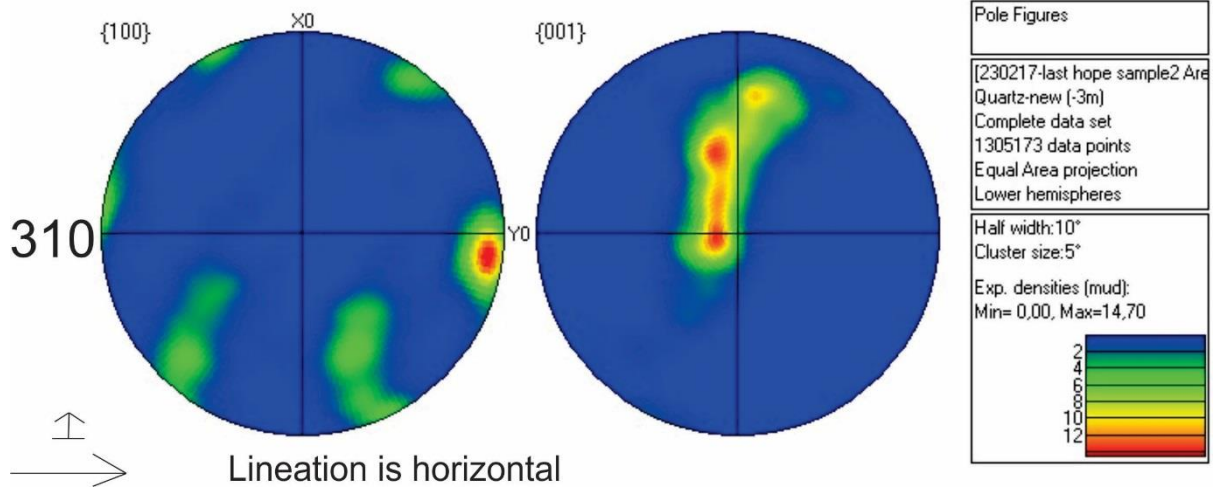
FIGURE 39: POLE FIGURE OF SAMPLE 2 CRYSTAL PREFERRED ORIENTATION. Y0 IS LINEATION, ALSO MARKED BY HORIZONTAL ARROW WHILE X0 IS PERPENDICULAR TO FOLIATION PLANE, MARKED BY SMALL ARROW. LEFT POLE PLOT MARKS THE ORIENTATION OF THE BASAL QUARTZ SLIP SYSTEM WHILE THE RIGHT SHOW THE ORIENTATION OF THE C-AXIS. THE BASAL SLIP SYSTEM FORMS A HEXAGONAL PATTERN FORMING A PLANE ALMOST PERPENDICULAR TO FOLIATION PLANE WITH A MAXIMA SUB PARALLEL TO LINEATION. RIGHT POLE PLOT SHOWS THE C-AXIS POLES FORMING A WEAK S-SHAPED PATTERN INDICATING THAT MOST QUARTZ C-AXIS ARE PERPENDICULAR TO LINEATION OR IN THE UPPER RIGHT QUADRANT, CORRELATING TO THE SLIGHT CLOCKWISE TILT OF THE HEXAGONAL BASAL SLIP PATTERN. OVERALL A DEXTRAL AND THUS TOP 130 SENSE OF SHEAR.
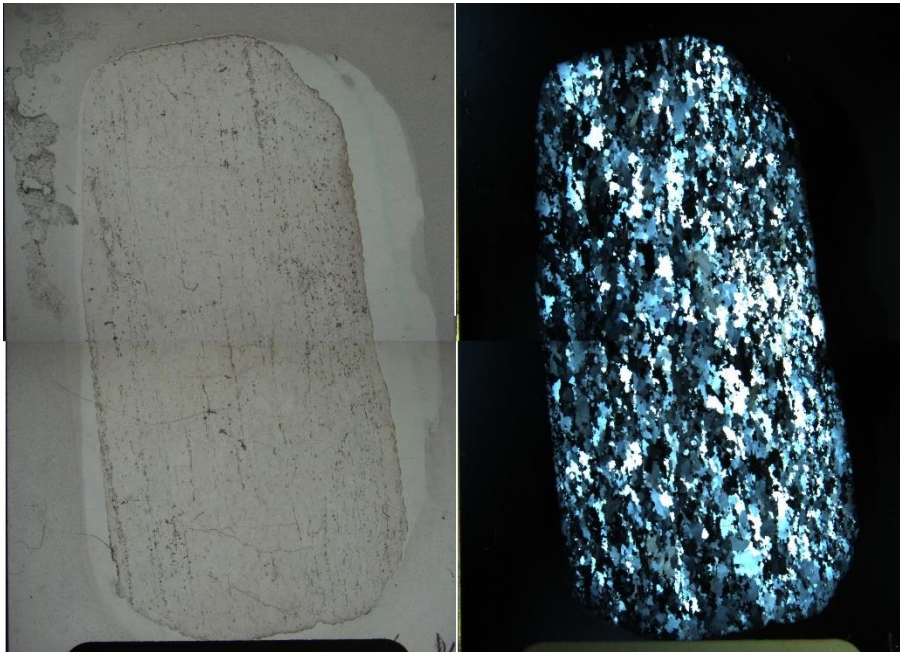
FIGURE 40: OVERVIEW OF SAMPLE 5. LINEATION IS VERTICAL. BROWN ELONGATED CHLORITE GRAINS CAN BE SEEN IN PPL MAKING VERTICAL A VERTICAL LINEATION WHILE XPL SUGGESTS SOME DIAGONAL PATTERN IN THE QUARTZ EXTINCTION.

Description:
Anhedral grains of quartz occurred in size varying from 80 to 160 microns featuring straight to oblate grain boundaries pinned by elongated grains of chlorite. The main form of deformation mechanism is interpreted to be grain boundary migration due to the lobate boundaries and relatively large grains. Some small rounded sub grains due indicate a degree of sub grain rotation.
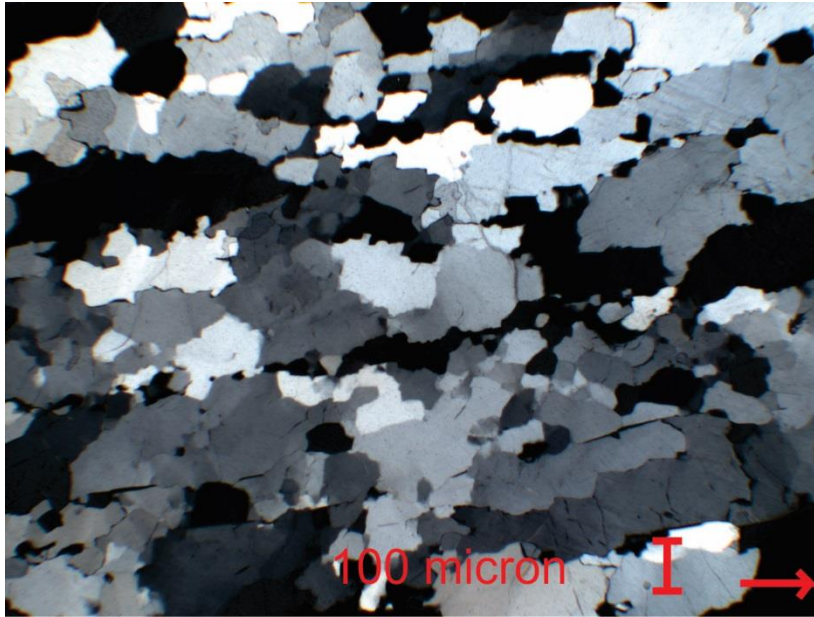
FIGURE 41: CLOSE UP OF SAMPLE 5, RED ARROW MARK LINEATION. LOBATE BOUNDARIES INDICATE GRAN BOUNDARY MIGRATION TO BE THE DOMINANT RECRYSTALLIZATION MECHANISM.

## Quartz sample grain size and fabric

Mode of equivalent radius of the grains was 40 to 60 microns with a rather large variance suggesting a wide span of sizes (Figure 42 a) and a long tail suggesting a local maximum of larger grains. The maxima persist into the three-dimensional projections (Figure 42 b) with a larger portion of grains becoming member of the modal grain size. Volume-wise 90 % is taken up by grain larger than 50 microns even though these make up 60 % of the grains. Overall inverse grain roundness is 1,36 indicating that grains are elongated or lobate in shape (Figure 43) and are weighted to be more elongated the larger they are, suggesting that smaller grains are more rounded than larger grains. Overall the grains show a rather strong alignment of long axes 10 degrees anticlockwise to lineation and a weighted aspect ratio of 0,47.

Fabric analysis (Figure 44) indicate a fabric elongated 7-9 degrees anticlockwise to lineation and a bulk aspect ratio of 0,692 from PAROR and 0,713 from SURFOR. Difference in alpha angle (180-99-7 = 88) indicate a monoclinic fabric shape and a dextral sense of shear.

Sample 5 quartz girdle (Figure 45) show two planes of a-axes almost perpendicular to each other tilted clockwise corresponding to the tilted axis that can be envisioned connecting the two quartz c-axis maximums indicating a dextral sense of shear.
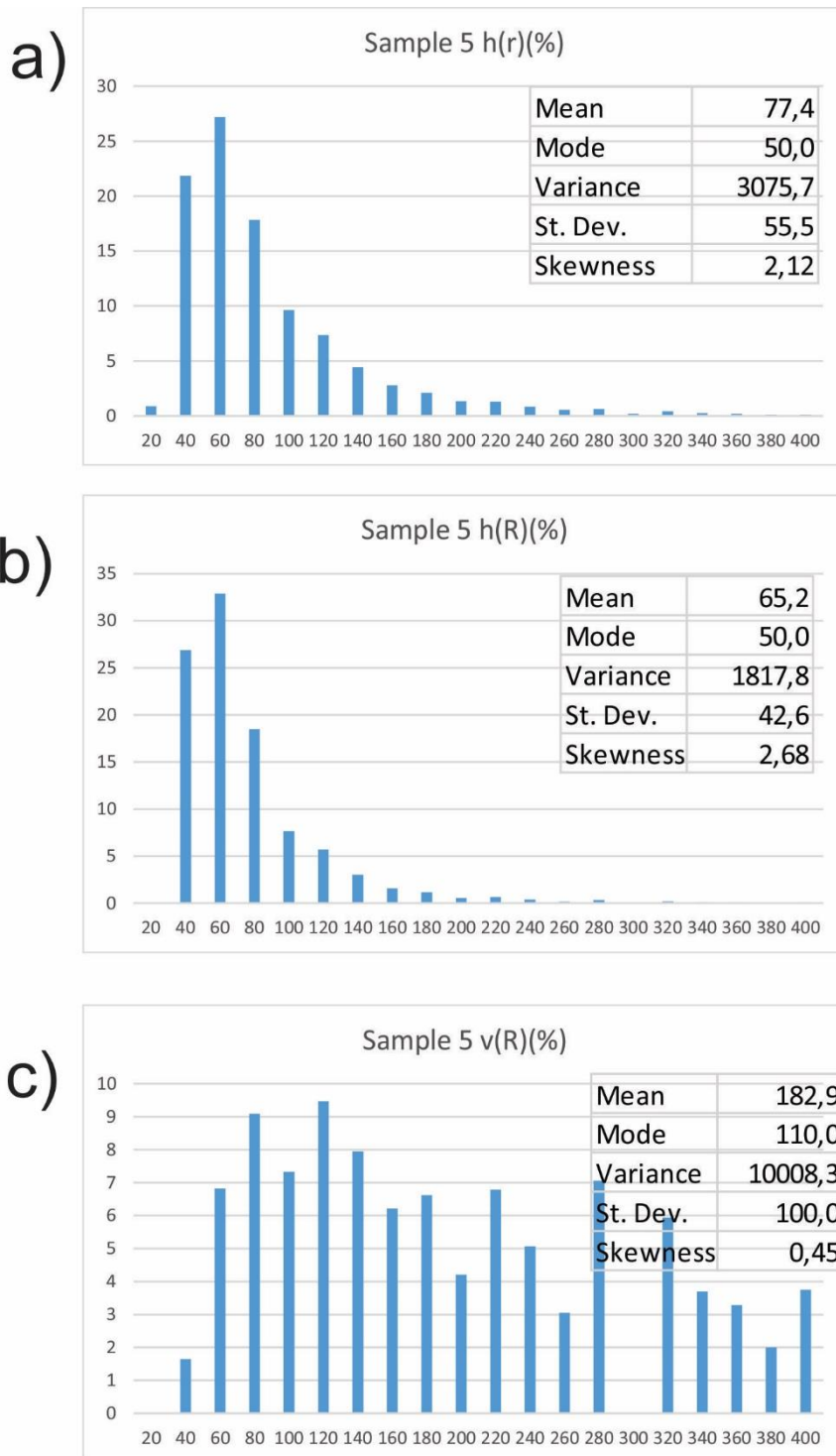
FIGURE 42: GRAIN SIZE DISTRIBUTIONS OF SAMPLE 5. ALL PLOTS ARE IN PERCENTAGE. X-AXIS IS SAMPLE RADIUS IN MICRONS. A) PLOT OF GRAIN EQUIVALENT RADIUS DERIVED FROM AREA OF GRAINS. MODE IS ABOUT 50 MICRON. B) PLOT OF EQUIVALENT GRAIN RADIUS DERIVED FROM VOLUME OF GRAINS PROJECTED FROM THE GRAIN AREA HISTOGRAM. MODE IS ABOUT 50 MICRON, MEAN HAVE DROPPED TO 65 MICRON INDICATING A DISTRIBUTION MORE WEIGHTED WITH SMALLER GRAINS COMPARED TO THE AREA EQUIVALENT GRAIN DISTRIBUTION. C) VOLUME IN PERCENTAGE TAKEN UP BASED ON GRAIN SIZE. MOST OF THE VOLUME IS MADE OUT BY A FEW LARGE GRAINS.
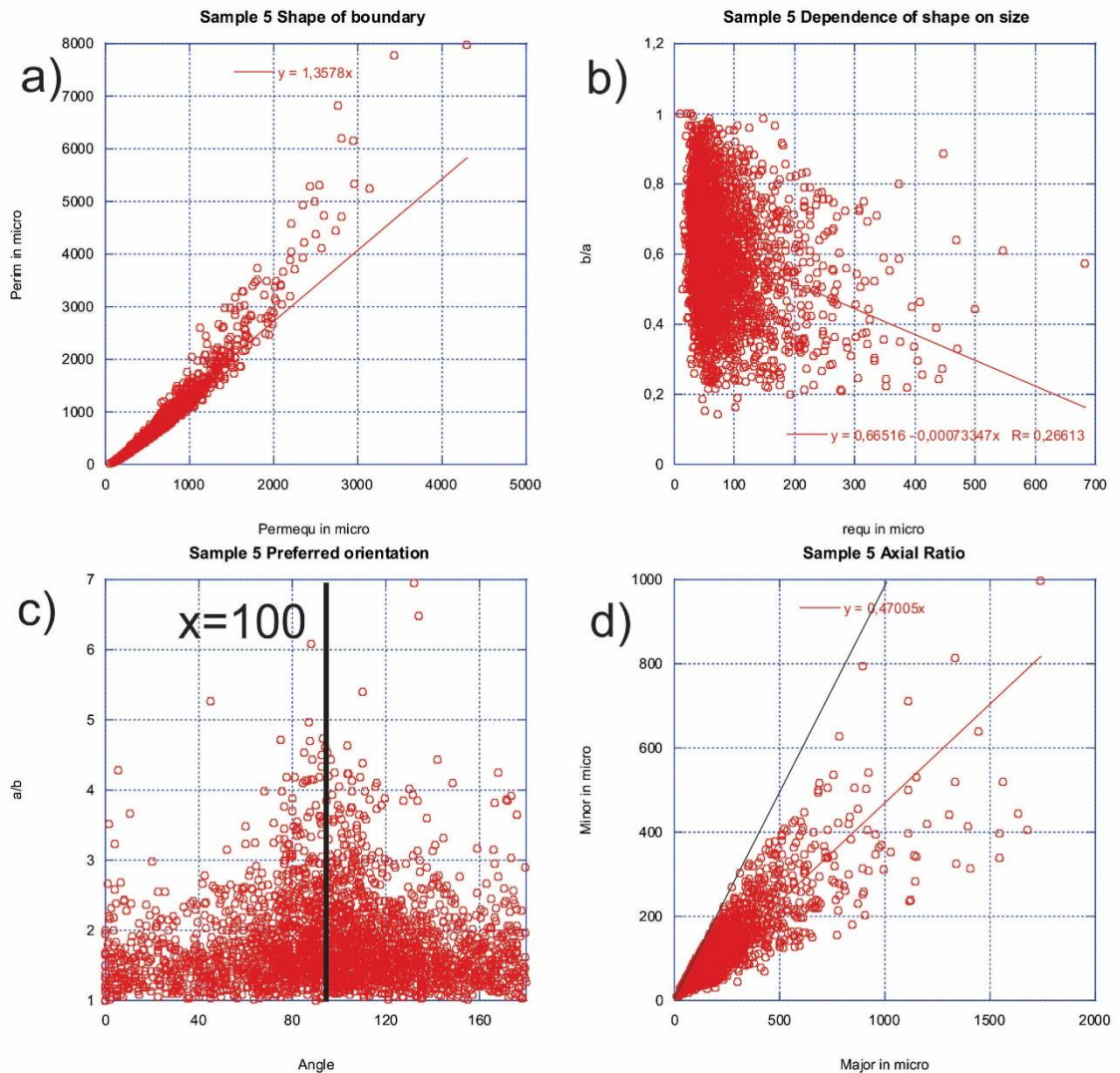
FIGURE 43: GRAIN CORRELATION DATA. A) COMPARISON BETWEEN PERIMETER OF GRAIN WITH PERIMETER OF AN EQUIVALENT GRAIN. GRAINS ARE GENERALLY NON-ROUNDED INDICATED BY SLOPE BEING MORE THAN 1. SMALLER GRAINS TENDING TO BE MORE ROUNDED THAN LARGER GRAINS. B) AXIAL RATIO TO GRAIN SIZE COMPARISON INDICATING A CORRELATION BETWEEN GRAIN SIZE AND ASPECT RATIO. CONFORMING A) BY PRODUCING A SLOPE THAT IS TILTED TOWARDS LARGER GRAINS BEING MORE LOBATE THAN SMALLER MORE ROUNDED GRAINS. C) ASPECT RATIO TO INCLINATION OF LONG AXIS PLOT. INDICATING THAT THERE IS AN PREFERRED ORIENTATION OF LONG AXIS OF PARTICLES AT ABOUT 100 DEGREES ANTICLOCKWISE TO A POINT. TRANSLATING TO 10 DEGREES CLOCKWISE TO LINEATION. D) WEIGHTED AXIAL RATIO INDICATING AN AVERAGE AXIAL RATIO OF 0,47. BLACK LINE MARKS 1/1 AXIAL RATIO.
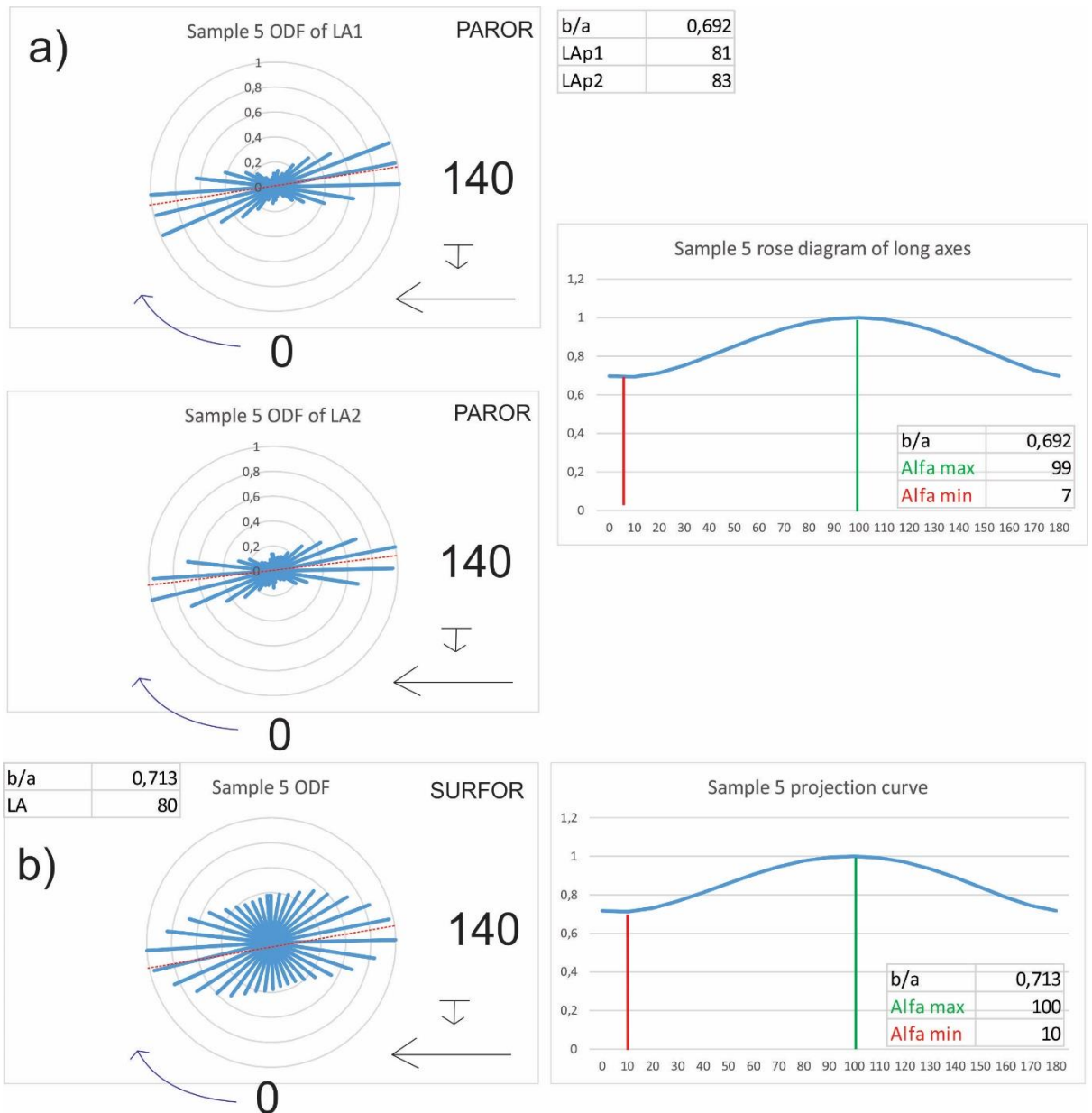
FIGURE 44: GRAIN PARTICLE AND ORIENTATION FABRIC. ROSE DIAGRAMS ON THE LEFT CORRELATING TO PROJECTION CURVES TO THE LEFT. PAROR HAVE TWO ROSE DIAGRAMS WITH LA1 BEING PROJECTED FROM ORIENTATION OF LONG AXIS WHILE LA2 BEING PROJECTED FORM NORMAL TO SHORT AXIS. 140 MARKS RIGHT HAND ORIENTATION OF LINEATION, 0 WITH ARROW INDICATE THE ROSE DIAGRAM AXIS, WHICH IS INVERSE COMPARED TO THE PROJECTION CURVE. LINEATION IS HORIZONTAL INDICATED BY LARGE ARROW WITH UP NORMAL TO FOLIATION INDICATED BY SMALL ARROW. RED LINE ON ROSE DIAGRAMS INDICATE FABRIC LONG AXIS PREFERRED ORIENTATION A) PAROR ROSE DIAGRAM INDICATE A LONG AXIS PREFERRED ORIENTATION 7-9 DEGREES ANTICLOCKWISE TO LINEATION WITH AN ASPECT RATIO OF 0,692. DIFFERENCE BETWEEN ALFA MAX AND ALFA MIN IS 92 DEGREES INDICTING A SINISTRAL MONOCLINIC SHAPE WITH 0 AS REFERENCE POINT TRANSLATING TO A DEXTRAL MONOCLINIC SHAPE WITH RESPECT TO LINEATION (180-99+7 = 88). B) SURFOR ROSE DIAGRAM INDICATE AN OVERALL MONOCLINIC SHAPE WITH AN ASPECT RATIO OF 0,713, SOMEWHAT HIGHER THAN PAROR AND A LONG AXIS PREFERRED ORIENTATION OF 10 DEGREES ANTICLOCKWISE TO LINEATION.
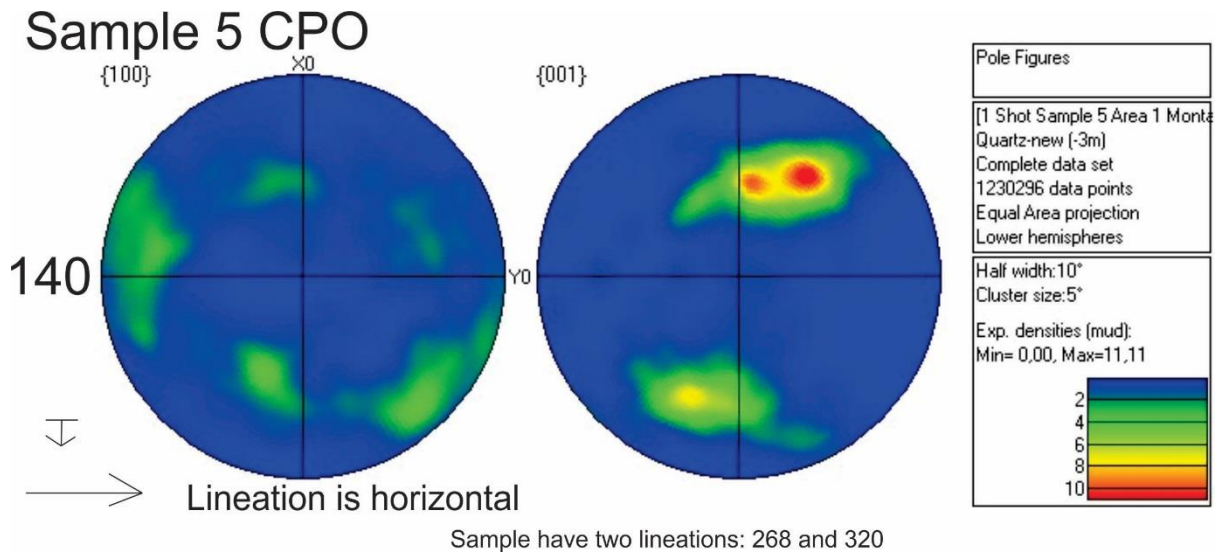
FIGURE 45: POLAR PLOTS OF QUARTZ AXIS PREFERRED ORIENTATION. LINEATION IS HORIZONTAL, LEFT HAND ORIENTATION IS 140. LEFT PLOT IS BASAL SLIP, RIGHT PLOT IS C-AXIS. LEFT PLOT INDICATE TWO PLANES OF PREFERRED ORIENTATION FOR THE A-AXIS. THE LOWER ONE BEING MORE PRONOUNCED THAN THE UPPER ONE. RIGHT PLOT YIELD TWO MAXIMA, THE UPPER RIGHT BEING MORE PRONOUNCED THAN THE LOWER LEFT CORRESPONDING TO THE LEFT BASAL PLOT.

Koppangen phyllites

Field description
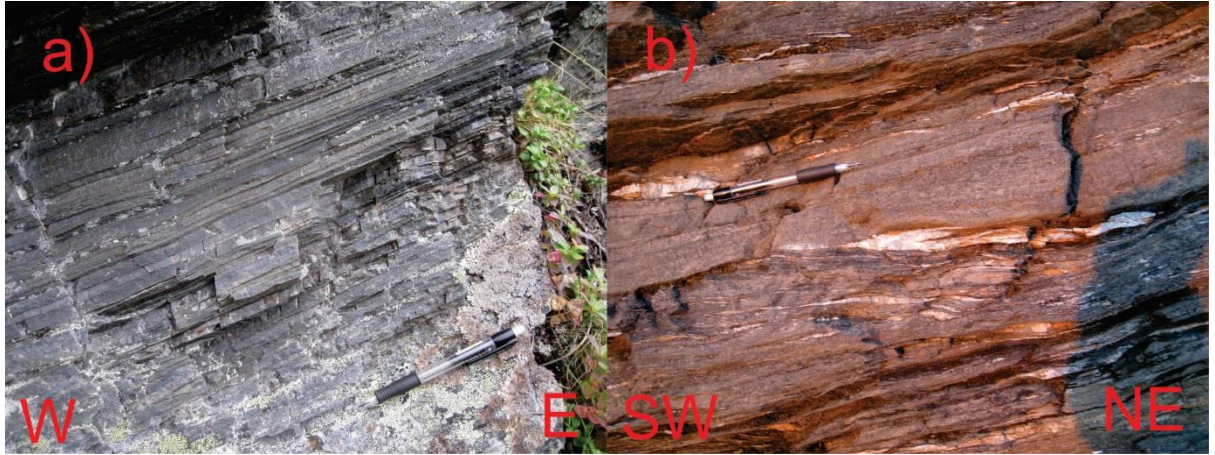
FIGURE 46: OVERVIEW OF KOPPANGEN PHYLLITES. A) INTERFINGERING UNITS OF LIGHT GREY QUARTZITE AND DARKER PHYLLITE CREATING EROSION RESISTANT OUTCROPS. THE PHYLLITE LAYERS FEATURE SINISTRAL TOP WEST S-C FABRIC. B) PHYLLITES WITH LENSES OF QUARTZ INDICATING S1 FOLIATION FOLDED AND CUT ABRUPTLY BY S2 FOLIATION. PEN ALONG S2 FOLIATION.

Petrology

The unit seemed to be more easily weathered than the gneiss and would form steep weathered slopes and tended to be covered with vegetation unless forming peaks. The weathering tended to be purple, white and yellow and go rather deep into samples. There was variation in unit weather resistance as some units seemed to weather and erode visibly while at other locations the unit could make steep peaks. Mineral content varied from no visible minerals except quartz lenses to visible mica and amphibole needles that could be cm long. Cm sized euhedral pyrite could occur, possibly correlating to large scale fold hinges. The unit would occur as a coherent unit from the edge of the underlying garnet schist to the chlorite schist/phyllites overlaying it or as one of several units occurring as interfingering schist, phyllites and chlorite phyllites. The quartz content of the unit varied in the succession and would at some locations become more quartz rich toward the overlaying contact with the Lyngen nappe. appearing as a quartzite interlayered with thin mm scale layers of phyllite. This gradual transformation from easily weathered phyllite to more erosion resistant quartzite interlayered with phyllite was prevalent North of Furuflaten, but was not detected further South. The contact between the overlaying Lyngen Magmatic complex would be gradual with a change from black phyllites to greener chlorite phyllites and then chlorite schist.

Structures

This unit tended to reliantly feature shear bands, folded quartz lenses and kinks. Dethatched isocline fold hinges of plagioclase/quartz were common, forming a S1 foliation. S2 Foliation was usually dipping gently west with a W-E lineation. At some locations both W-E and NW-SE lineation could be observed.
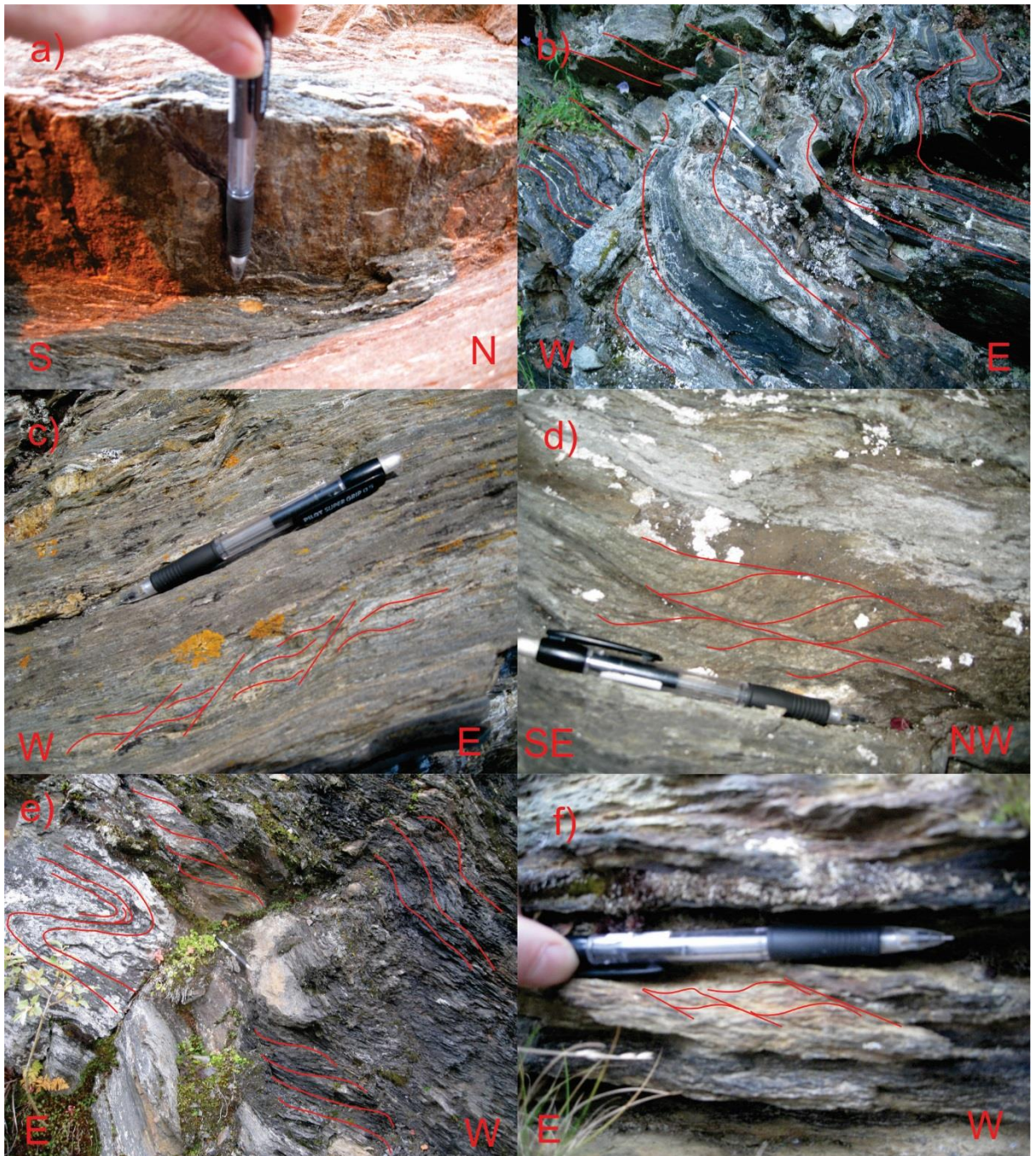
FIGURE 47: OVERVIEW OF PHYLLITE STRUCTURES. RED MARKINGS INDICATE FOLIATION AND SHEAR BANDS. A) W-E LINEATION. B) ASYMMETRIC FOLDING. C) SINISTRAL TOP WEST S-C' FABRIC IN PHYLLITE, LINEATION MARKED BY PEN. D) DEXTRAL TOP ROUGHLY WEST S-C FABRIC, PEN FOR SCALE E) OUTCROP WITH DEXRAL TOP WEST S2 S-C FABRIC AND FOLDED S1 FOLIATION . PEN FOR SCALE. F) S-C' FABRIC. PEN FOR SCALE.

Thin section description

Three thin sections were made from this unit.

Sample 10 is from a lens of quartzite found in the Koppangen phyllite in Rypedalen west of Kvalnesfjellet. The outcrop showed clear west dipping lineation and formed a step in the nearby river.

Sample 14 was taken along the banks of one of the rivers feeding Storvatnet from the west, a few hundred meters further up from sample 7 and 12. The outcrop had a peculiar red/yellow/purple weathering and a west dipping foliation.

Thin section 15 was gathered North of Lyngseidet by a dam up from Rottenvik, high up in the phyllite section where the unit formed a slightly west dipping plateau like the Nordmannvik unit tends to do.

Thin section 10 – Koppangen Quartzitic mylonite
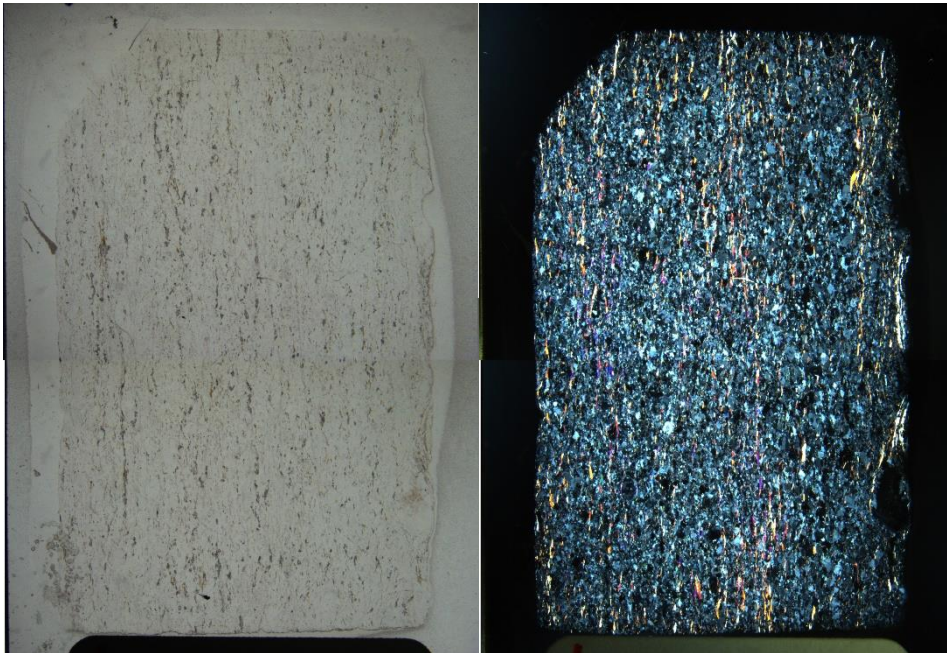
FIGURE 48: OVERVIEW OF THIN SECTION 10. LEFT IS PPL, RIGHT IS XPL. FIELD OF VIEW IS ABOUT 3 BY 5 CM. LINEATION IS VERTICAL. THIN SECTIONS SHOW LITTLE IN WAY OF MICA AND NO MAJOR PORPHYROCLASTS OR SIGNIFICANT STRUCTURES. SLIGHTLY WAVY FOLIATION.

Minerals: Plagioclase (55 %), quartz (15 %), K-feldspar (10 %), muscovite (10 %), biotite (5 %), epidote (5 %)

Accessories: Titanite, zircon

Occurrence: plagioclase and quartz occur as matrix, with K-feldspar occurring as porphyroclasts. Biotite and muscovite forms needles sub parallel to lineation, folding around plagioclase porphyroclasts. epidote occur spread out as single anhedral crystals.
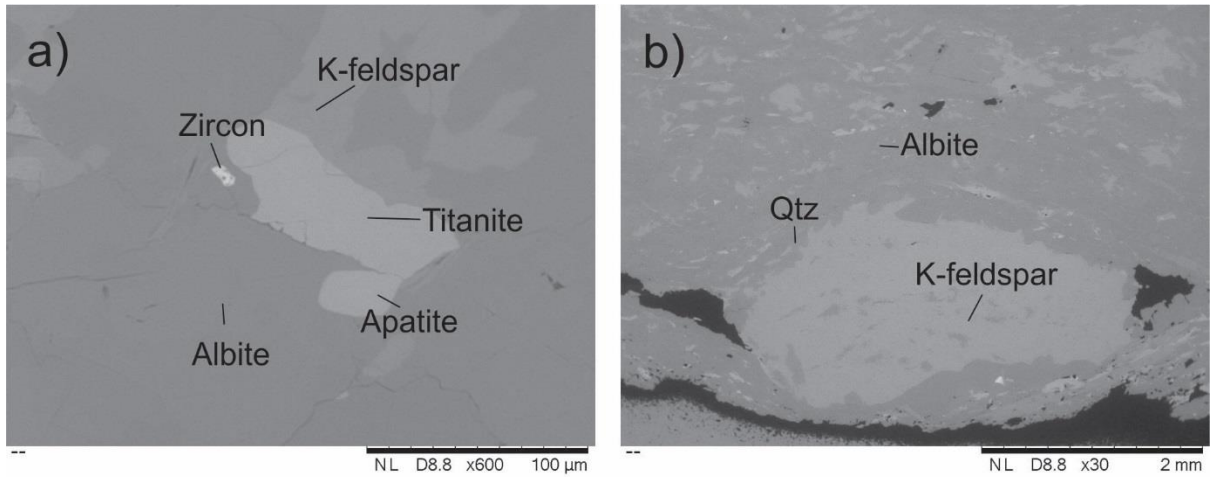
FIGURE 49: BACKSCATTER PICTURES FORM SAMPLE 10. BLACK BAR IS SCALE. A) ZIRCON, TITANITE AND ZIRCON SURROUNDED BY DARKER ALBITE AND K-FEDLSPAR. B) GRAIN OF K-FELDSPAR SURROUNDED BY QUARTZ AND ALBITE AND POSSIBLY SMALL WHITE GRAINS OF ZIRCON.

Description:

Porphyroclasts of plagioclase and K-feldspar occur in a bimodal matrix of quartz, plagioclase, epidote, biotite and muscovite. The plagioclase porphyroclasts are around 2 mm in diameter and has an elongated anhedral shape aligned parallel to foliation. Grain boundaries are rounded to serrated and there is a mantle of smaller grains, some of which show undulatory extinction. The very fine grains are assumed to be from the larger porphyroclast. Grains of muscovite and epidote are folded around the porphyroclasts and their strain shadow continuing to form tails. Foliation is made up by muscovite, biotite and epidote. It is continuous, rough shaped and anastomosing. The matrix is bimodal with two populations. One population is medium sized plagioclase grains with serrated boundaries and undulatory extinction. The second population is smaller, fine to medium, anhedral grains of quartz and plagioclase. Some grains show undulatory extinction and the boundaries are rounded.

Structures:

Muscovite make outlines that might be the remains of porpyroclasts of plagioclase. These outlines sometimes show dextral sigma clast patterns and outline a consistently dextral S-C' fabrics which tended to have C-planes 25-30 degrees to lineation.
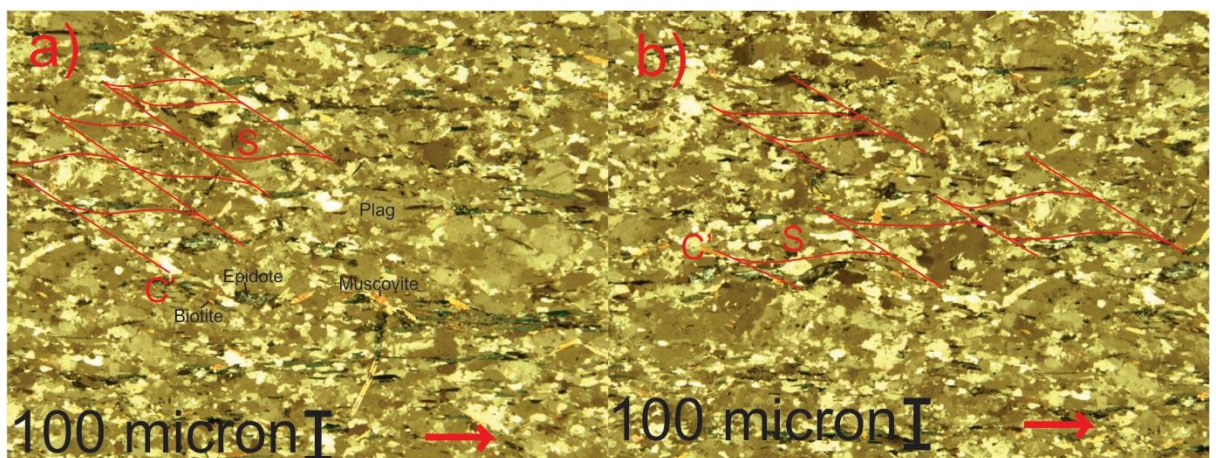
FIGURE 50: RED ARROW SHOW LINEATION. RED MARKINGS INDICATE S AND C' PLANES A) AND B) SHOW WEAK S-C' FABRIC MARKED OUT BY WAVY ALIGNED MICA MINERALS.

Thin section 14 – Nordmannvik Garnet mica schist
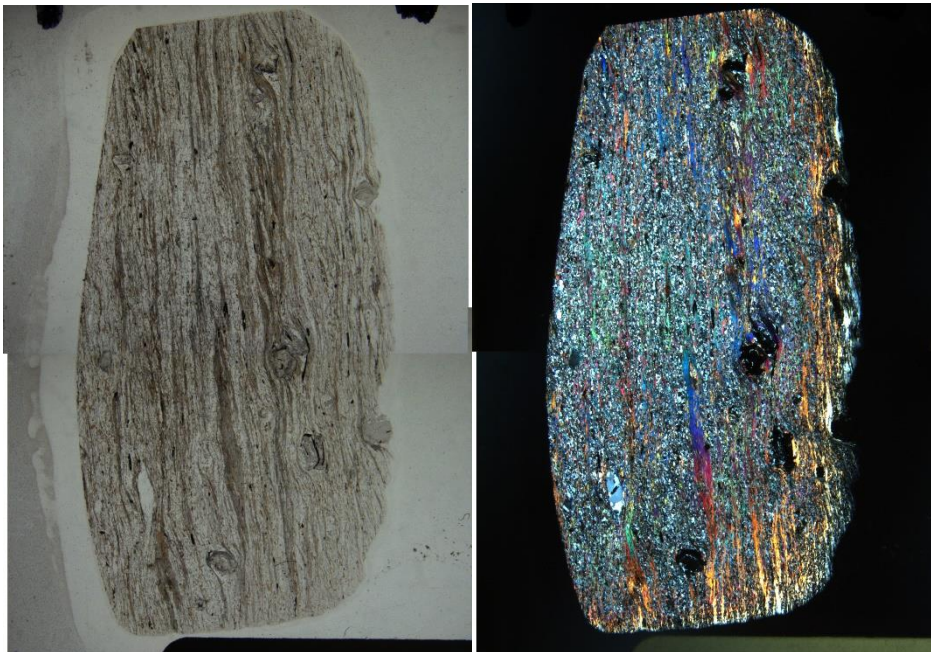
FIGURE 51: OVERVIEW OF SAMPLE 14. PORPHYROCLASTS OF GARNET IN A HETEROGENOUS GROUNDMASS OF BIOTITE, MUSCOVITE AND QUARTZ.

Minerals: Quartz (40 %), muscovite (20 %), biotite (15 %), garnet (10 %), plagioclase (5 %), hornblende (5 %), calcite (2 %), epidote (2 %), chlorite (1 %),

Accessories: Apatite, sulphide (indicated in SEM), ilmenite, zircon, rutile, tourmaline

Occurrence: Porphyroclasts of garnet occur in a matrix of muscovite, biotite, plagioclase and quartz. Muscovite and biotite make a spaced foliation.
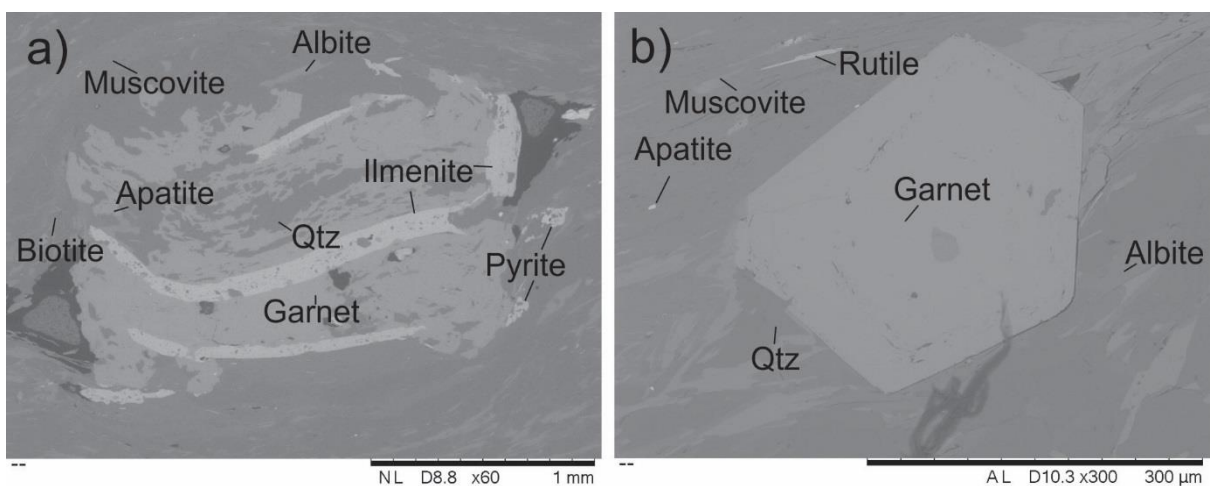
FIGURE 52: BACKSCATTER PICTURES OF TWO GARNETS IN SAMPLE 14. A) ANHEDRAL GARNET WITH INCLUSIONS OF ILMENITE AND QUARTZ FORMING ALMOST A DEXTRAL SIGMA CLAST WITH THE TWO EMPTY FIELDS MARKING TAILS. B) EUHEDRAL GARNET WITH ZONING INDICATED BY QUARTZ INCLUSIONS.

Description:

Garnet occur as porphyroclasts up to 1,5 mm in diameter. Small garnets can be euhedral while the largest occur as anhedral fragments. Several grains of garnet can make aggregate porphyroblasts. The small euhedral garnets show zonation marked by rims of micron sized opaque minerals. Inclusions of ilmenite are common and occurs as up to 0,1 mm elongated grains between the garnets. Some of the ilmenite inclusions run through the garnet grain from one edge to the other, curving gently. Clouds of fine grained minerals form spiral patterns or distinct areas in some of the garnets. These less than 10 micron grains are assumed to be also ilmenite. Other inclusions that occur is quartz, titanite and a anhedral low birefringence mineral that might be zoisite (SEM shows calcium). Some of the quartz inclusions make trains that are parallel to the ilmentite inclusions. This is also the case where the clouds of fine grained opaque minerals have a spiral-forming texture. Here the quartz makes bands that form disconnected semi circles. Garnet fragments that make aggregate porphyroclasts are separated by masses of fine, micron-sized muscovite and sometimes biotite, though biotite occurs as larger, more tabular grains. These masses of muscovite appear folded and bent at some locations. Pressure shadows of quartz, muscovite, biotite and chlorite form around the porphyroblasts forming long distinct tails.

Muscovite forms a gradational spaced foliation; alternating between quartz rich microlithons and muscovite and biotite rich cleavage domains. It usually occurs as tens of microns wide elongated grains sub parallel to foliation unless bending around porphyroclasts. In some areas, the foliation becomes more continuous and here the muscovite can be subtly folded crating an S-C texture. Slightly larger grains occur in the pressure shadows of porphyroclasts; becoming up to 50 microns wide. A single 0,1 mm wide elongated grain occurs, markedly larger than the main population of muscovite.

Biotite usually occurs as tabular grains up to 0,1 mm wide elongated sub-parallel to lineation. Some grains however seem to be orientated perpendicular to lineation as they show strong pleochroism when the lower polarizer is oriented perpendicular to foliation. These can be up to 0,2 mm wide and of rectangular shape, sometimes featuring polysynthetic twins and cracks filled with quartz. Inclusions of high relief zircon with pleochroic halos are common in the biotite observed in the matrix, but does not appear to occur in biotite present in the porphyroclasts' pressure shadows.

Hornblende occurs as 0,3 mm wide rounded or anhedral to tabular subhedral grains oriented parallel to lineation in the latter case. Some have inclusions of quartz and fine grained opaque minerals similar to the opaque clouds seen in garnet, making distinct curved lines of inclusions. One porphyroclast made of two distinct grains of chloritoid is separated by a mass of elongated micas that connect the two.

Ilmenite occurs as subhedral crystals 0,1 mm wide elongated parallel to lineation in the matrix. They have tails of muscovite and biotite and anhedral inclusions of quartz, muscovite and biotite. Some of the quartz inclusions show undulatory extinction. Ilmenite also occurs as inclusions in the garnet, then it is similar size to the ilmenite in the matrix.

Chlorite occurs in the tail of one of the bigger garnet porphyroclasts and in some of the mica rich cleavage domains with grains sizes similar to that of biotite.

Quartz usually occurs in the matrix as 50 to 200 microns large anhedral grains where the smaller grains tend to be in the cleavage domains. The larger grains tend to be pinned by mica and show elongation along lineation. Boundaries tend to be straight to curved and there is no undulatory extinction except in some of the larger grains and in grains present as inclusions in ilmenite. Patches of up to 0,6 mm wide larger grained quartz occur, these tend to taper out parallel to foliation. Grains show undulatory extinction and lobate grain

boundaries with sub grains about 50 microns wide.

Crystals of plagioclase up to 1mm wide occur, featuring inclusions of titanite, tourmaline and muscovite and possibly opaque minerals. It has a poikiloblastic texture with inclusions of anhedral plagioclase of different extinction than the parent crystal. The porphyroclasts feature thin patchy mantles of 50 micron wide grains and tails of biotite and muscovite. Calcite occurs as 50 micron wide disconnected ribbons in some of the quartz microlithons and as single grains in others. It also occurs as constituents in areas with grains of quartz larger than the usual 50 microns that folds the foliation around it like a porphyroclast. Epidote occurs as single around 0,1, up to 0,2 mm anhedral grains spread out in then thin section. At one location epidote forms around a 0,1-mm wide grain of titanite at opposite sides of the grain.

Structures

Some of the porphyroclastic garnets form sigma clasts with straight tails. These sigma clasts consistently feature tails that taper out dextrally and some feature strain shadows of muscovite that curve clockwise. Two fragments of amphibole are separated by tracking fibres of muscovite that taper out dextrally. Muscovite also form elongated lozenge shapes with differing aspect ratios, tending to taper out dextrally, forming mica fish. Some with large aspect ratios have tips that taper out sinistrally. The mica fish coincide with the presence of a 20 degree tilted S-C' fabric that is indicated by systematic and limited folding of the foliation. The shear bands tend to coincide with the tapering tips of the mica fish, cutting across the foliation. Some of the elongated opaque minerals show unsymmetrical tips that are arranged with the tips tapering out dextrally and can also feature dextrally tapering tails of biotite. The biotite crystals that seems to be elongated perpendicular to lineation have a lozenge shape with dextrally tapering crystal faces.
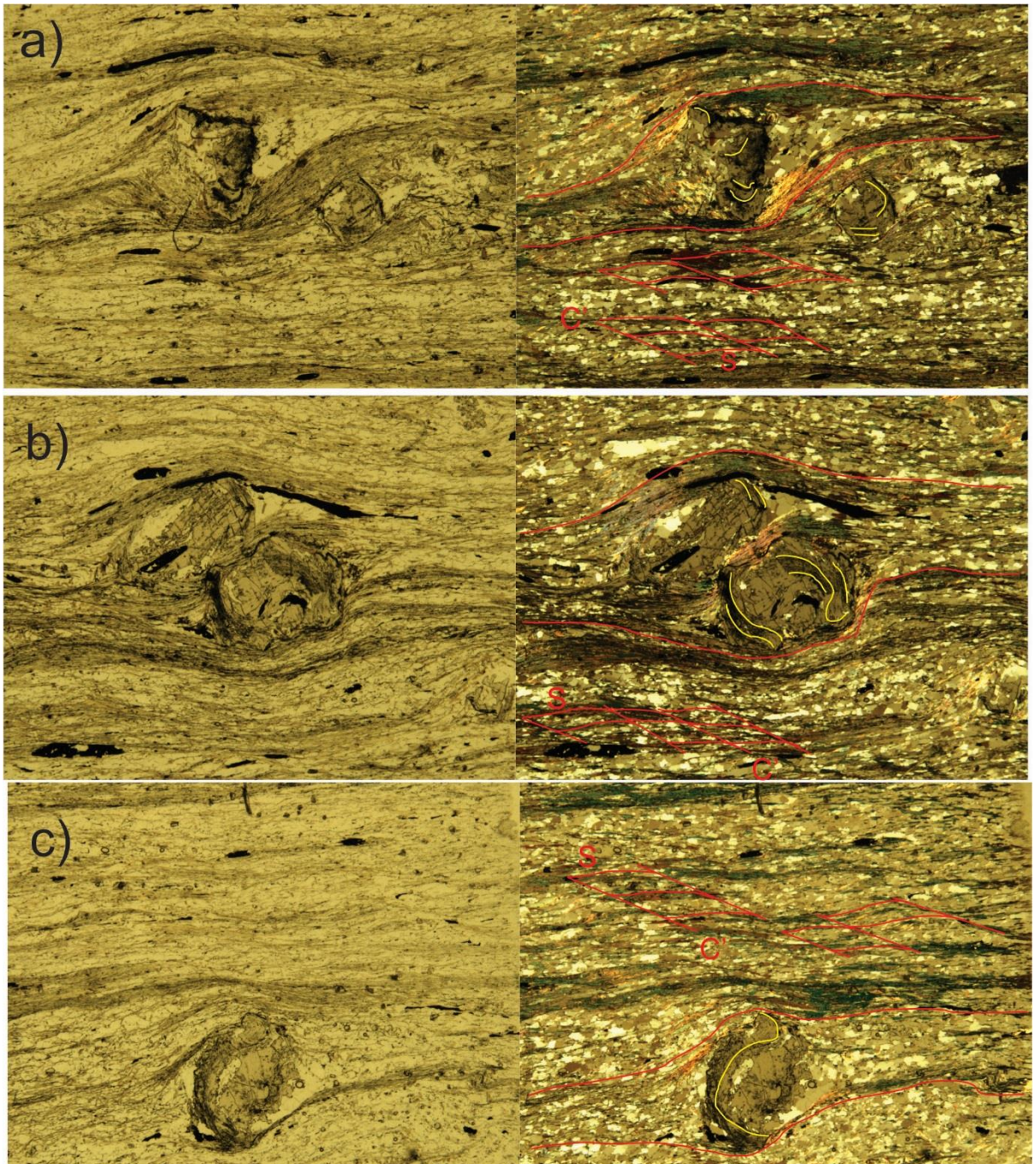
FIGURE 53: SENSE OF SHEAR INDICATORS IN SAMPLE 14, LEFT IS PPL, RIGHT IS XPL, RED ARROW MARK LINEATION. A) DEXTRAL SIGMA CLAST WITH DEXTRAL S-C' FABRIC. MUSCOVITE INDICATE AREAS OF HIGH PRESSURE, WITH PRESSURE SHADOWS INDICATING LOW PRESSURE. OPAQUE INCLUSIONS INDICATE EARLIER FOLIATION, SUGGESTING SYN-TECTONIC GROWTH AND POSSIBLY DEXTRAL SENSE OF SHEAR. B) AND C) SIMILAR TO A, BUT CLEARER OPAQUE POSSIBLE SYN-GROWTH FOLIATION. SUGGESTING ASYMMETRIC GROWTH DEVELOPMENT AND A ROTATION OF AROUND 180 DEGREES OR CHANGING SENSE OF SHEAR.

Thin section 15 – Koppangen Quartzite
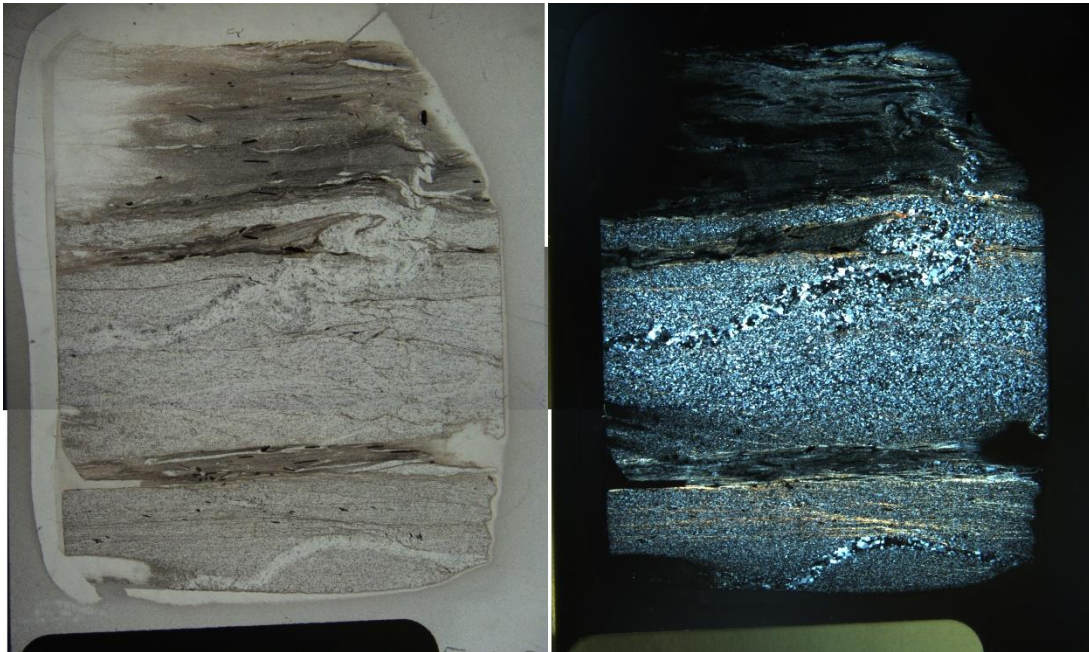
FIGURE 54: OVERVIEW OF THIN SECTION FROM SAMPLE 15. FIELD OF VIEW IS ABOUT 3 BY 5 CM. LINEATION IS HORIZONTAL. INTERFINGERING LAYERS OF MOSTLY QUARTZ AND MUSCOVITE WITH BLACK SPECS OF OPAQUES. FOLDED QUARTZ LAYERS.

Minerals: Quartz (70 %), muscovite (25 %), opaques (4 %), zoisite (1 %)

Occurrence: Bands of coarse and fine grained quartz. Some bands feature single lone floating mica while others feature small mica aligned parallel to foliation.
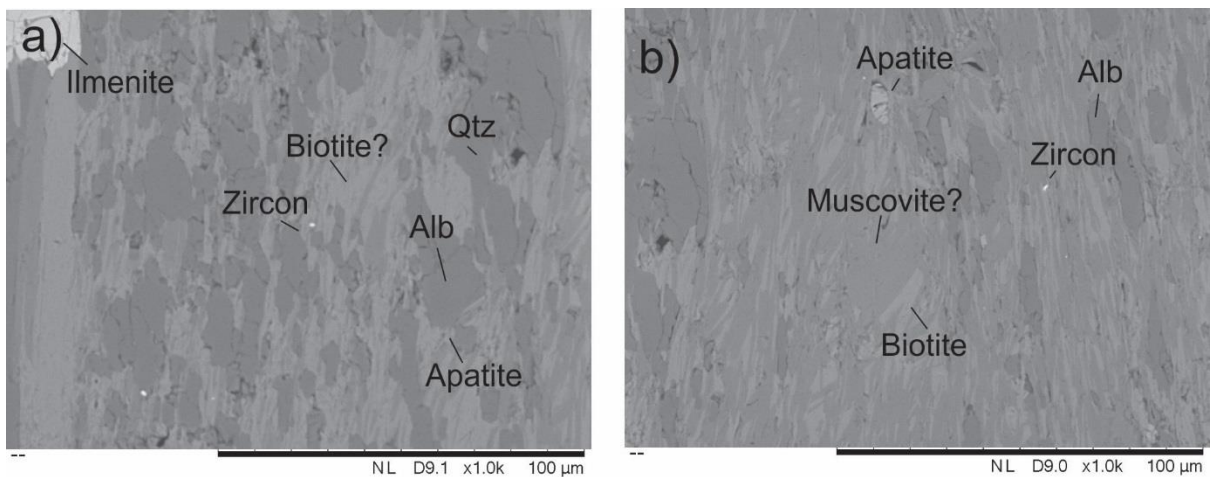
FIGURE 55: BACKSCATTER PICTURES OF SAMPLE 15. VERTICAL LINEATION. A) MOSTLY ALBITE AND SOME BIOTITE AND QUARTZ WITH OPAQUE MINERALS OF ILMENITE AND SMALL GRAINS OF ZIRCON. B) CONTINUATION OF A), OVERLAP TO THE LEFT, SHOW THE TRANSITION INTO A DOMAIN WITH MOSTLY MUSCOVITE AND BIOTITE. NOTE THAT THE MINERAL IDENTIFICATIONS ARE SOMEWHAT UNCERTAIN AS THEY COULD NOT BE VERIFIED WITH A TRANSMITTED LIGHT MICROSCOPE DUE TO SCALE.

Description:

Quartz occur as anhedral grains with several modes of grain size depending on microlithon. It varies from a few microns to 0,3 mm. The largest grain sizes from bands that traverse the thin section diagonally with folds that have axial traces sub parallel and perpendicular to lineation. Areas of grains of around 50 microns wide alternates with areas featuring grain sizes of a few microns. Boundaries are abrupt to gradual and always accompanied by masses of fibrous mica. Grain boundaries are straight to curved and grains show no undulatory extinction.

Muscovite form a spaced to continuous foliation and areas rich in muscovite correlate to areas with the smallest quartz grain size. It usually occurs as few to tens of microns wide fibres sub parallel to lineation, but can also be oriented in a conjugated fashion in some areas. Between the muscovite rich domains muscovite make a continuous foliation with gradual variations in concentration when traversing perpendicular to lineation. The bottom section of the thin section appears to be more muscovite rich than the mid-section and the middle section feature an area with thin bands of muscovite that run diagonally across lineation. These bands are also visible in the quartz, albeit subtly.

Opaque minerals occur as tabular to shredded shaped grains usually elongated parallel to lineation. They are most common in mica rich areas, and only a few can be observed in the mid-section rich in quartz. They feature anhedral inclusions of quartz a few microns wide that tend to show undulatory extinction.

Zoisite occur in the lower section of the thin section and appear to be absent from the middle area. It occurs as 0,1 mm wide anhedral shredded grains with inclusions of quartz. Under electron microscope the thin section appears as repeating bands of silicon, iron/aluminium/sodium and potassium that probably reflects the dominant minerals of quartz, biotite/albite and muscovite, indicating iron rich biotite.

Structures:

Mica formed sinistral "mini" mica fish, but also outlined dextral S-C faric as seen in Figure 56.
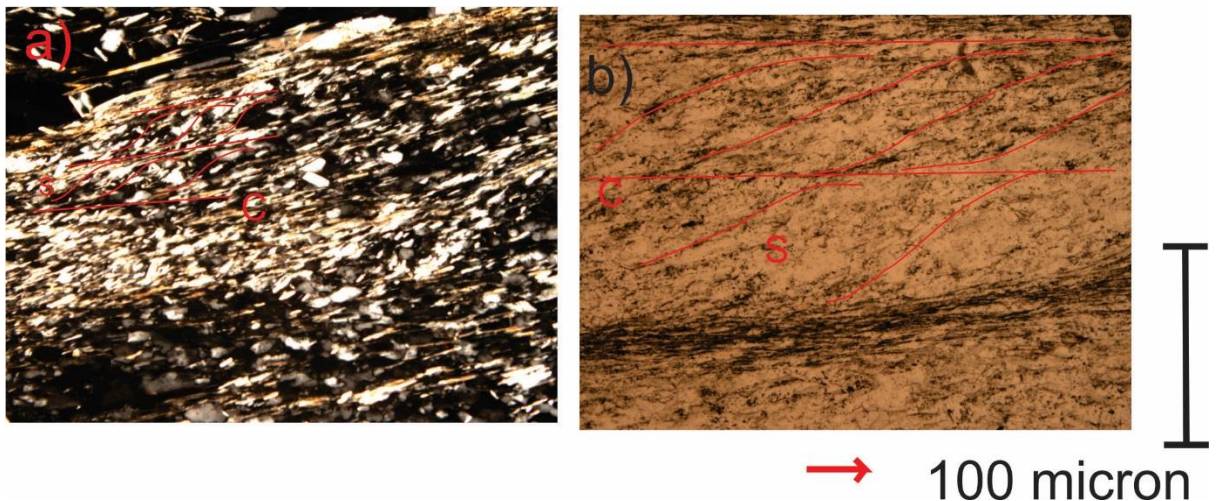
FIGURE 56: STRUCTURES OBSERVED IN SAMPLE 15. RED ARROW MARK LINEATION. A) AND B) SHOW DEXTRAL S-C FABRIC.

Lyngen chlorite schist

Field description

FIGURE 57: OUTCROP PICTURES OF FEATURES IN THE KJOSEN CHLORITE SCHSIT. A) BRECCIA OF HOST ROCK ALONG EDGE OF GRANODIORITIC INTRUSION. B) INTRUSION SEEN IN A) FROM FURTHER AWAY, CONCORDANT TO FOLIATION. C) SHEARED LENSES OF QUARTZ IN A CHLORITE SCHIST, LOOKING WEST. HAMMER FOR SCALE.

Petrology

The unit appeared to be easily erodible and would tend to form deeply incised rivers when in contact with more erosion resistant units like the gneiss. Glacier rivers tended to follow this unit south of Nordkjosbotn. It appeared as a deep green to black rock varying from massive very fine grained to foliated coarser grained. Intrusions of a white tonalite/granodiorite occurred along with brecciated host rock and lenses of quartz was common.

Structures

A few structures interpreted to be shear bands was observed indicating top east sense of shear. Foliation would usually dip 30-40 degrees to the west and have a W-E lineation.

Locally foliation could fold or change regularly to a sub vertical orientation (it was not clear) with a wavelength of 30 meters, showing a horizontal N-S lineation.

FIGURE 58: S-C' FABRIC TO THE LEFT AND S-C FABRIC TO THE RIGHT IN GREENSCHIST. PEN FOR SCALE, LOOKING SOUTH.

Lyngen amphibolite

FIGURE 59: AMPHIBOLITE UNITS IN THE FIELD. A) AMPHIBOLITE SCHIST WITH STRETCHING LINEATION ORIENTED W-E AS INDICATED BY COMPASS. B) AMPHIBOLITE MIGMATITE WITH BLACK-GREEN AMPHIBOLE AND WHITE PLAGIOCLASE. GPS FOR SCALE.
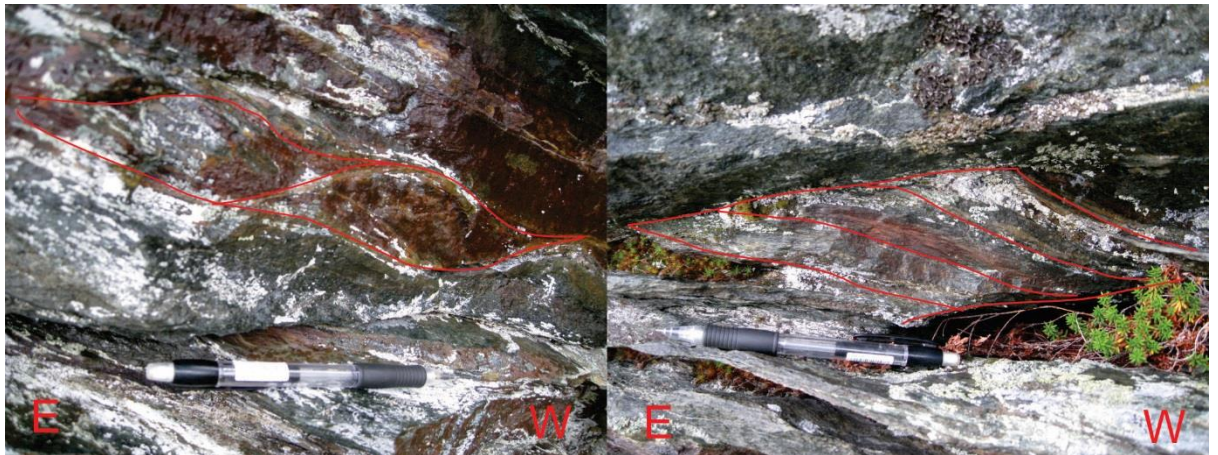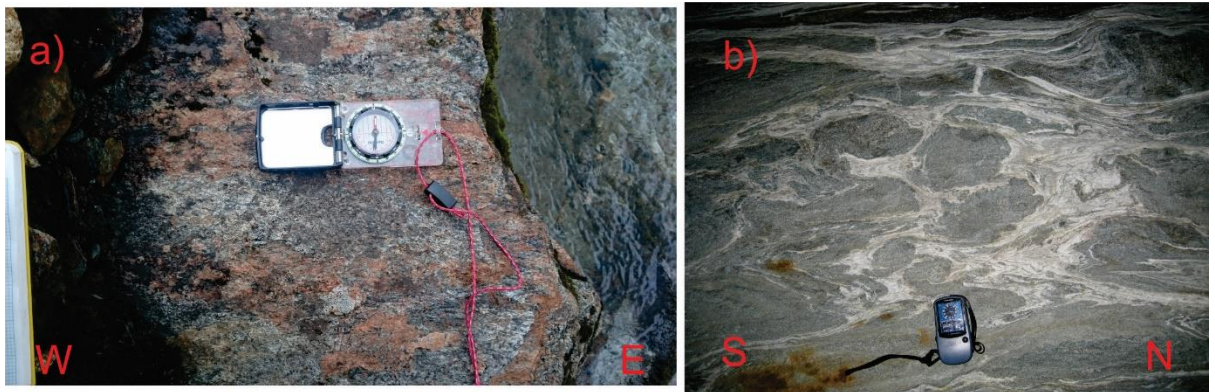
Petrology

The amphibolite appeared as a black to green intermingled with white rock. The proportions between white plagioclase and black/dark green amphibolite would vary. By the underlying phyllite contact it would appear as a amphibole schist with fine to very coarse needles of amphibole elongated parallel to lineation in a silvery foliated matrix of sericite and/or plagioclase. Further from the underlaying contact up it would appear more massive, sometimes with a spaced foliation, with rounded fine to coarse grains of plagioclase in a matrix of amphibole. Higher up it could have a migmatic texture as seen in figure 5 with portions of intermixing darker amphibolite and white plagioclase. The transition between amphibolite and meta gabbro appeared gradual.

Structures

The unit featured a west dipping foliation and W-E lineation that would vary in intensity through the section, generally decreasing in intensity upwards.

Thin section description

Two thin sections were made from this unit.
Sample 8 was taken from an outcrop at the east slope of Perstinden. This outcrop featured sinistral macro scale shear bands and formed a small hill in the terrain.

Sample 13 was taken west of Storvatnet, higher up along the river than previously mentioned samples in the area. The outcrop featured a clear lineation and was part of a straight riverbed that was hardly eroded into by the river.
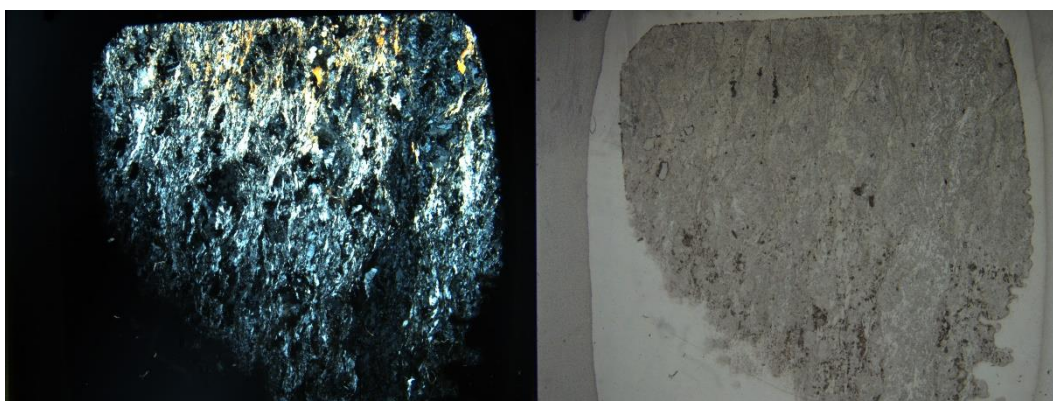
FIGURE 60: OVERVIEW OF SAMPLE 8 THIN SECTION, FIELD OF VIEW 3 BY 2,5 CM. LEFT IS XPL, RIGHT IS PPL. BOTH SHOW A WAVY FABRIC.

Minerals: Hornblende (50 %), zoisite (20 %), plagioclase (15 %, oligoclase judging by SEM data), epidote (10 %), chlorite (4 %), quartz (1 %)

Accessories: Titanite, rutile

Occurence: The epidote/zoisite occur as porphyroclasts in a matrix of bent actinolite and chlorite and anhedral plagioclase that range from oligoclase to anorthosite in composition.

Description:
Amphibole occur as thin fibrous grains forming a spaced anastomosing to conjugate foliation, occurring locally with chlorite. This foliation folds around aggregates of plagioclase, epidote and more columnar shaped amphibole. The amphiboles appear shredded and coexist with a low birefringence mineral thought to be epidote. Plagioclase occur as 50 to 200 micron large grains with undulatory extinction and inclusions that is thought to be zoisite due to low birefringence, high relief and occurrence. Epidote/zoisite of sizes varying from tens of microns to hundreds of microns in diameter occur as columnar grains usually with plagioclase and a few quartz grains.

Plagioclase composition varies from Oligoclase to Bytwnite with more Ca-rich members occurring in smaller grains inside less Ca-rich grains. Amphibole show a composition that suggests hornblende with high magnesium content.

Plag comp	Na atom C %	Ca atom C %	Al atom C %	Si atom C %		Anorthite %	
1	2,22	6,64	13,25	16,17	Small grain in	74,94356659	Bytownite
2	5,52	3,05	10,62	20,93		35,58926488	Andesine
3	5,93	2,35	9,81	20,92		28,38164251	Oligoclase
4	6,32	2,18	9,95	20,94		25,64705882	Oligoclase

FIGURE 61: TABLE OF ELEMENT COMPOSITION FROM A EDS SCAN OF GRAINS OF PLAGIOCLASE IN SAMPLE 8. VARIATION IN SODIUM CONTENT AND CALCIUM CONTENT. MOST GRAINS HAVE A SODIUM CONTENT OF 5-6

Amp comp	Na atom C %	Ca atom C %	Al atom C %	Si atom C %	Fe atom C %	Mg atom C %	Mg %
1	1,83	3,62	6,26	19,46	1,34	8,48	0,86
2	1,01	5,02	4,91	18,16	1,96	8,46	0,81
3	1,01	3,72	4,1	19,16	1,54	9,73	0,86
4	0,38	0,85	8,73	11,36	2,57	12,05	0,82

FIGURE 62: TABLE OF ELEMENT CONTENT DERIVED FROM EDS SCAN OF AMPHIBOLE GRAINS IN SAMPLE 8. AMPHIBOLE NUMBER 4 IS ABNORMAL COMPARED TO THE REST AND MIGHT BE ANOTHER MINERAL. REST INDICATE COMPOSITION RESEMBLING HORNBLENDE.

Structures:

Sample 8 featured large shear bands outlined by elongated grains of amphibole that crossed diagonally across the thin section, interspacing larger amphibole and epidote grains. Sense of shear is hard to determine due to intensity and quantity. Both sinistral and dextral S-C' fabric is common, one terminating into the other as seen in Figure 63. C-planes varied from 20 to 40 degrees with the dextral S-C' fabric being generally steeper than the sinistral S-C' fabric. Overall the sense of shear was interpreted to be sinistral as these shear bands were more common.
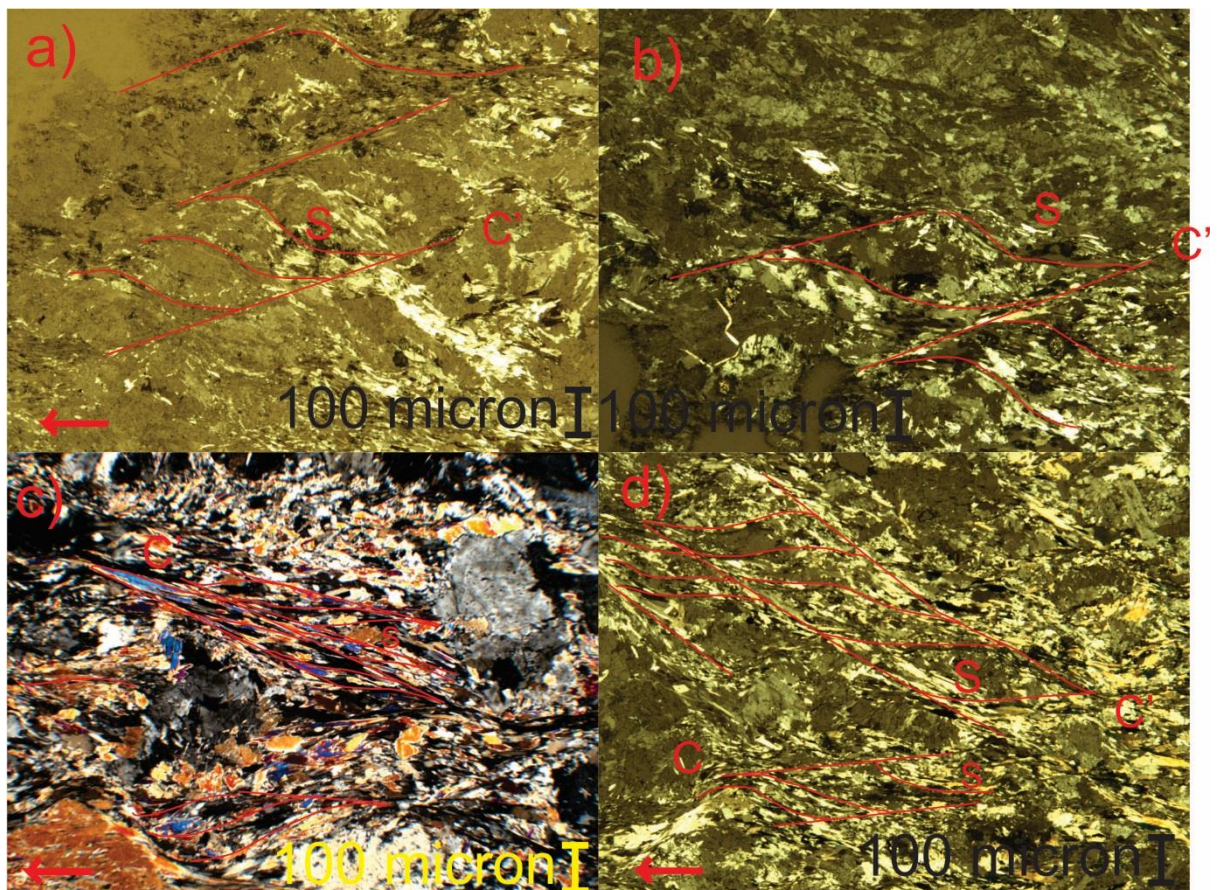
FIGURE 63: OVERVIEW OF SENSE OF SHEAR STRUCTURES OBSERVED IN SAMPLE 8 IN XPL. RED ARROW MARK LINEATION, RED MARKINGS INDICATE S- AND C-PLANES. A) AND B) SINSITRAL S-C' FABRIC OUTLINES BY ALIGNED AMPHIBOLE. C) STEEP DEXTRAL S-C' FABRIC. D) DEXTRAL S-C' FABRIC AND SINISTRAL S-C FABRIC CO-EXISTING AND SEEMINGLY INTERCEPTING.

Thin section 13 – Lyngen Amphibolite
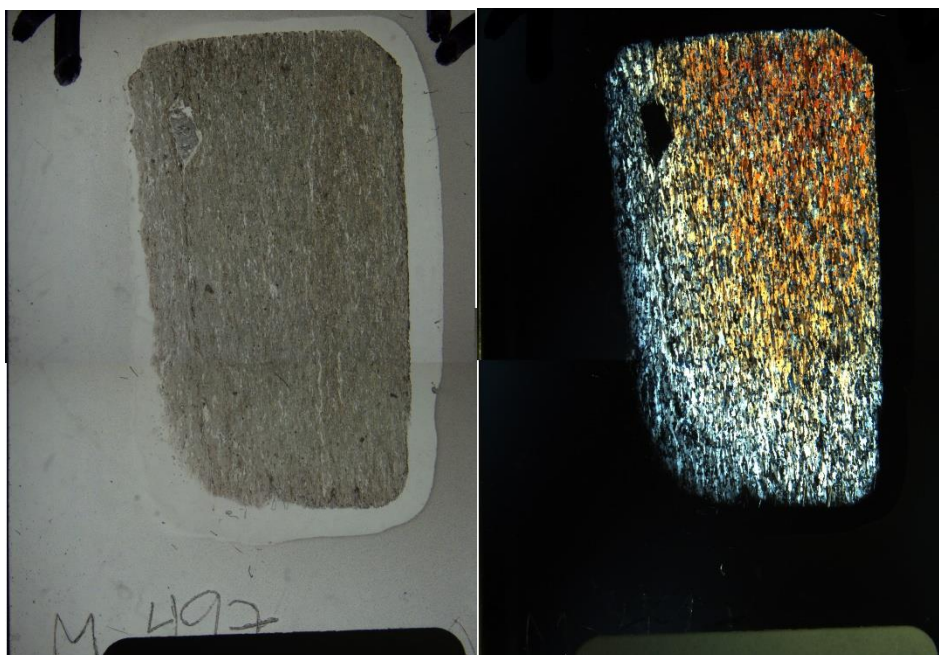
FIGURE 64: THIN SECTION SAMPLE 13 OVERVIEW. LEFT IS PPL, RIGHT IS XPL, FIELD OF VIEW 3 BY 5 CM. SINGLE CLAST OF PLAGIOCLASE VISIBLE IN EXTINCTION UPPER LEFT. WAVY FABRIC OF EPIDOTE, AMPHIBOLE AND PLAGIOCLASE VISIBLE IN XPL.

Minerals: Hornblende (65 %), epidote (10 %), albite (10 %), zoisite (10 %), quartz (5 %)

Accessories: Titanite, apatite, rutile, zircon

Occurrence: Amphiboles aligned sub parallel to lination, making up most of area, with the next most common mineral being clinozoisite-epidot that appear as anhedral rounded grains. Plagioclase occur as phenocrysts with zoisite needles. Smaller grains of quartz and albite make up matrix along with amphibole.
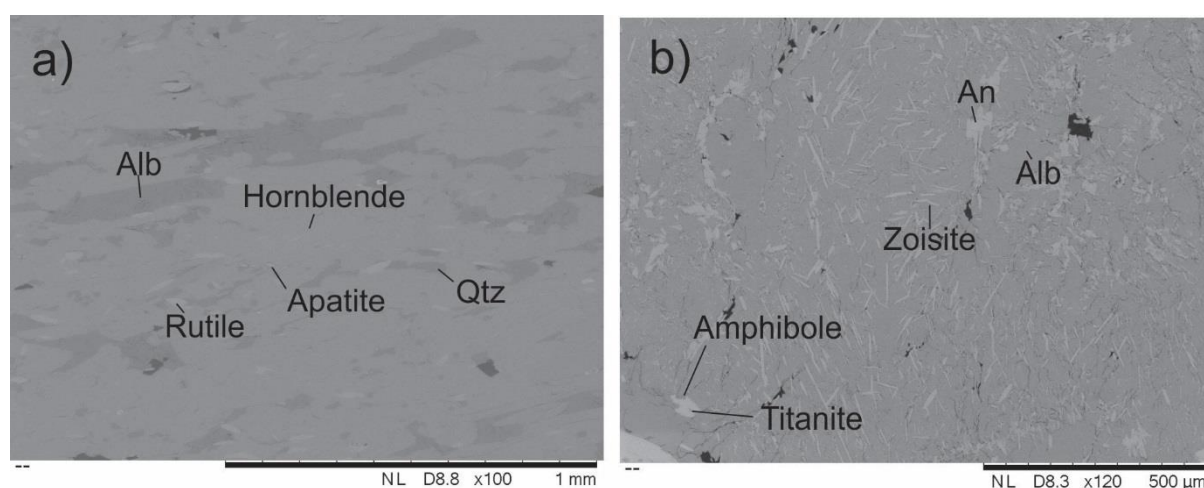
FIGURE 65: BSE IMAGE OF SAMPLE 13. A) MOSTLY HORNBLENDE SURROUNDED BY ALBITE AND QUARTZ WITH SOME ACCESSORY MINERALS PRESENT. B) CLOSE UP OF INGLE PLAGIOCLASE GRAIN SEEN IN SAMPLE 13 SHOWING INCLUSIONS OF ALBITE, ANORTHITE AND ZOISITE NEEDLES WITH MULTIPLE ORIENTATIONS.

Description:
Hornblende occur as coarse-sized elongated grains parallel to lineation with a uniform grain size distribution. This makes a continuous foliation that is slightly folded diagonally across the lineation. Grain boundaries are curved to straight and the grains are anhedral to subhedral. Usually only one set of cleavage is visible.

Epidote occurs as sub rounded to rounded anhedral coarse sized grained with a uniform distribution. They are distributed evenly through the thin section, but also tend to mark out the slight folding foliation by slight elongation and subtle variation in concentration.

Zoisite occur as sub rounded to rounded anhedral coarse sized grains in the matrix, distinguished by epidot by the parallel extinction. It also appears in plagioclase porphyroclasts as euhedral needle shaped inclusions tens of microns in size.

Plagioclase occurs in the matrix as coarse subhedral grains, with undulatory extinction and rounded sub grains. No twins are visible and the identification is relying on the presence of inclusions. A single plagioclase porphyroclasts is present. It is 1,5 mm across and is elongated parallel to foliation. The amphibole foliation is folded around it to a limited degree. The edges is jagged and it features three distinct clusters of radiating needles of zoisite, based on SEM observations of Ca content. It has a thin uneven mantle that is most prominent at the corners of the clast.

Quartz appear as coarse elongated grains parallel to foliation that forms single and rough bands of grains. Boundaries are straight to curved and there is no undulatory extinction.

Structures: As with sample 8 this thin section feature both sinistral and dextral S-C' fabric outlined by amphibole and epidote grain boundaries. It was rather regular and incorporated a single porphyroclast of plagioclase. Angle of C-planes was usually around 20 to 30 degrees, being steepest around the plagioclase porphyroclast. Overall the sense of shear is uncertain as the distribution of sinistral and dextral bands are very similar. The plagioclase porphyroclast suggests a dextral sense of shear due to the flow pattern.
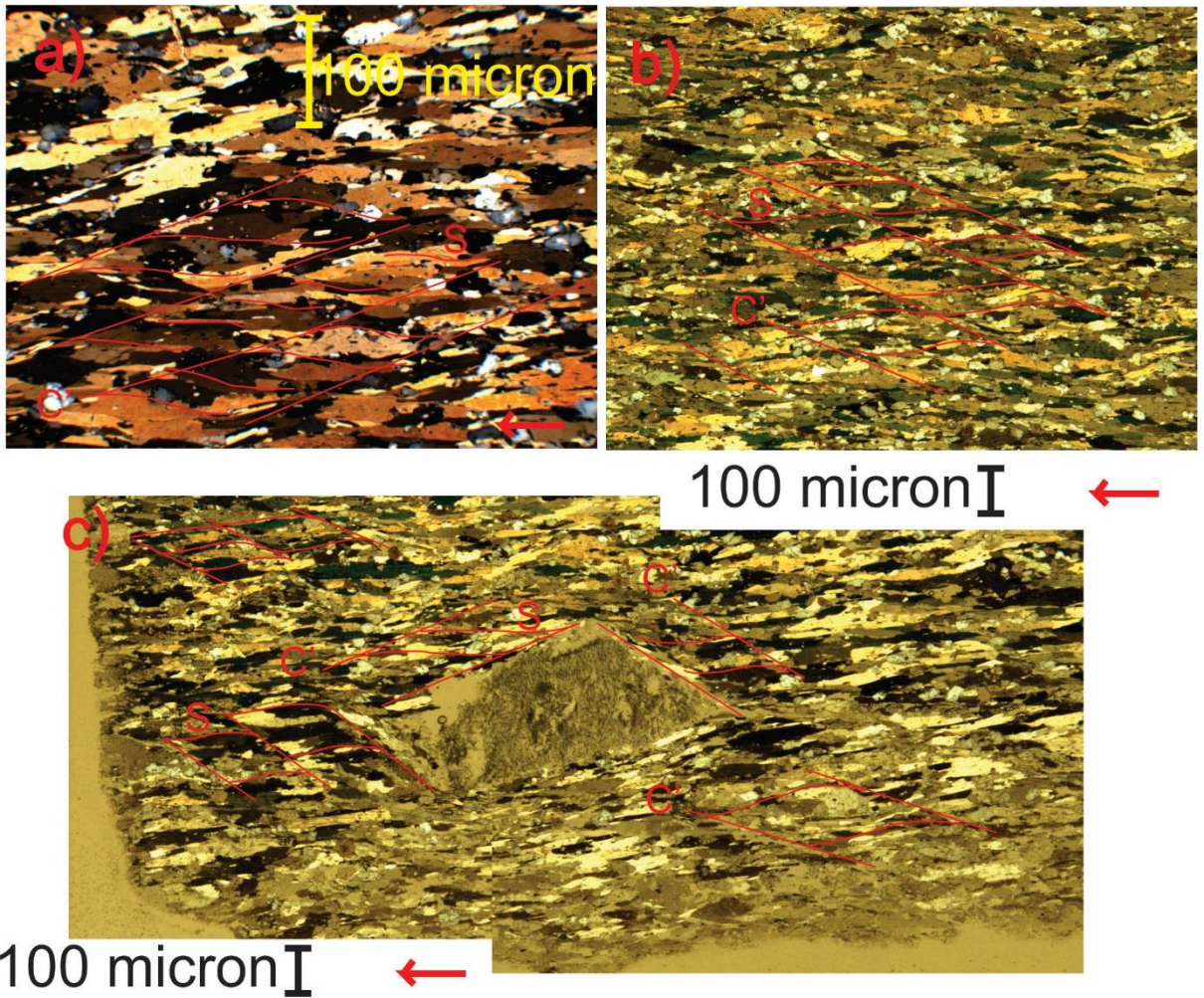
FIGURE 66: STRUCTURES OBSERVED IN SAMPLE 13. RED ARROW MARKS LINEATION, RED MARKINGS INDICATE C- AND S-PLANES. A) SINISTRAL S-C' FABRIC OUTLINES BY AMPHIBOLE. B) DEXTRAL S-C' FABRIC OUTLINED BY AMPHIBOLE. C) PDEXTRAL PLAGIOCLASE SIGMA CLAST OUTLINED BY DEBTRAL S-C' FABRIC AND SINISTRAL S-C' FABRIC.

Amphibolite quartz samples

One thin sections were gathered from a quartz lens in a massive green amphibolite outcrop south of Rørnesfjellet. The lenses occurred as cm thick continuous layers parallel to foliation, sheared brittly in a ductilly sheared parent rock.

Thin section 4 – Lyngen, Quartz sample from amphibolite schist
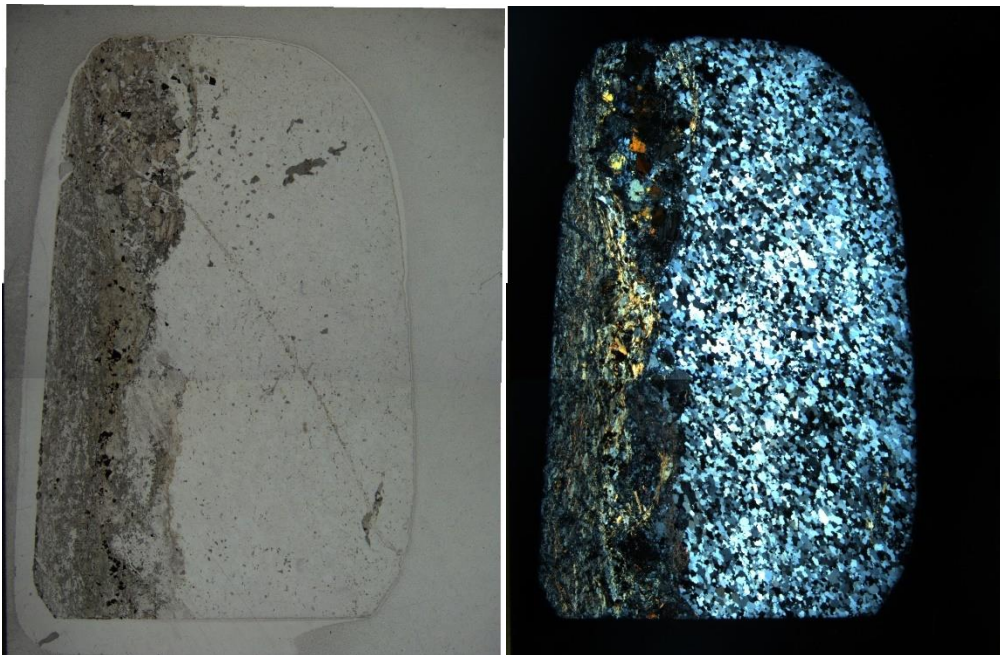
FIGURE 67. SAMPLE 4 THIN SECTION OVERVIEW. LEFT IS PPL, RIGHT IS XPL. FIELD OF VIEW IS 3 BY 5 CM. (FIX)

Minerals: Quartz, hornblende, tremolite-actinolite, sericite/muscovite, clinozoisite/epidote

Accessories: Rutile, titanite

Description: Quartz occur as the only mineral in two thirds of the tin section and in a vein cutting diagonally across whole of the thin section. The grains are anhedral with a bimodal distribution and straight to curved grain boundaries and show some undulatory extinction. Numerous triple points indicate annealing, with some rounded grains that might indicate sub grain rotation. Grains show systematically max birefriengence when oriented with lineation horizontal similar to sample 3, only with larger grains. Some of the minerals thought to be quartz in the fracture might be plagioclase/feldspar due to seemingly lower birefringence and simple twins/twinning. It might also be deformation lamellae, but the lamellae are not orientated systematically, but seemingly at random. Albite occur as clusters of grains along the edge of the quartz vein, often with alterations of sericite. Grain sizes vary and grain boundaries appear lobate with two domains of extinctions; one with undulatory

extinction and one with abrupt. Deformation are interpreted to be sub grain rotation and bulging, occurring in two domains with bulging being more common close to the vein and sub grain rotation more common further into the host rock.

Hornblende occur in bands along the quartz vein, parallel to lineation and draped around aggregates of muscovite. Tremolite-actinolite occur as parallelogram-shaped agglomerates of broken grains bordering the vein and host rock, suggesting a brittle deformation mechanism. Muscovite occur as fibre shaped grains elongated parallel to lineation while epidote/clinozoiste occur as anhedral grains associated with hornblende. Opaque grains of pyrite occurred with layers of iron oxide, only identified by SEM.

Structures:

Some dextral S-C' fabric was visible, but not very clear.
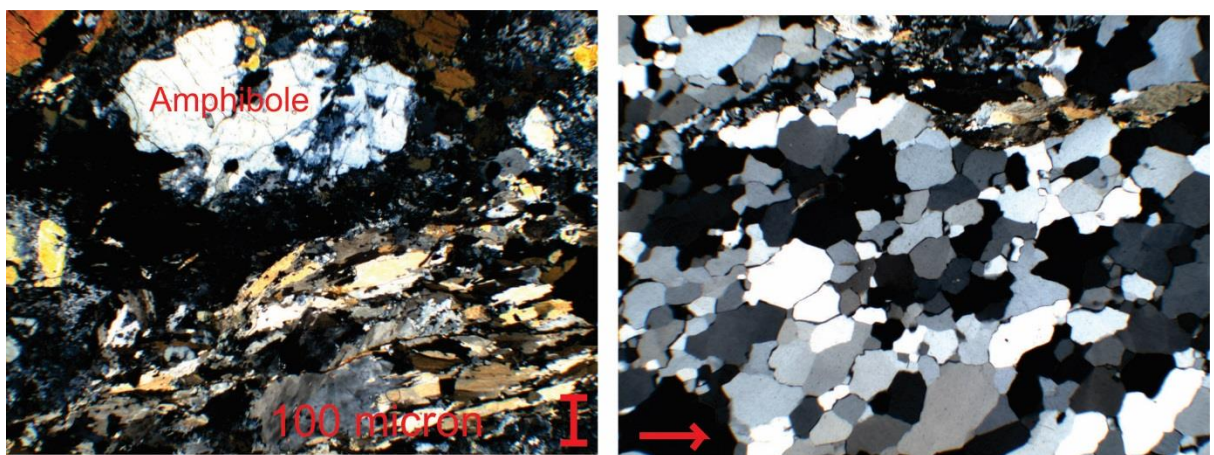
FIGURE 68: CLOSE-UP OF SAMPLE 4 THIN SECTION. RED ARROW INDICATING LINEATION. LEFT XPL IMAGE SHOWS LARGER AMPHIBOLES WITH WHITE BIREFRINGENCE AND SMALLER AMPHIBOLES WITH LIGHT YELLOW BIREFRIENGENCE. RIGHT IMAGE SHOW QUARTZ WITH STRAIGHT GRAIN BOUNDARIES INDICATING HEALING.
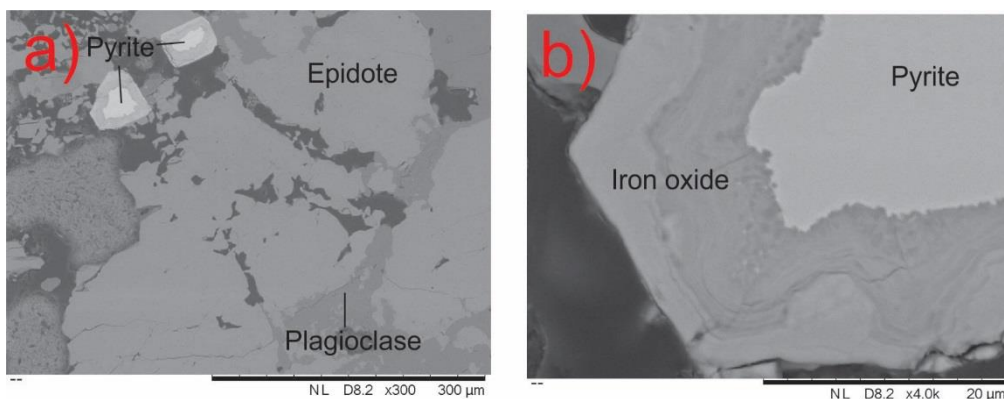
FIGURE 69: BSE IMAGES OF SAMPLE 4. EPIDOTE AND PLAGIOCLASE TOGETHER WITH ZONED PYRITE. B) CLOSE UP OF PYRITE REVEALS THAT THE PYRITE IS ZONED WITH AN COATING OF IRON OXIDE.

Quartz sample

One thin section was gathered from this unit, a greenish looking outcrop of clearly W-E lineated outcrop situated west of Store Russetinden in a glacier scoured valley. The quartz lens was a few cm thick and occurred as a lens flattened parallel to foliation.

Thin section 1 – Lyngen, Quartz sample from a chlorite schist
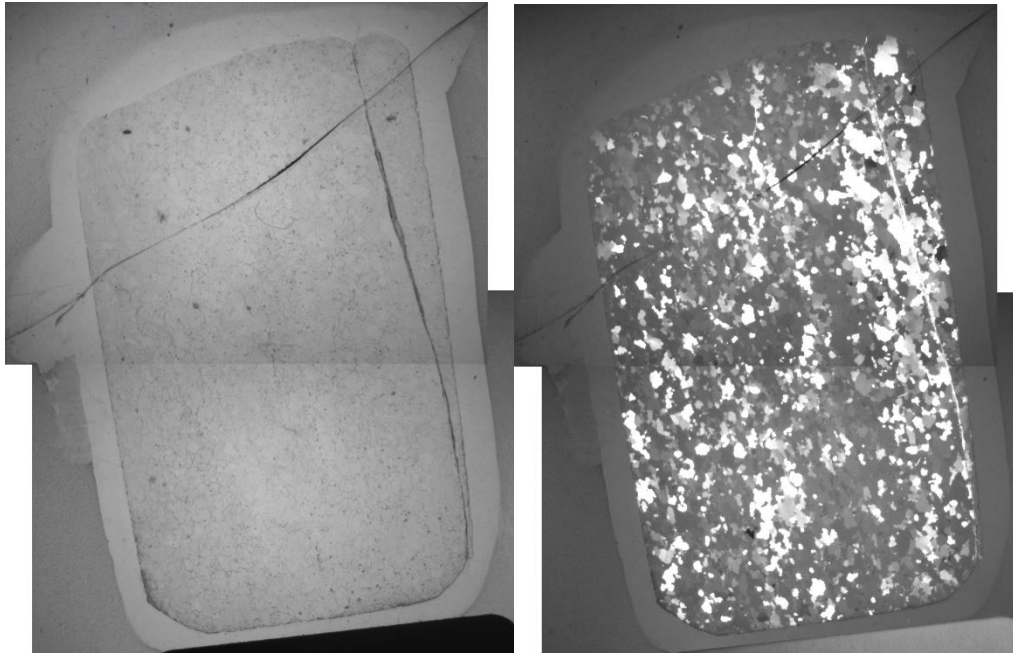
FIGURE 70: OVERVEW OF SAMPLE 1. PPL TO THE LEFT, XPL TO THE RIGHT, FIELD OF VIEW ABOUT 3 BY 5 CM. VERTICAL VEIN OF CHLORITE/MUSCOVITE RUNNING ALONG LINEATION. XPL INDICATE SOME ELONGATION OF GRAINS RUNNING DIAGONALLY AND SOME WEAK DOMAINS OF EXTINCTION.

Anhedral grains of quartz show undulatory extinction and lobate grain boundaries with many triple points. A substantial portion of grains are oriented with c-axis in the foliation plane, normal to lineation evident by always being in extinction. Grain distribution is seriate with clusters of more equigranular grains and there is some degree of elongation parallel to lineation. Deformation processes is interpreted to be grain boundary migration due to lobate grain boundaries. Grain boundaries might correlate with crystal orientation as grains that are permanently extinct tend to have more irregular interlobate grain boundaries while grains with changing birefringence have polygonal grain boundaries and triple points.

Recrystallized fabric, c axis perpendicular to thin section plane in majority of grains. Anhedral grains of quartz show undulate extinction, especially grains that are not aligned with the c axis perpendicular to thin section plane (might be due to these grains being in extinction). Signs of grain boundary migration. Many triple points. Grains with oblique orientation with respect to c have irregular interlobate grain boundaries, some amoeboid. While grains with a perpendicular orientation have polygonal boundaries with triple points(GBAR?). The grain distribution is seriate with clusters of more equigranular sizes. A small degree of grain shape preferred orientation observed in lineation direction. Acicular amphibole and more fibrous muscovite and biotite occur in a single vein that run parallel to lineation. This vein also contain albite with grains of titanite.
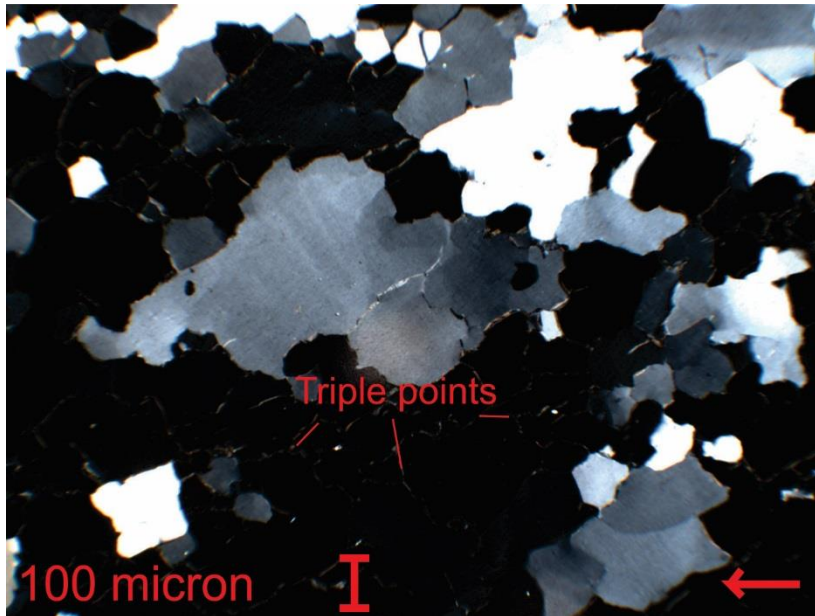
FIGURE 71: LOBATE GRAIN BOUNDARIES INDICATE GRAIN BOUNDARY MIGRATION WITH TRIPLE POINTS INDICATING A DEGREE OF HEALING.

Quartz grain size and fabric

The quartz equivalent radius grain distribution show a mode of around 50 microns with a second local maxima at 250 microns (Figure 72). Equivalent radius projected from spheres based on the area cross sections enhances the mode and removes many of the smaller grains from the distribution. Volume distributions suggests that 35 % of the grains only account for 5 % of the total volume with the local maxima at 250 microns occupying 10 %. Grains have an overall perimeter to equivalent perimeter ratio of 1,313 suggesting that grains are elongated and/or have irregular grain boundaries (Figure 73). Axial ratio to radius plots suggests that larger grains tend to be more elongated than smaller grains. The grain distribution show a preferred long axis elongation orientation at 20 degrees anticlockwise to the lineation while axial ratio is plotted by linear fit to be 0,54.

The particle fabric (Figure 74) suggests a long axis preferred orientation of 16 to 19 degrees anticlockwise to lineation and an axial ratio of 0,827. Fabric is slightly monoclinic indicated by delta alpha (180 – 109 + 16 = 87) and indicate a dextral sense of shear. Grain boundary orientations indicate an overall dextrally elongated parallelogram like fabric with a axial ratio of 0,851, slightly higher than the PAROR analysis.

Quartz preferred orientation (Figure 75) indicate quartz c axis orientations forming a hexagonal pattern in a plane perpendicular to foliation. A-axes form a maximum perpendicular to foliation that is elongated diagonally in a clockwise manner. Overall the girdle indicates a sinistral sense of shear.
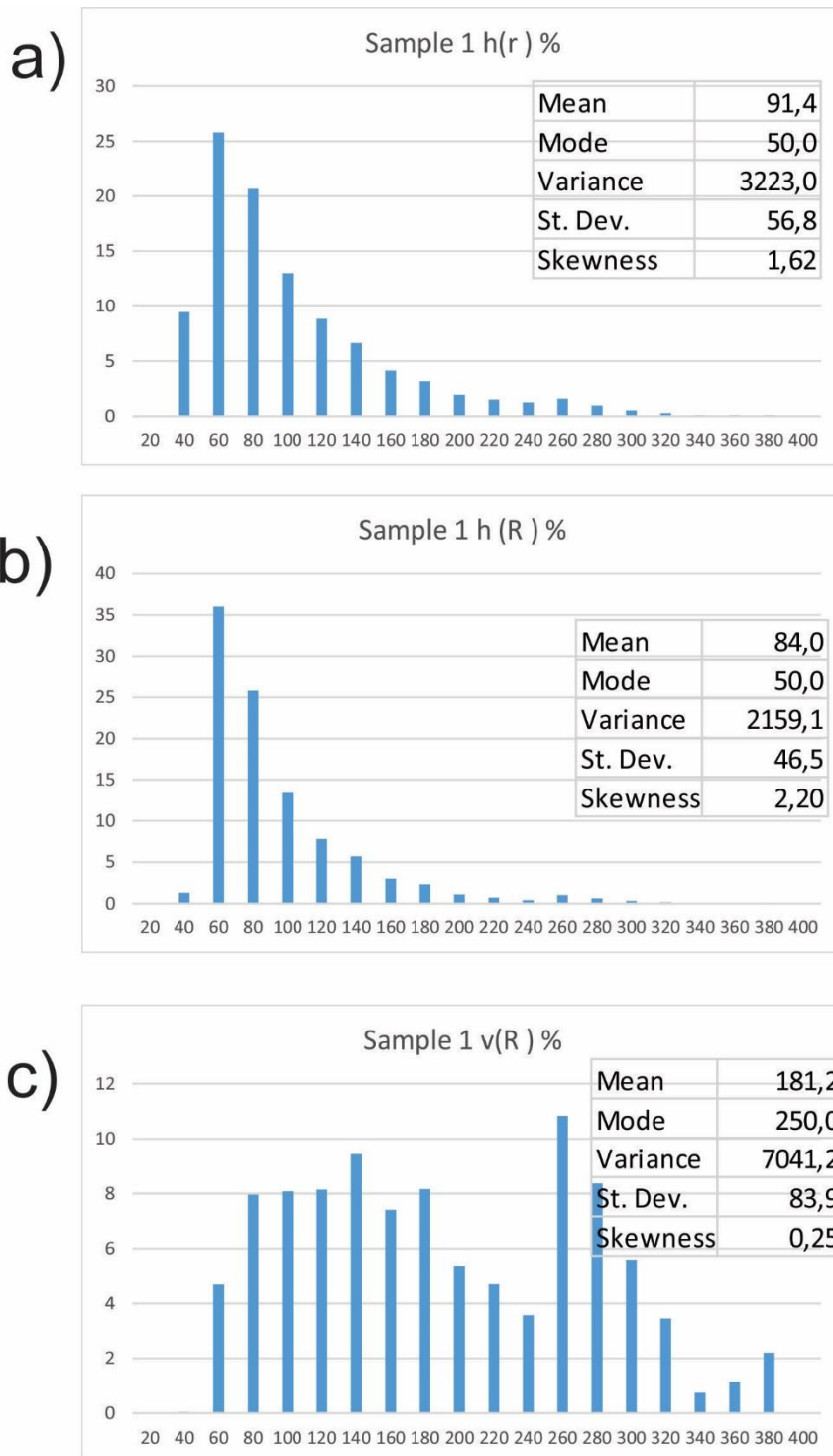
FIGURE 72: GRAIN SIZE DISTRIBUTION OF SAMPLE 1. Y-AXIS ARE PERCENTAGE OF LENGTH AND VOLUME FOR c). X-AXIS SHOW EQUIVALENT GRAIN RADIUS. A) EQUIVALENT RADIUS GRAIN SIZE DISTRIBUTION BASED ON GRAIN AREA. MODE IS ABOUT 50 MICRON, AND MEAN 91,4 MICRON WITH A FAIR NUMBER OF LARGER GRAINS. B) EQUIVALENT RADIUS GRAIN SIZE DISTRIBUTION BASED ON PROJECTED EQUIVALENT GRAIN VOLUME. MODE IS ABOUT 50 MICRONS, MEAN IS 84,0 MICRONS. THE DISTRIBUTION BEING MORE SKEWED AND WITH A SMALLER STANDARD DEVIATION. C) PERCENTAGE OF VOLUME BASED ON EQUIVALENT GRAIN RADIUS. ONLY 5 % OF THE VOLUME IS OCCUPIED BY THE MOST NUMEROUS GRAINS. OVERALL THE DISTRIBUTION INDICATE TWO POPULATIONS; ONE CENTRED AT 50 MICRONS AND ONE CENTRED AT 250 MICRONS, MOST VISIBLY IN THE VOLUME DISTRIBUTION.
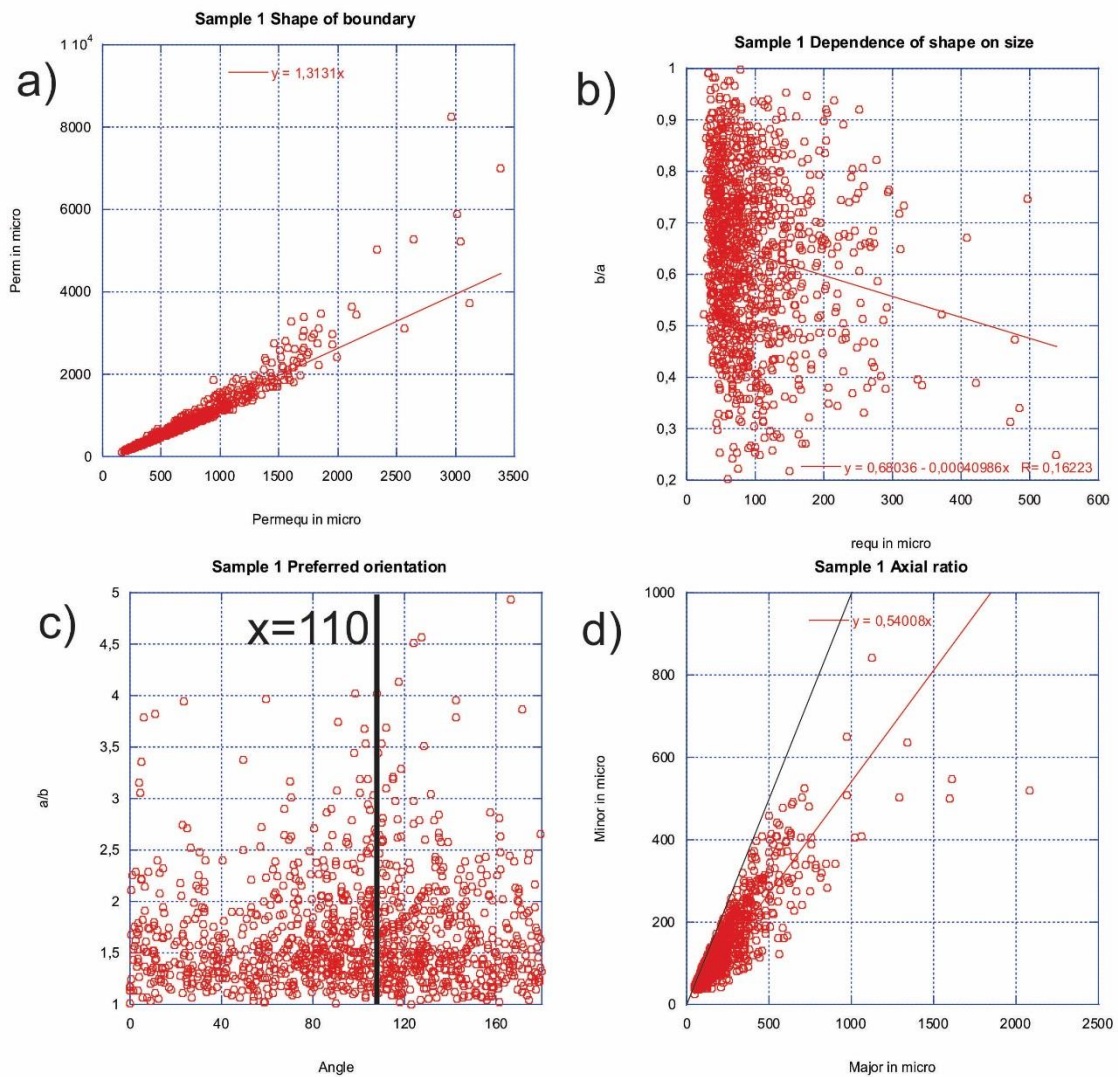
FIGURE 73: GRAIN ATTRIBUTES CORRELATION PLOTS. A) PERIMETER COMPARED TO EQUIVALENT PERIMETER OF GRAINS PLOT INDICATE THAT GRAINS ARE NOT PERFECTLY ROUNDED. LARGER GRAINS MIGHT BE LESS ROUNDED THAN SMALLER GRAINS. B) AXIAL RATIO TO EQUIVALENT RADIUS PLOT. LARGER GRAINS ARE MORE WEIGHTED TO HAVE A SMALLER AXIAL RATIO THAN SMALLER GRAINS. C) ASPECT RATIO TO LONG AXIS ORIENTATION. GRAINS SHOW AN PREFERRED ORIENTATION OF 110 DEGREES TO REFERENCE POINT WHICH TRANSLATES TO 20 DEGREES ANTICLOCKWISE WITH LINEATION AS REFERENCE POINT. D) SHORT AXIS TO LONG AXIS COMPARISON SHOWING THE WEIGHTED MEAN AXIAL RATIO TO BE 0,54. BLACK LINE IS 1/1.
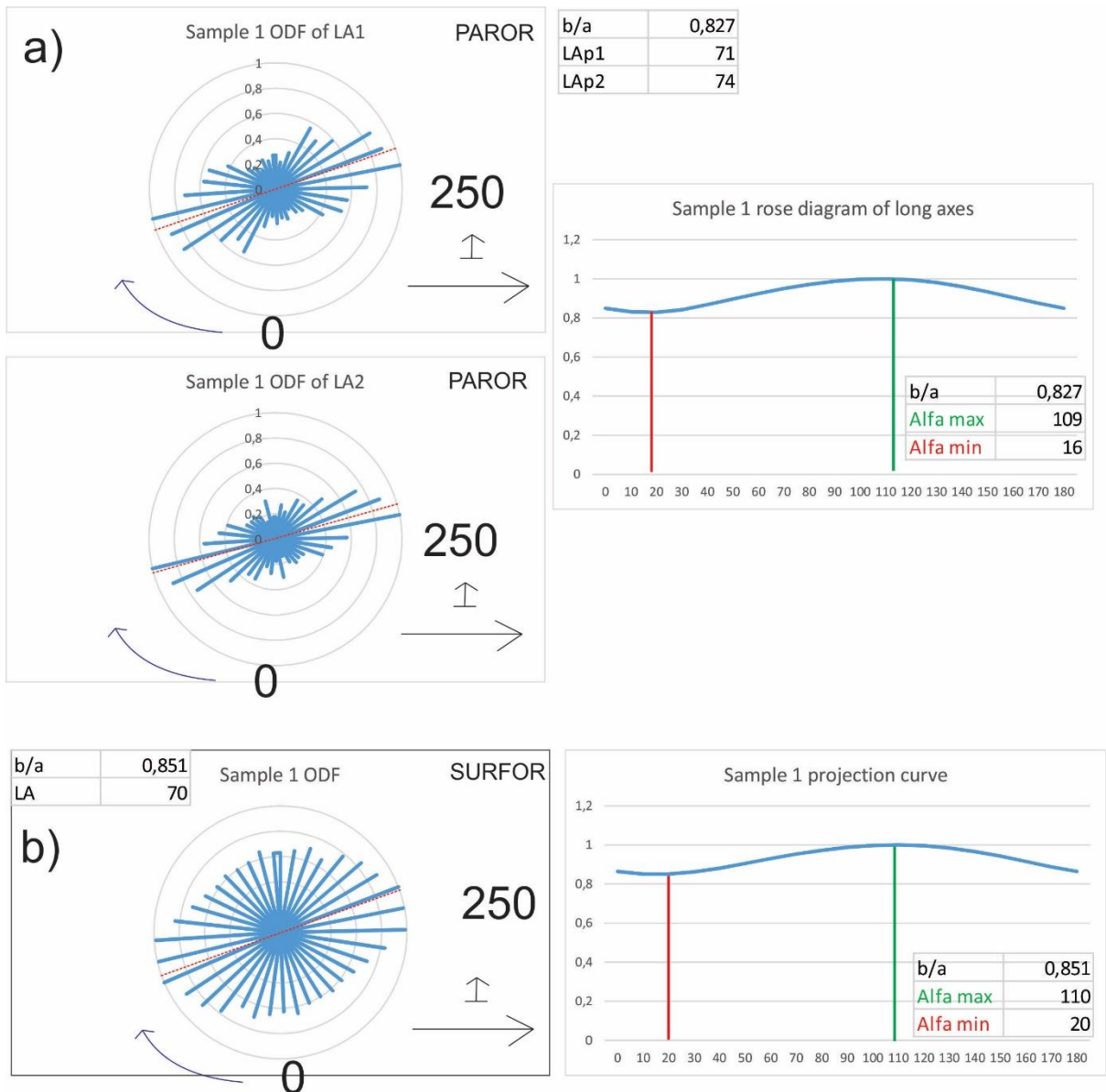
FIGURE 74: PARTICLE ORIENTATION AND FABRIC PLOTS. LEFT SHOW ROSE PLOTS OF PAROR AND SURFOR. PAROR HAVE TWO ROSE PLOTS BASED ON THE LONG AXIS AND THE NORMAL TO THE SHORT AXIS RESPECTIVELY. LINEATION IS MARKED BY HORIZONTAL ARROW, NORMAL TO FOLIATION IS MARKED BY SMALL ARROW. 250 INDICATE THE RIGHT-HAND SIDE ORIENTATION OF LINEATION. 0 WITH AN ARROW IS THE ROSE DIAGRAM NUMBER LINE WHICH RELATES TO THE LA1, LA2 AND LA PREFERRED ORIENTATION VALUES. RIGHT SIDE SHOW PROJECTION LINES EQUIVALENT TO ROSE DIAGRAMS TO THE LEFT. NOTE THAT THE AXES ARE INVERSED COMPARED TO THE ROSE DIAGRAMS. ALFA MAX CORRESPOND TO LONG AXIS PREFERRED ORIENTATION OF THE ROSE DIAGRAMS WHICH ARE MARKED WITH A RED LINE. A) FABRIC BULK LONG AXIS ORIENTATION INDICATE PREFERRED ORIENTATION OF 16-19 DEGREES ANTICLOCKWISE TO LINEATION. ALFA MAX – ALFA MIN = 180 – 109 + 16 = 87 INDICATING A DEXTRAL MONOCLINIC SHAPE AND SENSE OF SHEAR WITH AN ASPECT RATIO OF 0,827. B) SURFOR ROSE DIAGRAM INDICATE AN OVERALL FABRIC ASPECT RATIO OF 0,851 WHICH IS SLIGHTLY HIGHER THAN THE SURFOR DIAGRAM.
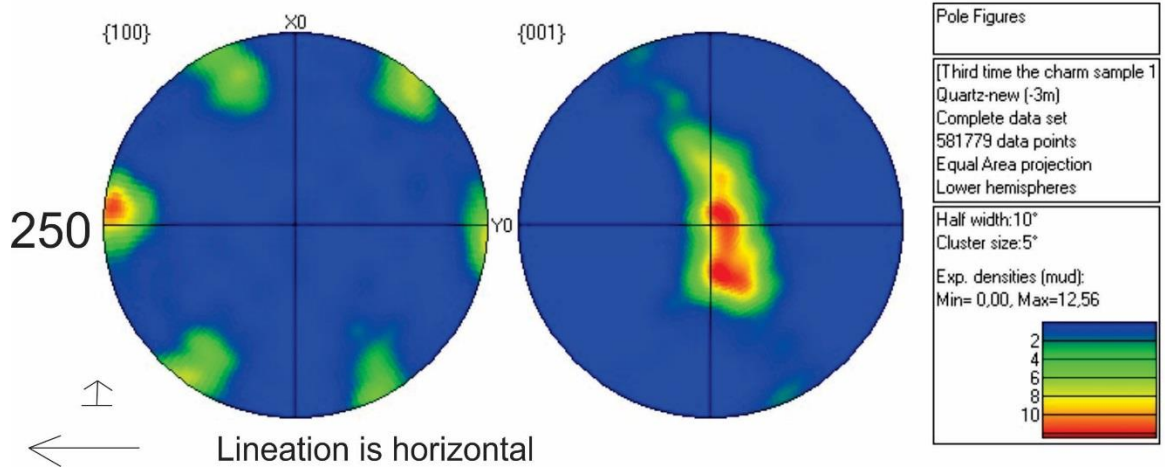
FIGURE 75: CRYSTALLOGRAPHIC PREFERRED ORIENTATION OF GRAINS PLOTS. LINEATION IS HORIZONTAL INDICATED BY LARGE ARROW, NORMAL TO FOLIATION IS INDICATED BY SMALL ARROW. 250 IS ORIENTATION OF LEFT HAND SIDE LINEATION. LEFT BASAL ORIENTATION PLOT SHOW A HEXAGONAL PATTERN OF THE QUARTZ A-AXES FORMING A PLANE NORMAL TO FOLIATION PLANE WITH A MAXIMA PARALLEL TO LINEATION. RIGHT C-CRYSTAL AXIS PREFERRED ORIENTATION PLOT INDICATE A MAXIMA IN THE FOLIATION PLANE SUB NORMAL TO LINEATION WITH A TOP-LEFT-BOTTOM RIGHT ELONGATION. INDICATIONS OF SINISTRAL SENSE OF SHEAR.

Lyngen meta gabbro

FIGURE 76: OUTCROP OF GABBRO FORMING PEAKS IN THE DISTANCE.

Petrology

The gabbro tended to form the highest peaks and appeared as a dark green to black massive rock. Where it did form valleys it would feature sparse vegetation and a marshy terrain. Up close it had a silky luster and a smooth feel, probably from epidote. Cutting it open revealed bands of folded granular plagioclase that could form a weak foliation. These bands alternated with a green coarse grained matrix of amphibole and epidote

Thin section description

Thin section 6 – Lyngen Meta gabbro
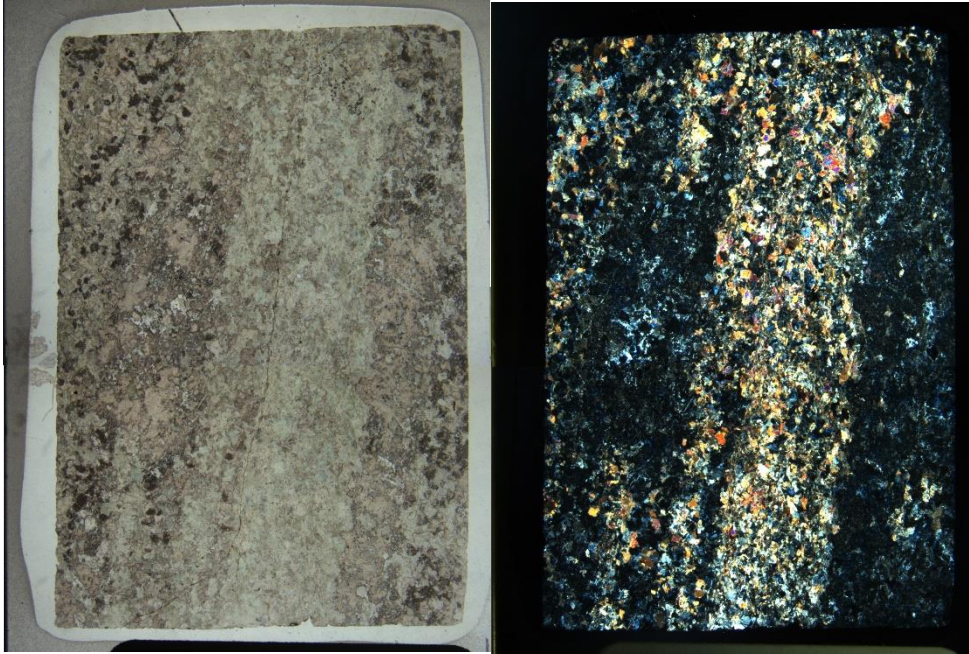
FIGURE 77: SAMPLE 6 OVERVIEW. DOMAINS OF AMPHIBOLE AND EPIDOTE/PLAGIOCLASE VISIBLE BY YELLOW BIREFRINGENCE AND DARK-BLUE BIREFRINGENCE. FIELD OF VIEW IS 3 BY 5 CM.

Minerals: Epidote-clinozoiste (40 %), Tremolite-Actinolite (20 %), chlorite (15 %), hornblende (10 %), albite (15 %)

Accessories: Apatite, Titanite

Occurrence: There are two domains in the thin section: A zoisite, albite, chlorite, epidote domain that looks dark blue and a hornblende, chlorite domain that looks yellow. Chlorite seems to replace hornblende. Albite and zoisite is suspected to replace plagioclase.
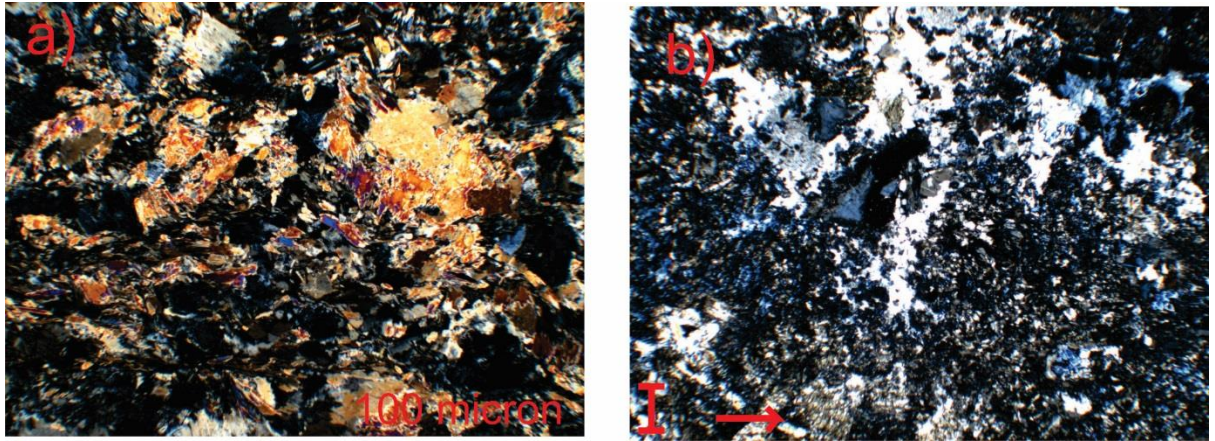
FIGURE 78: SAMPLE 6 CLOSE UP, XPL. A) AMPHIBOLE IN YELLOW, EPIDOTE IN BLUE WITH DARKER AREAS OF CHLORITE. B) BLUE EPIDOTE AND WHITE PLAGIOCLASE FORMING MOATS AROUND THE EPIDOTE SURROUNDED BY BLACK CHLORITE.

Description:

Randomly orientated amphibole, mostly actinolite-tremolite, occur surrounded by chlorite to different degrees. Small amphibole fragments that occur at some locations are left in fibres of chlorite with similar orientation as the amphibole grains. At other locations only some chlorite occurs with the amphiboles, also to a degree, having similar orientation as the amphiboles. At other locations, the chlorite occurs as distinct veins cutting through the amphiboles. Hornblende is less associated with chlorite, but can be seen occurring with moats of albite and epidote. The thin section can be divided into two domains: One domain consisting of mostly epidote and albite. Amphibole occur as small fragments in a composite of chlorite that maintains the orientation of the amphibole grains. The epidote occurs as a filthy looking mass with birefringence colours varying from first order grey to anomalous blue with yellow alterations. The albite occurs between these mattes of epidote as semi connected moats (Figure 79).
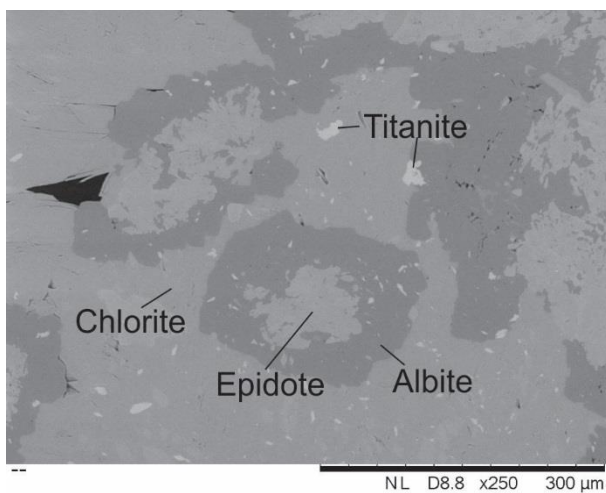
FIGURE 79: BSE OF SAMPLE 6. EPIDOTE WITH A MOAT OF ALBITE SURROUNDED BY CHLORITE.

Overall petrology

Samples taken below the Lyngen magmatic complex were generally rich in quartz, plagioclase and biotite and containing some garnet and amphibole (Figure 80). Phyllite samples show epidote to be present and more muscovite compared to the underlaying schist and gneiss. Plagioclase grains analysed with EDS indicate higher calcite content in the gneiss than in the amphibole, while garnet grains in the schist indicate higher content of manganese and calcite and lower content of iron and magnesium.

Sample	Mineral (%)											
Gneiss	Quartz	plagioclase	Biotite	Muscovite	garnet	Chlorite	Amphibole	Ilmenite	Pyrite	Calcite	K-feldspar	Epidote
9	20	65	15	-	1	-	-	-	-	-	-	-
11	60	1	10	10	5	5	-	3	3	2	-	-
Schist												
7	10	60	15	1	5	-	20	4	-	5	-	-
12	30	10	25		5					10		-
16	60	-	5	20	-	5	-	-	-	-	-	-
Phyllite												
10	15	55	5	10	-	-	-	-	-	-	10	5
14	40	5	15	20	10	1	5			2	-	2
15	70	-	-	25	-	-	-	4	-	-	-	1
Amphibolite												
8	1	15	-	-	-	4	50	-	-	-	-	30
13	5						65	-	-	-	-	20
Meta gabbro												
6	-	15	-	-	-	15	30	-	-	-	-	40

FIGURE 80: OVERVIEW OF RELATIVE MINERAL CONTENT IN SAMPLES. OVERALL THERE IS AN INCREASE IN AMPHIBOLITE AND EPIDOTE UP SECTION. MUSCOVITE CONTENT INCREASES UP SECTION INTO THE PHYLLITES, PARTIALLY CORRESPONDING TO A DECREASE IN BIOTITE. BIOTITE, MUSCOVITE, GARNET, ILMENITE AND CALCITE IS PRESENT UP INTO THE PHYLLITES. PLAGIOCLASE- AND QUARTZ-CONTENT IS LOW IN THE AMPHIBOLE AND META GABBRO COMPARED TO UNDERLAYING UNITS.

	Quartz deformation mechanism			
	Gneiss	Bulging	SGR	GBM
Sample	3		x	
	Schist			
	2		x	x
	5			x
	Amphibolite			
	4			x
	1			x

FIGURE 81: DEFORMATION MECHANISMS. OVERALL THE DOMINANT DEFORMATION PROCESSES IN THE QUARTZ SAMPLES IS GRAIN BOUNDARY MIGRATION AND SUB GRAIN ROTATION. NO INDICATIONS OF BULGING WAS OBSERVED.

Overall sense of shear

The sense of shear indicators indicates overall a top west sense of shear with some exceptions. Figure 82 indicate that the gneiss is mostly top east, while the phyllites and overlaying units indicate a top west sense of shear. The microstructures in Figure 83 seconds this picture to a degree and hint of the possibility of grouping sense of shear into two categories: Top west and top SE. S-C' and S-C fabric was present in all samples examined with angle between dominant foliation and C-planes generally between 20-30 degrees, up to 40 degrees in the amphibolite.

Macro	Sense of shear	Top movement direction	Rough sense of shear
Garnet gneiss			
Sigma clasts	Dextral	107	E
Sigma clasts	Dextral		E
Sigma clasts	Dextral	274	W
Phyllite			
Shear bands	Dextral		W
Shear bands	Sinistral		W
Sigma clasts	Sinistral	88	E
Shear bands	Dextral	268	W
Shear bands	Sinistral	282	W
Shear bands	Dextral	288	W
Chlorite schist			
Shear bands	Dextral	282	W
Amphibolite			
Shear bands	Dextral	270	W

FIGURE 82: OVERVIEW OF MACRO SENSE OF SHEAR INDICATORS. UNITS ARE GROUPED STRATIGRAPHICALLY GOING FROM THE LOWER LAYING GNEISS AND DOWN TO THE HIGHER-LAYING GABBRO. OVERALL A TOP WEST SENSE OF SHEAR WITH SOME EXCEPTIONS.

Lithology / Sample	Delta clasts	Sigma clasts	S-C fabric	S-C' fabric	Mica fish	CPO	SURFOR/PAROR	Sense of shear	Top movement direction	Rough top sense of shear
Garnet gneiss										
9	**	-	-	**	***	-	-	Dextral	138	SE
11	-	*	*	-	**	-	-	Sinistral	294	W
Garnet schist										
2	-	-	-	-	-	***	***	Sinistral	130	SE
7	*	*	-	**	-	-	-	Dextral	270	W
12	*	-	-	**	*	-	-	Dextral	292	W
14	-	**	-	***	***	-	-	Dextral	322	NW
Phyllite										
5	-	-	-	-	-	*	***	Dextral	320	NW
10	-	*	-	***	-	-	-	Dextral	286	W
15	-	-	**	-	*	-	-	Dextral	266	W
16	-	-	-	***	***	-	-	Dextral	130	SE
Amphibolite										
1	-	-	-	-	-	***	***	Dextral	250	W
8	-	-	*	**	-	-	-	Sinistral	276	W
13	*	-	**	**	-	-	-	Sinistral/Dextral	266/086	W/E

FIGURE 83: OVERVIEW OF MICRO SCALE SENSE OF SHEAR. QUALITY OF THE SENSE OF SHEAR INDICATORS ARE MARKED WITH GREEN, YELLOW AND RED INDICATING GOOD, QUESTIONABLE AND POOR QUALITY RESPECTIVELY. NUMBER OF STARS INDICATE HOW CLEAR THE SENSE OF SHEAR INDICATORS WERE DEEMED TO BE WITH ONE STAR BEING UNCERTAIN, 2 OK AND 3 GOOD. OVERALL A TOP WEST SENSE OF SHEAR CONCLUDED. BUT, MANY OF THE INTERPRETATIONS ARE QUESTIONABLE.

Discussion

What do the quartz samples indicate?

All quartz samples show some indications of dynamic recrystallization by the presence of irregular and bulging grain boundaries (Hirth & Tullis, 1992) indicating strain induced in a high temperature environment. Subgrain rotation was most evident in the gneiss quartz sample (sample 3), with small rounded grains and sweeping extinction, while other samples showed more indications of grain boundary migration and a degree of static recrystallization(Trepmann, Lenze, & Stöckhert, 2010) evident by straight grain boundaries and 120 degree triple points. As such it seems that the gneiss has been subjected to a lower temperature or increased strain rates compared to the overlaying units. The schist, phyllite and overlaying units in the contact between the Lyngen magmatic complex and the underlaying Nordmannvik gneiss have undergone deformation in temperatures higher than 600 degrees at relatively high temperatures or low strain. Alternatively, there was water present in the more foliated units shifting the regime boundaries as seen in Figure 84 changing regime 2 into regime 3. This might be a possibility as some of the samples showed evidence of both sub grain rotation and grain boundary migration occurring.
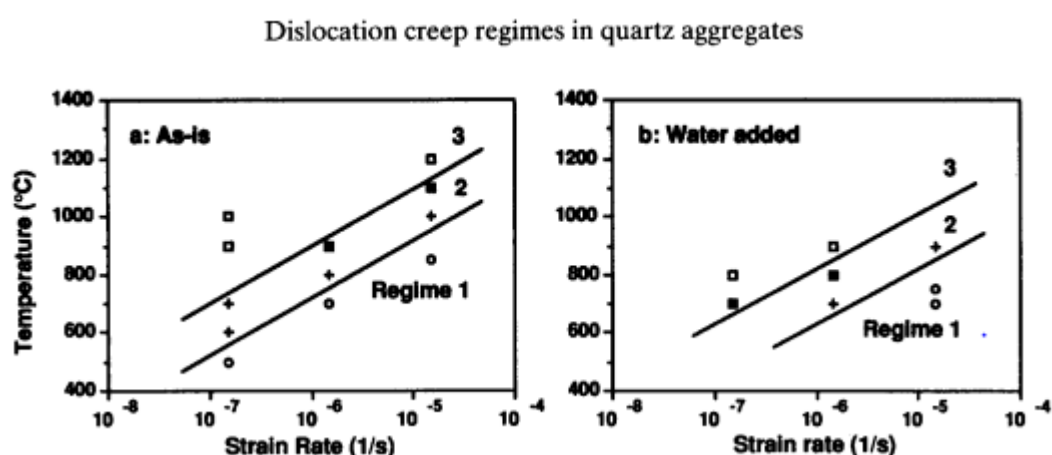
FIGURE 84: DYNAMIC RECRYSTALLIZATION REGIMES, FIGURE TAKEN FROM (HIRTH & TULLIS, 1992). REGIME 1 IS STRAIN INDUCED GRAIN BOUNDARY MIGRATION, REGIME 2 IS SUB GRAIN ROTATION AND REGIME 3 IS GRAIN BOUNDARY MIGRATION AND SUB GRAIN ROTATION.

CPO

Sample 1 (Figure 75) indicate at top 250 sense of shear, sample 2 (Figure 39) indicate a top 130 sense of shear and sample 5 (Figure 45) indicate a top 320 sense of shear, all non-coaxial. Taken together this seems like a rather random collection of samples. The intensity of the lattice oriented orientation varies as well, with sample 1 c-axes appearing more strongly oriented in two close clustered maximums compared with the other samples. The pattern of two locally clustered maximum repeat through all the samples to a degree. Sample 5 is different as it features two separate clusters of c-axis orientations at 90 degrees to two planes of a-axis orientations that converge in a monoclinic fashion to lineation. Perhaps sample 5 CPO contains mostly recrystallized grains while sample 1 for comparison

might indicate a larger proportion of non-recrystallized grains(Heilbronner & Tullis, 2006). This might be supported to a degree by more bulging grain boundaries in sample 5 compared to sample 1 and a slightly higher perimeter to equivalent perimeter slope of 1,36 to 1,31. The presence of small grains of mica might also be the reason, affecting the orientation of <a> axes. Another possibility might be a limited degree of overprinting creating two maximum. Sample 5 indicate that the quartz dynamic recrystallization favoured rhomb <a> glide thus creating two separated maxima. Sample 1 indicate a transition to prism <a> glide by two maxima along the Z axis of the pole figure perpendicular to lineation. Sample 2 indicate a in between with respect to glide domains with a maximum along the z-axis and disconnected inclined maxima's, indicating glide along both prism <a> and rhomb <a>. Overall this indicate that sample 1 have been affected by higher temperatures or strain than sample 2 and 5, which is also is reflected in the grain maps (Figure 88) which show more grain boundary migration influences and larger grains compared to sample 1 and 2.

Fabric and orientations

All samples were quartz that has been interpreted to feature grain boundary migration as main deformation mechanism. Sample 1 grain size distribution (Figure 72) feature one maximum and one local maxima indicating that there is either two dynamic recrystallization mechanisms going on at the same time, say a regime 3 grain boundary migration plus subgrain-rotation or an earlier generation of quartz grains being recrystallized. High strain conditions indicated by the lattice preferred orientation might favour the latter interpretation
Sample 2 has a smaller mode than the other sample distributions and have the volume distributed almost equally between smaller and larger grain sizes (Figure 36) possibly reflecting the presence of both subgrain rotation and grain boundary mechanism as deformation mechanisms.
Bulk fabric analysis (Figure 39, Figure 44 and Figure 74) indicate that bulk axial ratio varies from 0,692; sample 5, 0,816; sample 2 to 0,827; sample 1, possibly reflecting the dominant recrystallization mechanism again as more rounded grains would lead to a higher aspect ratio overall. Sample 1 and 2 have a similar aspect ratio even though the sense of shear is near opposite in the two locations. Sample 2 show that the long axes of grains are more aligned along the preferred axis orientation (Figure 85) compared to the other samples and show the smallest angle between foliation and preferred long axis orientation (Figure 38) with a value of 10 degrees compared to 20 degrees for sample 1 and 30 degrees for sample 2.

Sample	Weighted b/a	Bulk b/a shape	Bulk b/a long axes	Delta Weighted /Bulk shape	Delta Weighted /Bulk long axes
1	0.54	0.827	0.851	0.287	0.311
2	0.519	0.808	0.816	0.289	0.297
5	0.47	0.692	0.713	0.222	0.243

FIGURE 85: COMPARISON OF SHAPE/FABRIC AXIAL RATIOS. WEIGHTED AXIAL RATIOS DEPEND ON NUMBER OF GRAINS WHILE THE BULK FABRIC DEPENDS ON THE GRAIN SIZES. OVERALL SAMPLE 5 SHOW LESS MISALIGNMENT BETWEEN MEAN LONG AXIS ORIENTATION AND AXES IN GENERAL, CALL IT VARIANCE.

Sample 1 is indicated to be more strained due to a high degree of prism <a> sliding yet feature the highest bulk aspect ratio of the three samples while sample 5 show the least strain as such using the same reasoning on the CPO yet indicate the highest degree of

elongation along preferred long axis orientation. This might be due to the presence of mica impurities in the sample skewing the statistics.

While sample 1 and 2 have similar aspect ratio the volume distribution of the grain sizes is different with sample 1 having a modal grain size that makes up for 10 % of the volume while sample 2 modal grain size making out 5 %. This might be down to binning size or the grain map creation process that is suspected to ignore smaller grains or create them depending on structures like cracks and voids.

Sense of shear structures

Overall the sense of shear is interpreted to be top west in most of the units where shear markers have been looked for (Figure 83). A systematic exception exists, linked to the syncline east of Storvatnet where no top west indicators were seen at all. One sample taken across the Storfjorden a few kilometres away from the Lyngen/Nordmannvik metamorphic boundary is interpreted to show a top west (290) sense of shear suggesting that the shear zone might be wider than initially expected. It is suggested that the Lyngen nappes has been emplaced due west, possibly overprinting earlier SE directed sense of shear indicators. Lattice preferred orientations in quartz lenses taken in schist samples generally support this (Figure 39, Figure 45) assuming the schist was deformed by dissolution-crystallisation processes (Arnaud, Boullier, & Burg, 2004). Quartz lenses were common, and would often be oriented parallel to S2 or appear folded by the dominant S2 foliation that seemed to create the shear bands that was so prolific in the phyllites.

CPO from the amphibolite (Figure 75) also indicate a top west sense of shear, if the lenses formed by the same processes as suggested for the phyllite lenses is not known. Quartz lenses appeared to be more continuous in this unit, becoming more discontinuous corresponds possibly with strong lineation.

Shear sense indicators used to determine the microscopic sense of shear have generally tended to be S-C' and S-C fabric. It would usually appear weak, often not outlining before drawing out the foliation, and some have been as steep as 40 degrees making it possible that it is another type of fabric. There were also many instances of shear bands showing opposing sense of shear in the same thin section, leaving it very open for discussion which shear band represents the overall sense of shear(C. W. Passchier & Williams, 1996). This was especially the case in the amphibolite where shear bands with similar C-angle would be situated through the thin section seemingly at random. This might indicate that the shear zone influence only have a limited extent and influence on the amphibolite and overlaying gabbro. This degree of fluctuating sense of shear is not seen in the Nordmannvik however, though the samples are few.

Petrological aspects

The gneiss samples collected contained garnets that probably formed before the deformation event that made the dominant west dipping S2 foliation. Pre-tectonic garnets feature strain shadows and inclusions of rutile, titanite and quartz. Quartz inclusions were usually of smaller grain size than surrounding matrix indicating that the garnet formed surrounded by a smaller grain-sized matrix of quartz. They appear anhedral with cracks, sometimes with chlorite suggesting retrogradation reactions, and uneven grain boundaries. They also show higher content of iron and magnesium compared to some of the garnets observed in the schist. These garnets can occur small 300 micron wide euhedral grains with faint inclusions outlining earlier grain boundaries (Figure 52) and was probably formed after the deformation event due to the lack of strain shadows and evident overgrowth of foliation. Garnets that probably formed syn-tectonically feature curved inclusions that probably reflect the existing foliation during growth and thus indicate a rotation of around 180 degrees. They also grew asymmetrically, growing more in the low-pressure zone and thus ending up ellipse shaped due to the 180-degree rotation (Figure 53).

No K-feldspar was observed other than in a lens of quartzite, suspected to be of felsic origin. Biotite observed in the phyllite units seemed very enriched in iron and showed almost no potassium content in EDS. Plagioclase of andesine composition indicates a high metamorphic facies origin which fits the description of the unit being metamorphosed in lower amphibole conditions. (S. Elvevold, 1988)

No kyanite was observed, the few grains that resembled probably being calcite along the rim of the thin section showing kyanite-like birefriengence as a result. Perhaps the unit has undergone retrograde reactions turning kyanite and biotite into muscovite and quartz, as staurolite was not observed either. This development was seen in the field as well where biotite would become scarcer while progressing up section from the blue/grey gneiss into more muscovite rich schist. This might suggest that the nordmannvik/Lyngen contact feature previously high grade metamorphic gneiss retrograded into greenschist facies. The presence of muscovite and chlorite indicate this with the absence of kyanite.

The phyllites resembles the schist mineralogically and it could be hard to distinguish the two units, the presence of epidote seems to be the main difference, even present in the lens of quartzite, with even higher content of muscovite. Not much chlorite was observed however. The amphibolites would vary from a migmatite to a schist texture, indicating partial melting at some stage, probably unrelated to the shear zone, and featured plagioclase ranging from oligoclase to andesine (possibly bytownite) with the higher calcium content grains occurring surrounded by rims of low-calcium containing plagioclase. This suggests a lower amphibolite facies, a notion supported by the presence of hornblende.

Chlorite was observed, as well as albite and actinolite-tremolite, suggesting some retrogradation reactions to greenschist facies as higher facies minerals have been preserved. The meta-gabbro featured epidote and reaction rings of albite surrounded by chlorite possibly reflecting breakdown of calcium rich plagioclase and hornblende to epidote, albite and chlorite (Philpotts & Ague, 2009). Overall the conditions the last deformation event occurred in is interpreted to be somewhere in the greenschist facies range, possibly affecting the Nordmannvik gneiss all the way across Storfjorden (Sample 11)

Foliation and lineation

Sense of shear structures indicate a generally top west/north west sense of shear where the direction is mainly decided based on the orientation of the stretching lineation, which might not necessarily be reliable sense of shear indicator.(Lin & Williams, 1992) Foliation varies along strike, but generally keeps in the 180 to 220 range (right hand rule) with stretching lineation generally 70 to 90 degrees clockwise. West of Storvatnet there seems to cooccur two sets of lineation; one westerly and one NW while showing a consistent foliation. This might or might not be the case across the whole of the boundary, but the two locations that have been studied closely both show this pattern. Overall the boundary show some variation in foliation dip and lineation plunge up section with steepening in the higher units compared to the lower gneiss and schist. Along strike of the boundary lineation plunge and foliation dip show variations. The lineation especially is shallower around Storvatnet, generally steepening North towards Lyngseidet, a trend reflected to a lesser degree by the foliation (Figure 86). Overall the Nordmannvik/Lyngen boundary shear band dips around 15 degrees to the WNW being of an unknown thickness as the extent of it is unknown.

The synform east of Storvatnet is intriguing, the units in the east dipping limb show retrograde reactions by the presence of chlorite and feature stretching lineation, yet consistently indicate a top SE sense of shear. One way to interpret the synfom have been shown in Figure 87 where the foliation has been drawn so to fold it into a antiform and a synform. Perhaps the remnant of a duplex or a antistack from the Scandian event. There are problems with this interpretation though as the vertical foliation along the east synform limb is unexplained, and how this structure fits into an assumed WNW vergent shear band is unknown. If the shear band cut it off why does it indicate a NW-SE lineation and a SE top sense of shear seemingly made in greenschist facies conditions? If it is part of the shear band, why does it feature opposite sense of shear? Is it an indication of a larger scale SE verging folding that have passively turned sense of shear indicators along the limbs?(Stünitz, 1991)
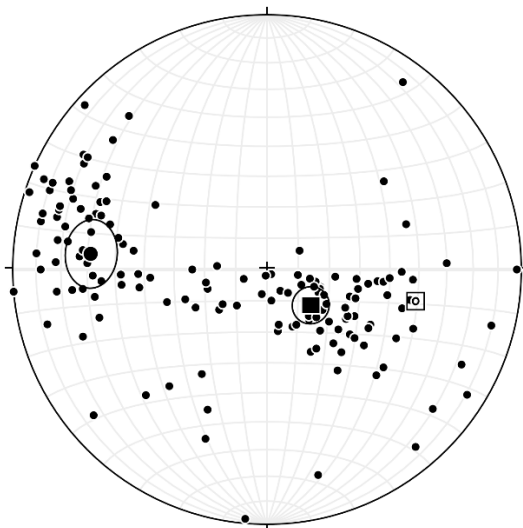
FIGURE 86: MEAN LINEATION ORIENTATION PLOTTED WITH A POINT, SURROUNDING CIRCLE INDICATING DEGREE OF VARIATION. FOLIATION POLES PLOTTED AS SQUARE, CIRCLE INDICATING DEGREE OF VARIATION. ANGLE BETWEEN THE MEANS ARE 74 DEGREES, INDICATING AN ANGLE OF 16 DEGREES BETWEEN FOLIATION DIP AND STRETCHING LINEATION PLUNGE. FOLIATION VARIATION IS SMALLER THAN LINEATION VARIATION.
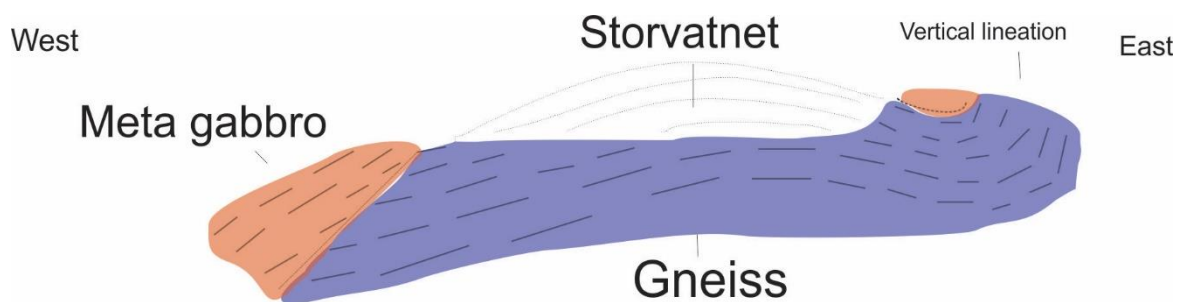
FIGURE 87: INTERPRETATION OF "STORVATNET SYNCFORM". FOLIATION IS INTERPRETED TO FOLD INTO A KILOMETER SCALE ANTIFORM EVIDENT BY THE HORIZONTAL FOLIATION MAKING OUT THE BASE OF THE STORVATNET BEFORE TURNING INTO A SYNFORM WITH A STEEPLY DIPPING EAST LIMB. THE WHOLE STRUCTURE DIPS NORTH AND THUS DISAPPEARS FROM THE SURFACE.

The big picture

Assuming the Lyngen nappe's last emplacement direction was NNW, how does this fit into the larger picture? How is the jump from lower amphibole facies to greenschist facies explained?

Looking further South to the corresponding Ofoten transect the same lithological situation is present; a greenschist facies Ofoten nappe complex transposed on top of an amphibolite facies Narvik nappe complex, separated by a shear zone. The situation is explained by upper crustal piggy back top east greenschist facies tectonism where the lower facies unit have been juxtaposed on top of earlier metamorphosed terrains (Mark G Steltenpohl, Andresen, Lindstrøm, Gromet, & Steltenpohl, 2003).

Yet (Fossen & Rykkelid, 1992) report of numerous top west and NW shear structures that overprint earlier top SE shear structures in the same transect. A picture that resembles the field data in the Lyngen/Nordmannvik boundary with both NW and W top sense of shear indicators, possibly overprinting earlier structures top to the SE kinematic indicators. These structures have been explained to result from meso-scale backfolds or flexural loading by eastward-advancing thrust sheets by (Mark G. Steltenpohl & Bartley, 1988), but they have not been interpreted kinematically(H. Steltenpohl, Bartley, Fossen, & Rykkelid, 1993). However, recent papers do not really mention any extensional west vergent structures when talking about the Rombak window or the nappe emplacements in Troms-Finnmark. That said late paleozoic extension might be required to explain the accumulation and preservation of thick Carboniferous salt deposits at deep late Paleozoic basins in the South Barents sea. (Angvik & Bergh, 2014) If we link offshore and onshore the Nordmannvik/Lyngen shear zone is in between. A driving force could be the exhumation of ductile middle crust due to isostatic rebounding after loss of brittle mantle resulting from the Scandian event (Luc & Gianreto, 2006) thus resulting in an extensional greenschist facies top west/north west shear zone with the degree of uplift controlled by distance to an inferred thrust front (H. Steltenpohl et al., 1993) being less prevalent than further South (Northrup, 1997).

Another possibility is that the Lyngen/Nordmannvik represents the upper hinterland directed shear band of an extrusion wedge(Grimmer, Glodny, Druppel, Greiling, & Kontny, 2015) with a normal -sense roof and a reverse-sense floor. Nordmannvik should in this case feature WNW sense of shear kinematic indicators that gradually turn into top to the SE

kinematic indicators down progressing down to the floor shear band. One of the samples taken for control further into the Nordmannvik did indicate top WNW. One sample alone says little and no greenschist facies metamorphism is reported for the Kåfjord/Nordmannvik tectonic boundary(S. Elvevold, 1988) unless the extrusion wedge incorporates the Vaddas nappe as well, which does feature greenschist facies mylonite(Dallmeyer & Andresen, 1992). So a scenario is suggested: The Lyngen ophiolite was formed 469-481 Ma (Augland et al., 2014a) as an incipient arc (A. Kvassnes et al., 2004) before being accreted on to possibly Laurentia and eroded during an early Caledonian tectonic event and then covered with the Balsfjord group sediments. The Scandian event thrusts the nakkedal complex on top of the Balsfjord group creating an inverse metamorphic gradient (Bjørlykke & Olaussen, 1981) and the Lyngen gabbro piggy-back on to Nordmannvik, causing a extrusion wedge in a middle-crust greenschist regime resulting in hinterland dipping shear bands by the Lyngen/Nordmannvik boundary that should fade in intensity down though the Nordmannvik unit, turning into top-east floor shear bands. If this is so, greenschist facies kinematic indicators should be common in the Nordmannvik unit.

Conclusion

The final emplacement occurred in greenschist facies conditions and was WNW relative to the underlaying Nordmannvik unit as indicated by kinematic indicators. The mechanism for this displacement is speculation, but could be extensive shear due to orogen-collapse or extrusion wedging.

Acknowledgments

References

Andersen, T. B. (1998). Extensional tectonics in the Caledonides of southern Norway, an overview. *Tectonophysics, 285*(3), 333-351. doi:http://dx.doi.org/10.1016/S0040-1951(97)00277-1

Anderson, M., Barker, A., Bennett, D., & Dallmeyer, R. (1992). A tectonic model for Scandian terrane accretion in the northern Scandinavian Caledonides. *Journal of the Geological Society, 149*(5), 727-741.

Andersson, A. (1985). *The Scandinavian alum shales*: Sveriges geologiska undersökning.

Andresen, A., Agyei-Dwarko, N. Y., Kristoffersen, M., & Hanken, N.-M. (2014). A Timanian foreland basin setting for the late Neoproterozoic–Early Palaeozoic cover sequences (Dividal Group) of northeastern Baltica. *Geological Society, London, Special Publications, 390*(1), 157-175.

Andresen, A., & Bergh, S. (1985). Stratigraphy and tectonometamorphic evolution of the Ordovician-Silurian Balsfjord Group, Lyngen Nappe, north Norwegian Caledonides. *The Caledanide Orogen-Scandinavia and related arcas, John Wiley and Sons, London*, 579-591.

Andresen, A., Fareth, E., Bergh, S., Kristensen, S., & Krogh, E. (1985). Review of Caledonian lithotectonic units in Troms, north Norway. *The Caledonide Orogen-Scandinavia and related areas. John Wiley, New York*, 569-578.

Andresen, A., & Steltenpohl, M. G. (1994). Evidence for ophiolite obduction, terrane accretion and polyorogenic evolution of the north Scandinavian Caledonides. *Tectonophysics, 231*(1), 59-70. doi:10.1016/0040-1951(94)90121-X

Angvik, T. L., & Bergh, S. G. (2014). Structural development and metallogenesis of Paleoproterozoic volcano-sedimentary rocks of the Rombak Tectonic Window: UiT Norges arktiske universitet.

Arnaud, F., Boullier, A. M., & Burg, J. P. (2004). Shear structures and microstructures in micaschists: the Variscan Cévennes duplex

(French Massif Central). *Journal of Structural Geology, 26*(5), 855-868. doi:10.1016/j.jsg.2003.11.022

Augland, L. E., Andresen, A., Gasser, D., & Steltenpohl, M. G. (2014a). Early Ordovician to Silurian evolution of exotic terranes in the scandinavian caledonides of the Ofoten-Troms area-terrane characterization and correlation based on new U-Pb zircon ages and Lu-Hf isotopic data. *Geological Society Special Publication, 390*(1), 655-678. doi:10.1144/SP390.19

Augland, L. E., Andresen, A., Gasser, D., & Steltenpohl, M. G. (2014b). Early Ordovician to Silurian evolution of exotic terranes in the Scandinavian Caledonides of the Ofoten–Troms area – terrane characterization and correlation based on new U–Pb zircon ages and Lu–Hf isotopic data. *Geological Society, London, Special Publications, 390*(1), 655-678. doi:10.1144/sp390.19

Bjørlykke, A., & Olaussen, S. (1981). *Sibirian Sediments, Volcanics and Mineral Deposits in the Sagelvvatn Area, Troms, North Norway*: Universitetsforlaget.

Boger, S. D., & Miller, J. M. (2004). Terminal suturing of Gondwana and the onset of the Ross–Delamerian Orogeny: the cause and effect of an Early Cambrian reconfiguration of plate motions. *Earth and Planetary Science Letters, 219*(1–2), 35-48. doi:http://doi.org/10.1016/S0012-821X(03)00692-7

Braathen, A., Nordgulen, Ø., Osmundsen, P.-T., Andersen, T. B., Solli, A., & Roberts, D. (2000). Devonian, orogen-parallel, opposed extension in the Central Norwegian Caledonides. *Geology, 28*(7), 615-618.

Chroston, P. N. (1972). A gravity profile across Lyngenhalvoeya, Troms, northern Norway. *Norsk Geologisk Tidsskrift. Supplement, 52*(3), 295-303.

Cloetingh, S. A. P. L., Wortel, M. J. R., & Vlaar, N. J. (1982). Evolution of passive continental margins and initiation of subduction zones. *Nature, 297*(5862), 139-142.

Corfu, F., Andersen, T. B., & Gasser, D. (2014). The Scandinavian Caledonides: main features, conceptual advances and critical

questions. *Geological Society, London, Special Publications, 390*(1), 9-43. doi:10.1144/sp390.25

Corfu, F., Gerber, M., Andersen, T. B., Torsvik, T. H., & Ashwal, L. D. (2011). Age and significance of Grenvillian and Silurian orogenic events in the Finnmarkian Caledonides, northern Norway. *Canadian Journal of Earth Sciences, 48*(2), 419-440. doi:10.1139/E10-043

Corfu, F., Ravna, E., & Kullerud, K. (2003). A Late Ordovician U–Pb age for the Tromsø Nappe eclogites, Uppermost Allochthon of the Scandinavian Caledonides. *Contributions to Mineralogy and Petrology, 145*(4), 502-513. doi:10.1007/s00410-003-0466-x

Corfu, F., Roberts, R. J., Torsvik, T. H., Ashwal,L. D. & Ramsay, D. M. (2007). Perigondwanan elements in the Caledonian nappes of Finnmark, northern Norway: implications for the paleogeographical framework of the Scandinavian Caledonides. *American Journal of Science*(307), 434-458.

Dallmeyer, R., & Andresen, A. (1992). Polyphase tectonothermal evolution of exotic caledonian nappes in Troms, Norway: Evidence from 40Ar39Ar mineral ages. *Lithos, 29*(1-2), 19-42.

Dunning, G. R. (1987). U–Pb zircon ages of Caledonian ophiolites and arc sequences: implications for tectonic setting. *Terra Abstr.*(EUG IV, Strasbourg), 179.

Eide, E. A., & Lardeaux, J. M. (2002). A relict blueschist in meta-ophiolite from the central Norwegian Caledonides—discovery and consequences. *Lithos, 60*(1–2), 1-19. doi:http://doi.org/10.1016/S0024-4937(01)00074-3

Elvevold, S. (1987). <Petrologiske undersøkelser av kaledonske bergarter i takvatnomradet, Troms.pdf>.

Elvevold, S. (1988). *Petrologiske undersøkelser av kaledonske bergarter i Takvatnområdet, Troms.* University of Tromsø.

Fossen, H., & Rykkelid, E. (1992). Postcollisional extension of the Caledonide orogen in Scandinavia: Structural expressions and tectonic significance. *Geology, 20*(8), 737-740.

Furnes, H., & Pedersen, R. (1995). The Lyngen magmatic complex: Geology and geochemistry. *Geonytt, 22*, 30.

Gayer, R., Humphreys, R., Binns, R., & Chapman, T. (1985). Tectonic modelling of the Finnmark and Troms Caledonides based on high level igneous rock geochemistry. *The Caledonide Orogen–Scandinavia and Related Areas*, 931-952.

Gee, D. G., Fossen, H., Henriksen, N., & Higgins, A. K. (2008). From the early Paleozoic platforms of Baltica and Laurentia to the Caledonide orogen of Scandinavia and Greenland. *Episodes, 31*(1), 44-51.

Grenne, T., Ihlen, P. M., & Vokes, F. M. (1999). Scandinavian Caledonide Metallogeny in a plate tectonic perspective. *International Journal of Geology, Mineralogy and Geochemistry of Mineral Deposits, 34*(5), 422-471. doi:10.1007/s001260050215

Grenne, T., & Roberts, D. (1998). The Hølonda Porphyrites, Norwegian Caledonides: geochemistry and tectonic setting of Early–Mid-Ordovician shoshonitic volcanism. *Journal of the Geological Society, 155*(1), 131-142.

Grimmer, J. C., Glodny, J., Druppel, K., Greiling, R. O., & Kontny, A. (2015). Early- to mid-Silurian extrusion wedge tectonics in the central Scandinavian Caledonides.(Report)(Author abstract). *43*(4), 347. doi:10.1130/G36433.1

Heilbronner, R. (2000). Automatic grain boundary detection and grain size analysis using polarization micrographs or orientation images. *Journal of Structural Geology, 22*(7), 969-981. doi:10.1016/S0191-8141(00)00014-6

Heilbronner, R., & Barrett, S. (2014). *Image Analysis in Earth Sciences: Microstructures and Textures of Earth Materials*. Berlin, Heidelberg: Springer Berlin Heidelberg: Berlin, Heidelberg.

Heilbronner, R., & Tullis, J. (2006). Evolution of c axis pole figures and grain size during dynamic recrystallization: Results from experimentally sheared quartzite. *Journal of Geophysical Research: Solid Earth, 111*(B10), n/a-n/a. doi:10.1029/2005JB004194

Hibelot, T. (2013). Relationships Between Metamorphism And Deformation In The Nordmannvik Nappe, South Of Lyngseidet: A Focus On High Grade Relics.

Hirth, G., & Tullis, J. (1992). Dislocation creep regimes in quartz aggregates. *Journal of Structural Geology, 14*(2), 145-159. doi:10.1016/0191-8141(92)90053-Y

Kirkland, C. L., Daly, J. S., Eide, E. A., & Whitehouse, M. J. (2006). The structure and timing of lateral escape during the Scandian Orogeny: A combined strain and geochronological investigation in Finnmark, Arctic Norwegian Caledonides. *Tectonophysics, 425*(1), 159-189. doi:10.1016/j.tecto.2006.08.001

Kirkland, C. L., Daly, J. S., & Whitehouse, M. J. (2008). Basement-cover relationships of the Kalak Nappe Complex, arctic Norwegian Caledonides and constraints on neoproterozoic terrane assembly in the North Atlantic Region. *Precambrian Research, 160*(3-4), 245-276. doi:10.1016/j.precamres.2007.07.006

Kirkland, C. L., Stephen Daly, J., & Whitehouse, M. J. (2007). Provenance and terrane evolution of the Kalak Nappe Complex, Norwegian Caledonides: implications for Neoproterozoic paleogeography and tectonics. *The Journal of Geology, 115*(1), 21-41.

Krogh, E., Andresen, A., Bryhni, I., Broks, T., & Kristensen, S. (1990). Eclogites and polyphase P–T cycling in the Caledonian Uppermost Allochthon in Troms, northern Norway. *Journal of Metamorphic Geology, 8*(3), 289-309.

Kumpulainen, R., & Nystuen, J. (1985). Late Proterozoic basin evolution and sedimentation in the westernmost part of Baltoscandia. *The Caledonide Orogen—Scandinavia and Related Areas, 1*, 213-245.

Kvassnes, A., Strand, A., Moen-Eikeland, H., & Pedersen, R. (2004). The Lyngen Gabbro: the lower crust of an Ordovician Incipient Arc. *Contributions to Mineralogy and Petrology, 148*(3), 358-379. doi:10.1007/s00410-004-0609-8

Kvassnes, A. J. S., Strand, A. H., Moen-Eikeland, H., & Pedersen, R. B. (2004). The Lyngen Gabbro: the lower crust of an Ordovician

Incipient Arc. *Contributions to Mineralogy and Petrology, 148*(3), 358-379. doi:10.1007/s00410-004-0609-8

Lin, S., & Williams, P. F. (1992). The geometrical relationship between the stretching lineation and the movement direction of shear zones. *Journal of Structural Geology, 14*(4), 491-497. doi:10.1016/0191-8141(92)90108-9

Lindahl, I., Stevens, B. P., & Zwaan, K. B. (2005). The geology of the Vaddas area, Troms: a key to our understanding of the Upper Allochthon in the Caledonides of northern Norway. *NORGES GEOLOGISKE UNDERSOKELSE, 445*(5).

Luc, L. L., & Gianreto, M. (2006). A mechanism to thin the continental lithosphere at magma-poor margins. *Nature, 440*(7082), 324. doi:10.1038/nature04608

McKerrow, W., Mac Niocaill, C., & Dewey, J. (2000). The Caledonian Orogeny redefined. *J. Geol. Soc., 157*, 1149-1154.

Northrup, C. J. (1997). Timing Structural Assembly, Metamorphism, and Cooling of Caledonian Nappes in the Ofoten-Efjorden Arca, North Norway: Tectonic Insights From U-Pb and 40Ar/39Ar Geochronology.

Oliver, G., & Krogh, T. E. (1995). U-Pb zircon age of 469 5 Ma for a metatonalite from the Kjosen Unit of the Lyngen Magmatic Complex northern Norway. *NORGES GEOLOGISKE UNDERSOKELSE, 428*, 27-32.

Passchier, C. W., Trouw, R. A. J., & SpringerLink. (2005). *Microtectonics* (2nd, Revised and Enlarged Edition. ed.): Springer Berlin Heidelberg.

Passchier, C. W., & Williams, P. R. (1996). Conflicting shear sense indicators in shear zones; the problem of non-ideal sections. *Journal of Structural Geology, 18*(10), 1281-1284. doi:10.1016/S0191-8141(96)00051-X

Philpotts, A. R., & Ague, J. J. (2009). *Principles of igneous and metamorphic petrology* (2nd ed. ed.). Cambridge: Cambridge University Press.

Ramsay, D., Sturt, B., Zwaan, K., & Roberts, D. (1985). Caledonides of northern Norway. *The Caledonian Orogen: Scandinavia and*

related areas. Edited by DG Gee and BA Sturt. Wiley, Chichester, UK, 163-184.

Roberts, D. (2003). The Scandinavian Caledonides: event chronology, palaeogeographic settings and likely modern analogues. *Tectonophysics, 365*(1-4), 283-299. doi:10.1016/s0040-1951(03)00026-x

Roberts, D., Nordgulen, Ø., & Melezhik, V. (2007). The Uppermost Allochthon in the Scandinavian Caledonides: From a Laurentian ancestry through Taconian orogeny to Scandian crustal growth on Baltica. *Geological Society of America Memoirs, 200*, 357-377.

Roberts, D. D. G. G. (1985). An introduction to the structure of the Scandinavian Caledonides. *The Caledonide Orogen; Scandinavia and related areas; Vol. 1*, 55-68.

Roberts, R. J., Corfu, F., Torsvik, T. H., Ashwal, L. D., & Ramsay, D. M. (2006). Short-lived mafic magmatism at 560570 Ma in the northern Norwegian Caledonides: UPb zircon ages from the Seiland Igneous Province. *Geol. Mag., 143*(6), 887-903. doi:10.1017/S0016756806002512

Rykkelid, E., & Andresen, A. (1994). Late Caledonian extension in the Ofoten area, northern Norway. *Tectonophysics, 231*(1), 157-169. doi:10.1016/0040-1951(94)90127-9

Selbekk, R. S., Skjerlie, K. P., & Pedersen, R. B. (2000). Generation of anorthositic magma by H 2 O-fluxed anatexis of silica-undersaturated gabbro: an example from the north Norwegian Caledonides. *Geol. Mag., 137*(6), 609-621. doi:10.1017/S0016756800004829

Slabunov, A., Lobach-Zhuchenko, S., Bibikova, E., Sorjonen-Ward, P., Balangansky, V., Volodichev, O., . . . Arestova, N. (2006). The Archaean nucleus of the Fennoscandian (Baltic) Shield. *Geological Society, London, Memoirs, 32*(1), 627-644.

Slagstad, D. (1995). Lyngen Magmatic Complex Rypdalen Shear Zone: magmatic and structural evolution. *Geonytt, 22*, 67.

Slagstad, T., Melezhik, V., Kirkland, C., Zwaan, K., Roberts, D., Gorokhov, I., & Fallick, A. (2006). Carbonate isotope

chemostratigraphy suggests revisions to the geological history of the West Finnmark Caledonides, northern Norway. *Journal of the Geological Society, 163*(2), 277-289.

Steltenpohl, H., Bartley, E., Fossen, E., & Rykkelid, E. (1993). Postcollisional extension of the Caledonide orogen in Scandinavia: Structural expressions and tectonic significance: Comment and Reply. *Geology, 21*(5), 476-478. doi:10.1130/0091-7613(1993)021<0476:PEOTCO>2.3.CO;2

Steltenpohl, M. G., Andresen, A., Lindstrøm, M., Gromet, P., & Steltenpohl, L. W. (2003). The role of felsic and mafic igneous rocks in deciphering the evolution of thrust-stacked terranes: An example from the north Norwegian Caledonides. *American Journal of Science, 303*(2), 149-185.

Steltenpohl, M. G., & Bartley, J. M. (1988). Cross folds and back folds in the Ofoten-Tysfjord area, North Norway, and their significance for Caledonian tectonics. *Geological Society of America Bulletin, 100*(1), 140-151. doi:10.1130/0016-7606(1988)100<0140:CFABFI>2.3.CO;2

Steltenpohl, M. G., Moecher, D., Andresen, A., Ball, J., Mager, S., & Hames, W. E. (2011). The Eidsfjord shear zone, Lofoten–Vesterålen, north Norway: an Early Devonian, paleoseismogenic low-angle normal fault. *Journal of Structural Geology, 33*(5), 1023-1043.

Stephens, M. B. D. G. G. (1985). *A plate tectonic model for the evolution of the eugeoclinal terranes*

in the central Scandinavian Caledonides. (Vol. The Caledonide Orogen – Scandinavia and Related Areas): Wiley, Chichester.

Stünitz, H. (1991). Folding and shear deformation in quartzites, inferred from crystallographic preferred orientation and shape fabrics. *Journal of Structural Geology, 13*(1), 71-86. doi:10.1016/0191-8141(91)90102-O

Terry, M. P., Robinson, P., Hamilton, A., & Jercinovic, M. J. (2000). Monazite geochronology of UHP and HP metamorphism, deformation, and exhumation, Nordøyane, Western Gneiss Region, Norway. *American Mineralogist, 85*(11-12), 1651-1664.

Torsvik, T. H., Smethurst, M. A., Meert, J. G., Van der Voo, R., McKerrow, W. S., Brasier, M. D., . . . Walderhaug, H. J. (1996). Continental break-up and collision in the Neoproterozoic and Palaeozoic — A tale of Baltica and Laurentia. *Earth Science Reviews, 40*(3), 229-258. doi:10.1016/0012-8252(96)00008-6

Trepmann, C., Lenze, A., & Stöckhert, B. (2010). Static recrystallization of vein quartz pebbles in a high-pressure – low-temperature metamorphic conglomerate. *Journal of Structural Geology, 32*(2), 202-215. doi:https://doi.org/10.1016/j.jsg.2009.11.005

van Staal, C. R., & Hatcher, R. D. (2010). Global setting of Ordovician orogenesis. *Geological Society of America Special Papers, 466*, 1-11.

Yoshinobu, A. S., Barnes, C. G., Nordgulen, Ø., Prestvik, T., Fanning, M., & Pedersen, R. (2002). Ordovician magmatism, deformation, and exhumation in the Caledonides of central Norway: An orphan of the Taconic orogeny? *Geology, 30*(10), 883-886.

Appendix
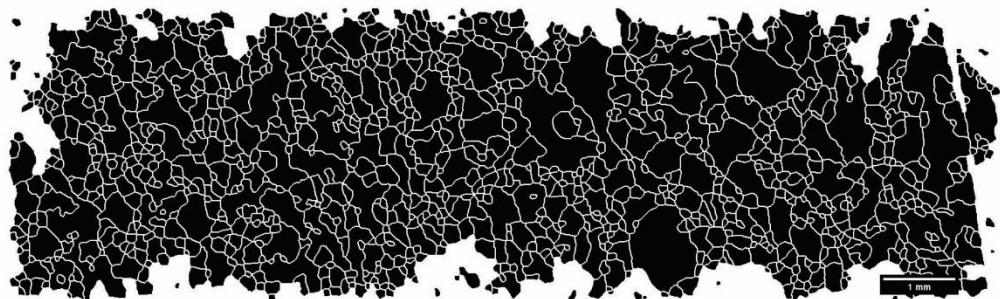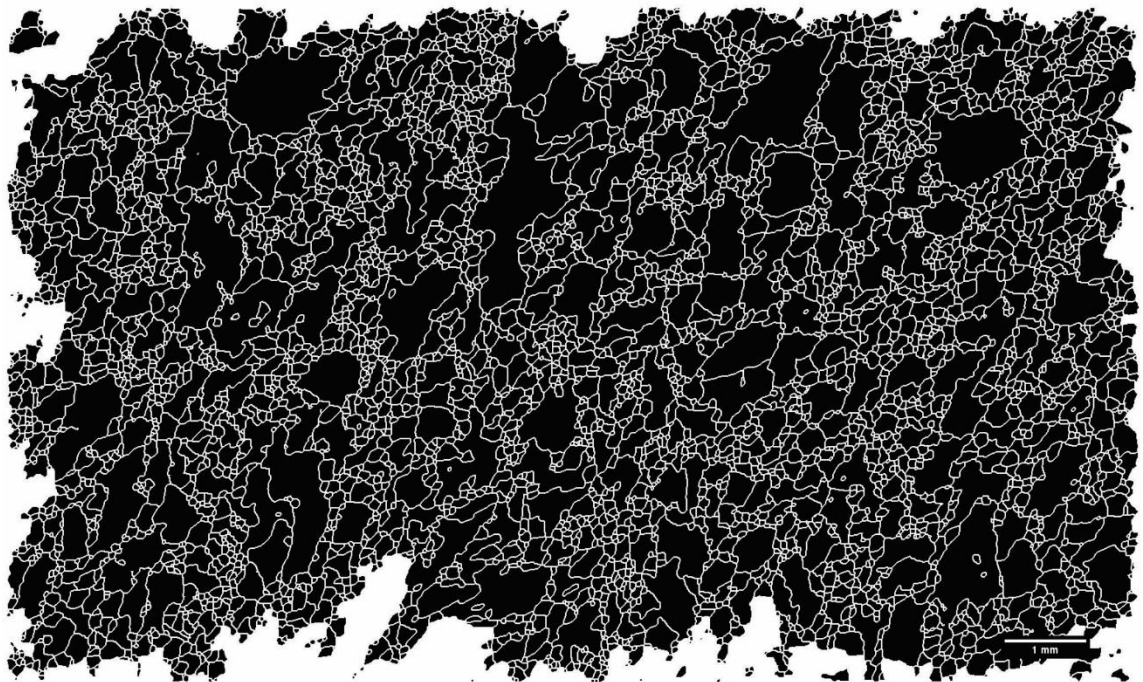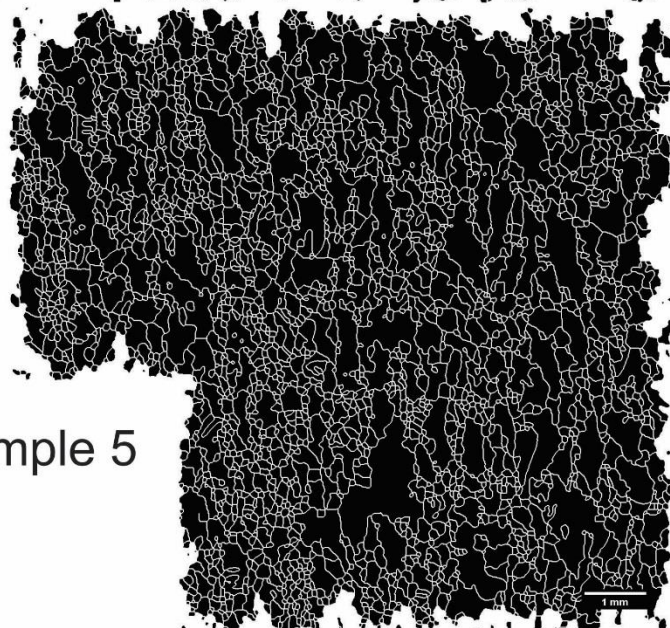
FIGURE 88: GRAIN MAPS USED AS BASIS FOR IMAGE ANALYSIS. NOTE 1 MM SCALE FOR EACH MAP. SAMPLE 1 HAS NOTICEABLY LARGER GRAINS, WHILE 1 AND 5 FEATURE CORES SURROUNDED BY SMALLER GRAINS.